THE ROLE OF P16^{INK4A} EXPRESSION IN THE AGE-RELATED RISK OF VENOUS THROMBOEMBOLISM

Jessica Caroline Cardenas

A dissertation submitted to the faculty of the University of North Carolina at Chapel Hill in partial fulfillment of the requirements for the degree of Doctor of Philosophy in the Department of Pathology and Laboratory Medicine.

Chapel Hill
2012

Approved by:

Frank C. Church, PhD

Nigel S. Key, MD

Norman E. Sharpless, MD

Herbert C. Whinna, MD, PhD

Alisa S. Wolberg, PhD

Abstract

JESSICA CAROLINE CARDENAS: The Role of $p16^{INK4a}$ Expression in the Age-related Risk of Venous Thromboembolism
(Under the direction of Dr. Frank C. Church)

Venous thromboembolism (VTE) is a pathophysiologically complex disease involving dysregulation of pro and anticoagulant processes in the vasculature. Aging is the strongest risk factor for VTE, although the mechanism is not well understood. Senescence is a physiologic process limiting cellular proliferation, caused by age-dependent expression of the cell cycle inhibitor $p16^{INK4a}$. $p16^{INK4a}$ expression and senescence could promote vascular dysfunction and predispose elderly individuals to VTE. This dissertation is focused on researching the contribution of $p16^{INK4a}$ expression and aging to venous thrombosis.

Murine *in vivo* vascular injury models are commonly used to study venous and arterial thrombosis. We found that $p16^{INK4a}$ overexpression in mice was associated with augmented venous thrombosis and increased thrombin generation. Bone marrow transplantation analysis demonstrated that this phenotype was dependent on $p16^{INK4a}$ expression in hematopoietic cells. Furthermore, $p16^{INK4a}$ transgenic mice display significant elevation monocyte and macrophage marker, F4/80 staining following IVC ligation. Depletion of monocytes and macrophages, abolished the difference in thrombus mass between $p16^{INK4a}$ overexpressing and wild-type mice. This suggests that $p16^{INK4a}$ expression in hematopoeitic cells, and specifically monocytes and macrophages, contribute to venous thrombosis.

Senescence in vascular endothelial cells is associated with phenotypic changes that could promote vascular dysfunction. We observed that senescence induced by serial passaging *in vitro* caused more rapid rates of clot formation, increased thrombin generation, and formation of denser fibrin networks on the endothelial cell surface. Furthermore, senescent endothelial cells generate less activated protein C due to downregulation of thrombomodulin expression. These results suggest that endothelial cell senescence promotes a procoagulant phenotype.

Age-related changes in venous thrombus formation and resolution have not been well defined. Aged mice display a prothrombotic phenotype in a $FeCl_3$ injury to the saphenous vein, however there was no difference compared to young mice in thrombus mass after IVC-ligation. This suggests the susceptibility of aged mice to venous thrombosis is coagulation stimulus dependent. Additionally, aging in mice is associated with changes in blood composition and plasma coagulability that differ from changes observed in human aging, suggesting mice are a challenging model to study hemostasis during aging.

Collectively these studies suggest that $p16^{INK4a}$ expression and cellular senescence contribute to venous thrombosis.

Acknowledgments

First of all, I must thank my dissertation committee, Dr. Alisa Wolberg, Dr. Herb Whinna, Dr. Ned Sharpless and Dr. Nigel Key for all of their guidance and support throughout this process. Every member made an invaluable contribution to this work and was always willing to provide helpful feedback. In particular, I would like to thank Dr. Alisa Wolberg for setting aside time to talk science with me whenever I needed her and also for introducing me to coagulation research. I would also like to specially thank Dr. Herb Whinna for putting up with my sass and coaching me through the mouse models aspect of my work. You have taught me an incredibly useful skill and are an irreplaceable sounding board for my wild ideas.

The Department of Pathology and Laboratory Medicine has always prioritized the needs of the graduate students. I would like to thank Dr. Charles Jennette for his support of our graduate program. Ms. Dorothy Poteat, for all of her effort in maintaining the sanity I am so thankful. Also, I must thank our director of graduate studies, Dr. Bill Coleman for all the time he puts into guiding each of us. He always has an open door and is willing to rearrange his schedule for a "mental health break".

I am so thankful to all of the past Church lab members and to Dr. Mac Monroe, Dr. Peter Chang, and Leana LeFrapper for all of their support. Of course, I have so much to thank my advisor Dr. Frank Church for. Frank is a particularly intuitive advisor, who treats every student differently based on his or her mentoring needs. He has always made time to meet with me and discuss data or new ideas and allowed me to pursue the projects and questions

that most interested me. Most importantly, Frank knew when I needed guidance and when I needed independence. He has taught me so much about how to answer a question, and more importantly how to ask one. For all his mentoring, I am eternally grateful. I must also give a special thank you to Dr. Chantelle Rein for single handedly keeping the peace. She has been a solid rock of support for me through finishing my research and writing my dissertation. She is a true friend and colleague and I will miss having her as a scientific teammate.

I have been blessed with such incredible friends in Texas, D.C. and North Carolina. Special thank you to Emily and Cori for always being only a phone call away. Thank you to Erin, Dana, Dan, Matt and Mary for providing a family when we were so far from ours. Kellie and Zach, you are the perfect partners in crime. I miss you both. Thank you Jen for keeping me well fed and entertained. And thank you Courtney; true friend who I will miss binging on sushi with a great deal.

Finally, have to give infinite credit to my family. They have supported me in any way I needed it and were always there for me through the highs and the lows. Especially my mother and father, Joe and Roxie, who are the most loving, generous, kind, and supportive parents anyone could ask for. They have encouraged me to live my life on my own but always provided a home to return to. I am so thankful for my sister, Jackie, who is my best friend and favorite person. And lastly thank you to my grandmother, Mia, from whom I have received so much of my strength.

I would also like to thank my funding sources, The UNC Integrative Vascular Biology NIH training grant (T32 HL697668) and the American Heart Association predoctoral fellowship (11PRE7630005).

Table of Contents

List of Tables

List of Figures

List of Abbreviations and Symbols

α	Alpha
α_1-PI	alpha 1-Protease Inhibitor (Antitrypsin)
α_2-AP	alpha 2-Antiplasmin
ABC	Avidin-Biotin Complex
ADP	Adenosine Diphosphate
ANRIL	Antisense Non-coding RNA in the INK4 Locus
APC	Activated Protein C
ApoE	Apolipoprotein E
aPTT	Activated Partial Thromboplastin Time
ARF	Alternative Reading Frame
AT	Antithrombin
ATP	Adenosine Triphosphate
β	Beta
BAC	Bacterial Artificial Chromosome
BSA	Bovine Serum Albumin
°C	Degree Celsius
$CaCl_2$	Calcium Chloride
CAD	Coronary Artery Disease
CAT	Calibrated Automated Thrombography
CBC	Complete Blood Count
CDK	Cyclin-Dependent Kinase

CDKN2A	Cyclin-Dependent Kinase Inhibitor 2A
CRP	C-Reactive Protein
d	deca
DNA	Deoxyribonucleic Acid
DVT	Deep Vein Thrombosis
EDTA	Ethylenediaminetetraacetic Acid
ELISA	Enzyme-Linked Immunosorbent Assay
eNOS	Endothelial Nitric Oxide Synthase
EPCR	Endothelial Protein C Receptor
ETP	Endogenous Thrombin Potential
f	femto
$FeCl_3$	Ferric Chloride
FV	Factor V
FVII	Factor VII
FVIII	Factor VIII
FIX	Factor IX
FX	Factor X
FXI	Factor XI
FXIII	Factor XIII
g	grams
G	Gauge
GWAS	Genome-Wide Association Study
Gy	Gray

HBS	HEPES Buffered Saline (20 mM Hepes, 150 mM NaCl, pH 7.4)
HCII	Heparin Cofactor II
H&E	Hematoxylin and Eosin
HEPES	4-(2-hydroxyethyl)-1-piperazineethane sulfonic acid
hrs	Hours
HTF-1	Mouse anti-Human Tissue Factor Antibody
HUVEC	Human Umbilical Vein Endothelial Cells
IB	Immunoblot
IHC	Immunohistochemistry
IL	Interleukin
INK	Inhibitor of Kinase
IVC	Inferior Vena Cava
k	kilo
L	Liter
LDLr	Low Density Lipoprotein Receptor
LPS	Lipopolysaccharide
LSCM	Laser Scanning Confocal Microscopy
μ	Micro
m	milli
M	Molar
MCP-1	Monocyte Chemotactic Protein-1
MDM2	Murine Double Minute 2
$MgCl_2$	Magnesium Chloride

min	Minute
MMP	Matrix metalloprotease
MP	Microparticle
mRNA	Messenger Ribonucleic Acid
n	nano
NaCl	Sodium Chloride
NO	Nitric Oxide
p	pico
PAI-1	Plasminogen Activator Inhibitor-1
PAP	Plasmin-Antiplasmin
PBS	Phosphate Buffered Saline (10 mM phosphate and 150 mM NaCl, pH 7.4)
PcG	Polycomb Group
PCI	Protein C Inhibitor
PCR	Polymerase Chain Reaction
PE	Pulmonary Embolism
PE-10	Polyethylene-10
PS	Phosphatidylserine
PT	Prothrombin Time
Rb	Retinoblastoma
RNA	Ribonucleic Acid
s	second
SA	Senescence Associated
SERPIN	Serine Protease Inhibitor

SNP	Single Nuleotide Polymorphism
TAFI	Thrombin Activatable Fibrinolysis Inhibitor
TNFα	Tumor Necrosis Factor α
TF	Tissue Factor
TFPI	Tissue Factor Pathway Inhibitor
TM	Thrombomodulin
tPA	Tissue-type Plasminogen Activator
TTP	Time to Peak
U	Units
uPA	Urokinase Plasminogen Activator
uPAR	Urokinase Plasminogen Activator Receptor
VTE	Venous Thromboembolism
vWF	von Willebrand Factor
WT	Wild-type
ZPI	Z Protein Inhibitor

Chapter 1

Introduction

Venous Thromboembolism and the Increased Risk with Age

1.1 Introduction.

Deep vein thrombosis (DVT) is characterized by the formation of occlusive or semi-occlusive thrombi typically in the deep veins of the limbs. The most serious and potentially fatal complication of a DVT is pulmonary embolism (PE), in which part of the thrombus breaks off (embolizes), traveling through the circulation before becoming lodged in the pulmonary artery. DVT and PE are collectively referred to as venous thromboembolism (VTE). The incidence of VTE is approximately 1 in 1000, with between 350,000 and 600,000 individuals affected by this disease each year in the United States[1,2]. There are many risk factors for VTE, both genetic and acquired/environmental. The strongest acquired risk factor is age[3]. Interestingly, the rate of VTE increase relatively slowly until the age of 50, after which there is a dramatic increase with an incidence of 1 in 100 over the age of 75[2,4]. In the U.S., over 250,000 VTE patients are hospitalized each year, contributing to the significant healthcare economic burden associated with cardiovascular disease. The national annual cost of VTE is estimated at $1.5 billion[5]. With the incidence of VTE predicted to increase dramatically in the future with the aging population, we can expect the economic burden to continue to rise.

Virchow's triad can be used to explain the etiology of thrombosis: changes in blood vessel (arterial and venous thrombosis) due to endothelial injury, secondary to diseases like atherosclerosis, trauma or chronic inflammation; changes in blood constituents (venous thrombosis) due to primary hypercoagulability (e.g., antithrombin deficiency or Factor V_{Leiden}) or acquired hypercoagulability (e.g., age, obesity, pregnancy, smoking, trauma/surgery, or cancer); and changes in blood flow (venous thrombosis) such as caused by stasis or vessel turbulence especially behind venous valve pockets. One or more aspects of Virchow's triad may change with advanced aging, although the relationship between VTE and age is poorly understood. Several publications have reviewed the effect of aging on hemostasis/thrombosis[6-8]. Here we review recent findings concerning age-related changes in the hemostasis system that may predispose elderly individuals to VTE.

1.2 Review of hemostasis.

Under normal, physiologic conditions, luminal flowing blood comes into contact only with circulating blood cells and the naturally anticoagulant vascular endothelium. Upon perturbation or injury to the vessel wall, sub-endothelial tissue factor (TF) expressed by cells such as fibroblasts and smooth muscle cells is exposed to the flowing blood, becoming available for complex formation with circulating activated factor VII (Figure 1.1). This TF/FVIIa complex initiates the coagulation pathway by activation of both factor X (FX) to activated factor X (FXa) and factor IX (FIX) to activated factor IX (FIXa) . FXa bound to its cofactor activated factor V (FVa) then cleaves prothrombin to its active form, thrombin. This is the initiation phase of coagulation. The relatively small amount of thrombin generated during the initiation phase can then activate factor XI, factor VIII and factor V and activate

platelets that will adhere to the site of injury by cleavage of the protease-activated receptors on the platelet surface. In addition, thrombin stimulates microparticle release from platelets and circulating monocytes. Rich in TF and phosphatidyl serine (PS), microparticules (MP) support FXa generation an are thus critical in promoting thrombin generation and further platelet activation. Even greater activation of FIX by FXIa and FX occurs on the PS-rich platelet surface by the FIXa and FVIIIa complex, also known as the TENase complex (Figure 1.1). Also on the platelet surface, FXa binds with its cofactor, FVa (all together referred to as the prothrombinase complex) generating a large volume burst of thrombin (Figure 1.1). This is termed the propagation phase of coagulation and this process cycles to produce more and more thrombin. The generation of thrombin is a key event in the coagulation cascade, as thrombin is the protease that cleaves circulating fibrinogen to fibrin. The more thrombin that is generated, the more fibrinogen can be cleaved to fibrin to form a fibrin clot, a structure which is stabilized and made insoluble through fibrin cross-linking by activated factor XIII (FXIIIa), a transglutaminase.

Therefore, blood clots are composed of activated plasma factors, trapped leukocytes and red blood cells, activated platelets, MPs and fibrin. Fibrin-rich venous clots and platelet-rich arterial clots differ in composition, suggesting that while thrombin is generated through the same mechanism, differences in shear flow rate favor fibrin deposition over platelet adhesion in the venous circulation, whereas shear rates in the arterial circulation favor platelet adhesion over fibrin deposition.

As aberrant or sustained clotting can be pathological, several very important anticoagulant and fibrinolytic pathways also regulate blood coagulation and clot dissolution. The protein C pathway is an essential anticoagulant regulatory pathway designed to inhibit

the propagation of thrombin (Figure 1.1). As part of their anti-thrombotic surface, vascular endothelial cells produce thrombomodulin (TM), a trans-membrane glycoprotein that binds to thrombin and in the presence of endothelial protein C receptor (EPCR) which binds zymogen Protein C. The TM/thrombin complex cleaves protein C bound to EPCR to activated protein C (APC) (Figure 1.1). APC can then interact with its cofactor, protein S, to inactivate FVa and FIIIa; thus down-regulating the further generation of thrombin. In addition to TM and EPCR, vascular endothelial cells also produce heparan sulfate and dermatan sulfate, molecules that increase the efficiency of thrombin inhibition by antithrombin and other serine protease inhibitors (SERPINs). Endothelial cells also produce key platelet inhibitors, including prostacyclin and nitric oxide, limiting the availability of lipids for coagulation factor complex formation.

In addition to pathways in place to control clot formation and prevent the generation of occlusive thrombi, fibrinolysis or clot dissolution must also be regulated. The fibrinolysis pathway is the pathway that dictates whether clots are sustained or dissolved (Figure 1.1). Endothelial cells and trapped leukocytes release both tissue and urokinase plasminogen activator (tPA and uPA, respectively), proteases which activate plasminogen to plasmin. Plasmin is a serine protease that cleaves cross-linked fibrin to produce fibrin degradation products, which are easily swept away and degraded in flowing blood. Inhibitors tightly regulate fibrinolysis. Plasmin is inhibited by α2-antiplasmin. The primary inhibitor of both tPA and uPA is plasminogen activator inhibitor (PAI-1). PAI-1 binds to the active site on tPA and uPA, blocking their ability to interact with plasminogen, therefore inhibiting fibrinolysis.

Blood coagulation is a complex cascade of proteases and protease inhibitors present in the circulation and synthesized by various cell types. Given this, alterations to plasma proteins and platelet and endothelial function have significant, detrimental effects on coagulation.

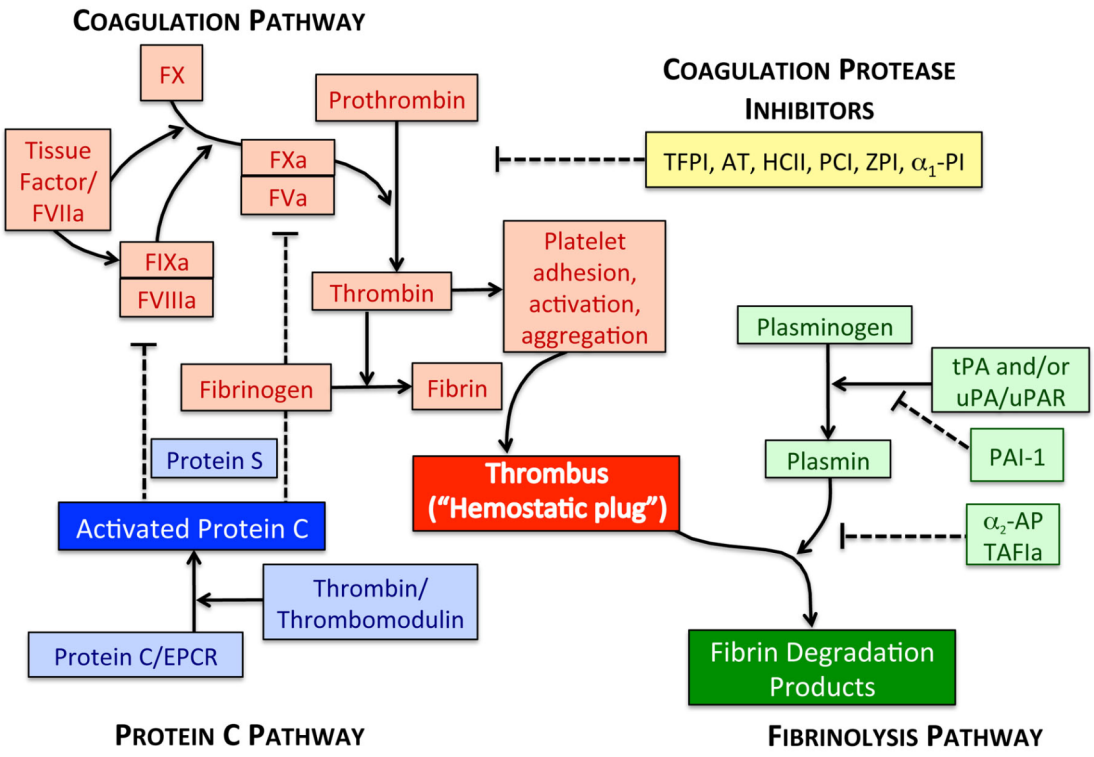

Figure 1.1. Coagulation Regulation: The coagulation pathway is composed of a cascade of proteases that activate platelets and ultimately generates thrombin to cleave fibrinogen to fibrin. This cascade is regulated by a number of protease inhibitors that limit the generation of thrombin, as well as the endothelial-derived protein C pathway which inactivates FVa and FVIIIa. The sustained presence of a thrombus is regulated by the fibrinolysis pathway, which controls fibrin degradation.

1.3 Age-related increases in coagulation factors.

A number of large-scale studies have measured the changes in coagulation factors with respect to age. One of the coagulation proteins most commonly reported to increase with age is fibrinogen[9], with levels ranging from 250 mg/dL in young, 20 year old subjects to 300 mg/dL in subjects over 65 years of age[10,11]. As the precursor to fibrin, fibrinogen availability is a key determinant in the formation of stable thrombi. Elevated fibrinogen is a strong risk factor for cardiovascular disease, and while its role in arterial disease is widely accepted, the contribution of elevated fibrinogen levels to venous thrombosis has been considered controversial. The first study attempting to correlate elevated fibrinogen with the risk of VTE included some of earliest patients in the Leiden thrombophilia study[12]. With limited numbers, elevated fibrinogen was considered weakly predictive of VTE, however, when later expanded to include more patients, a positive correlation was found among patients with fibrinogen levels in the 95th percentile having a 2.8-fold increased risk of VTE[13]. More recently, a study using mouse models showed that elevated fibrinogen plays a causative role in enhancing thrombosis in both arterial and venous models[14]. Therefore, elevated circulating fibrinogen in elderly individuals may predispose them to coagulation abnormalities in the arterial and venous circulation.

FVIII levels are also known to increase with age[15-17]. With its cofactor FIXa, FVIII is a potent activator of FX that in turn, cleaves prothrombin to thrombin. Thus, elevated FVIII has long been believed to be a risk factor for VTE, and as of recently, also for arterial thrombosis[18]. A prospective cohort study showed a 11-fold increase in the risk of VTE for individuals with FVIII levels above the 90th percentile[19].

FVIII circulates bound to von Willebrand Factor (vWF) and as such, age-related increases in vWF have also been observed[9]. vWF is an endothelial-derived protein that functions as a strong platelet tethering agent. It was thought that vWF only contributed to the risk of VTE through its association with, or effect on levels of FVIII[20]. However the 2002 LITE study showed that FVIII and vWF are in fact independent risk factors for VTE[21]. Mouse models have recently shown that both vWF and FVIII are independently critical for venous thrombus formation. vWF knock-out mice show impaired venous thrombus growth and platelet adhesion following $FeCl_3$ injury, a defect that was not fully corrected upon infusion of recombinant FVIII although FVIII infusion did increase thrombus stability[22]. These data support findings from the LITE study that even uncomplexed vWF and FVIII can both contribute to venous thrombosis.

FVII is a circulating zymogen that, when in complex with its cofactor TF, is a potent initiator of coagulation. Levels of FVII are reported to increase over 15 units/dL between the ages of 20 and 50 years[9,23]. Considering that increases in circulating FVII should be relatively harmless given that TF is typically not found circulating or even available on the endothelial surface in the absence of an injury or disease state, its contribution to VTE remains controversial[10,20,21,24]. Recent data in mouse models show that stress is a potent inducer of TF expression in mouse models of aging and obesity[25]. This suggests that during normal, physiologic aging and chronic pathologic conditions where individuals are more susceptible to stress, elevated TF may interact with FVII, thus making elevated FVII an important risk factor for VTE.

The zymogen FIX, a member of the TENase complex with cofactor FVIII, also undergoes an age-depended increase[26]. Given its importance in the activation of FX to

subsequently enable the generation of thrombin, elevated FIX levels are thought to be a risk factor for VTE. Data from the LETS study concluded that those with FIX levels above the 90th percentile had an odds ratio of 2.3 and were at elevated risk of VTE[27].

Other coagulation proteins known to increase with age include high molecular weight kininogen, prekallikrein and thrombin activatable fibrinolysis inhibitor (TAFI); however, these increases are not thought to significantly elevate the risk of VTE.

It is important to note that while procoagulant markers do increase with age, this may not always correlate with the risk cardiovascular disease. Multiple studies have reported increases in coagulation factors in healthy, elderly individuals who do not suffer from arterial or venous diseases[10,28,29]. These studies suggest that elevated procoagulant proteins may be a better marker of aging than of cardiovascular disease risk.

1.4 Age-related changes in anticoagulant factors.

Very little data exists in the literature to suggest that levels of natural anticoagulants diminish with age as a means of explaining the increased risk of VTE. In fact, particularly in women, levels of certain anticoagulants such as protein C, protein S and antithrombin (AT) reportedly increase with age[30], most commonly during menopause[31]. Levels of these same anticoagulants remained unchanged in aging men. Similarly, age-related increases in tissue factor pathway inhibitor (TFPI), the primary inhibitor of TF initiated coagulation, have been observed in both men and women[10,30,32].

Conversely, there is a growing body of evidence in mouse models to suggest that aging is associated with a reduction in endothelial-bound levels of anticoagulant TM[33,34]. A decrease

in available TM to bind thrombin would result in diminished APC generation. However, this data has yet to be confirmed in humans.

Given the above data, it appears that while changes in levels of natural anticoagulants with age alone do not contribute to the risk of VTE, the combination of increased procoagulants in the absence of concomitant increases in anticoagulants may predispose elderly individuals to venous and arterial disease.

1.5 Age-related changes in plasminogen activation.

The plasminogen activation system is the primary pathway regulating fibrinolysis. Well-documented age-related alterations to this pathway that result in impaired thrombus resolution have been reported. Plasminogen activator inhibitor (PAI-1) is an important inhibitor of fibrinolysis and elevated levels of this protein have been reported in aging and a variety of other disease states[9,31]. Data from the Framingham cohort found that PAI-1 antigen levels in plasma went from 19.4 ng/mL in men under 40 years old to 24.6 ng/mL in those 70 years and above, with similar increases found in women[9]. PAI-1 itself is cardioprotective and is thought to maintain vascular integrity, as evidenced by data in PAI-1 deficient mice which show increased cardiac fibrosis likely as a result of increased inflammation and endothelial leakage[35,36]. However, in humans, elevated PAI-1 levels are positively correlated with the risk of thrombotic events[37,38]. Plasma levels of tissue plasminogen activator (tPA) are also elevated with age[9,31,39]. The mechanism behind concurrent increases in both tPA and PAI-1 in elderly individuals are not known. Additionally, although levels of circulating plasminogen were found to decrease only slightly in women with age[40], levels of plasmin-α_2-antiplasmin (PAP) complex increase[41] with age.

The SERPIN α2-antiplasmin is an important inhibitor that inactivates plasmin, thus is an inhibitor of fibrinolysis. Collectively, the combined increases in fibrinolysis inhibitors PAI-1 and α2-antiplasmin even with concomitant increases in tPA could predispose elderly individuals to impaired thrombus resolution

1.6 Effect of age on platelet function.

Platelets are key mediators of primary hemostasis in that they are crucial in stopping early bleeding and provide a lipid-rich surface for the generation of coagulation proteases. Patients with low platelet counts (thrombocytopenia) as a result of infection, malnutrition, cancer, or genetics suffer symptoms ranging from minor fatigue to severe bleeding. Interestingly, aging in humans is associated with a decrease in circulating platelet counts[42-44], with an estimated decrease of 6 x 10^9/L for every 10 years of age[43]. It remains unclear whether this decrease in platelet counts is due to reduced hematopoiesis, decreased production from megakaryocytes or increased clearance by the speen.

Despite the reduction in platelet number, aging is associated with differences in platelet function. While there is very little current data in this area, historical data has given insight into how platelet biology changes with age. Increased platelet aggregation in response to ADP, collagen, and adrenaline has been observed in platelets from aged individuals, in addition to increased ATP release upon collagen stimulation[45,46]. Platelets from older individuals also display reduced ADP thresholds for aggregation compared to those from the young, further suggesting they are more sensitive to certain agonists[47]. It is thought that this hyperreactivity is due to increased platelet expression of receptors for these agonists[48,49]. Also, platelets from the elderly produce more thromboxane A2 which is involved in platelet

activation and formation of platelet aggregates[50]. This could have clinical implications for treating elderly patients with antiplatelet agents such as clopidogrel, an inhibitor of the platelet $P2Y_{12}$ receptor for ADP. A recent study found that the linear age-related increase in ADP-induced platelet aggregation was associated with reduced sensitivity to initial clopidogrel[51].

Aside from biological changes that occur with age in platelets themselves, age-associated changes in endothelial function could also promote platelet hyperreactivity. These include increased endothelial production of vWF, which could result in enhanced platelet tethering to endothelial cell surfaces[52]. Also, decreased production of endothelial nitric oxide synthase (eNOS) results in dowregulation of nitric oxide (NO) generation. NO is a potent inhibitor of platelet activation[53,54]. Decreased levels of this important inhibitor could result in dysregulation of platelet activation and the inappropriate release of procoagulant material from platelet granules.

1.7 Effect of aging on the vascular endothelium.

Understanding the interplay between the components of Virchow's triad is necessary to effectively diagnose and treat bleeding and thrombotic disorders. Increasing awareness of the complexities of these presentations, along with increasingly sophisticated technologies to analyze soluble, cellular, and physical dysfunctions in concert will shed new light on these pathologies and identify novel therapeutic targets. With such targets, we can achieve the The vascular endothelium plays an important role in regulating blood coagulation through its anticoagulant properties. These include production of the thrombin inhibitors TM, EPCR, heparan and dermatan sulfate, creating a physical barrier to block exposure of sub-

endothelial tissue factor from flowing blood, release of tissue factor pathway inhibitor (TFPI) to inhibit TF activity, and initiating fibrinolysis through release of plasminogen activators.

Endothelial dysfunction is a widely accepted consequence of aging and can turn the naturally anticoagulant endothelial cell surface into one that is more procoagulant. Many age-related changes have been reported to occur in the vascular endothelium, one of which is increased vascular permeability. The loss of cell-cell junctions with age results in vascular leakage, exposure of subendotheial proteins (i.e. TF), and leukocyte adhesion[55]. Aged endothelial cells also produce more anti-fibrinolytic PAI-1[56] and, in animal models, less anticoagulant TM upon treatment with endotoxin[34]. There is also increased production and secretion of pro-inflammatory cytokines interleukin-6 (IL-6) and interleukin-1β (IL-1β) from aged endothelium, promoting recruitment and binding of leukocytes to the cell surface[57]. Aging is also associated with a loss of eNOS production, resulting is reduced availability of NO to regulate vessel dilation and platelet activation[53,54].

1.8 Vascular inflammation and age.

The relationship between aging and chronic inflammation is well recognized, yet poorly understood. Similarly, the relationship between inflammation and aging is not fully apparent, however it is widely studied. Many of the procoagulant and antifibrinolytic proteins that increase with age are, in fact, acute phase reactants (i.e. fibrinogen, FVIII, and PAI-1) that are sensitive to and regulated by inflammatory cytokines. These cytokines also have a profound effect on vascular endothelial cells. In cell culture, stimulation with TNF-α results in the increased production of TF and PAI-1 and decreased production of TM by endothelial cells[58]. *In vitro*, endothelial cells will only contribute to thrombin generation on

their cell surface after such stimulation[59]. Circulating plasma levels of TNF-α reportedly increase with age[60,61], and, given its importance *in vitro*, this inflammatory cytokine could regulate thrombin generation *in vivo* by increasing endothelial procoagulant and decreasing protein production in endothelial cells.

IL-6 is another inflammatory cytokine that increases in an age-dependent manner[62]. IL-6 is capable of both pro and anti-inflammatory functions, limiting its own production and inhibiting other cytokines. IL-6 is also involved in acute phase responses to infection and trauma; it can stimulate the production of neutrophils from the bone marrow and promote the synthesis of C-reactive protein (CRP) by hepatocytes. CRP itself is proinflammatory and is used as a marker of inflammation. Increased CRP levels are predictive of cardiovascular disease and have recently been shown in a transgenic rabbit model to enhance thrombus formation after neointimal injury[63]. Cytokine expression may also promote TF release by circulating monocytes and recruit leukocytes to endothelial cells surfaces. Monocyte chemotactic protein-1 (MCP-1) is a chemokine produced by endothelial cells, monocytes and macrophages. The recruitment of leukocytes to dysfunctional endothelium may lead to propagation of cytokine release by these leukocytes and promote coagulation, as expression of MCP-1 and IL-6 are both risk factors for recurrent VTE[64]. Giving credence to the importance of inflammation in promoting VTE, data from the JUPITER study suggests patients on statins have reduced inflammation and a lower risk of VTE[65].

1.9 Immobility with age.

Venous thrombi are most likely to develop within a valve pocket where blood can form eddies or circular flow patterns, suggesting that irregular blood flow is a risk factor for

thrombosis. Immobility reduces the rate of blood flow leading to the stagnation of blood, referred to as stasis. Stasis not only causes the pooling of blood and procoagulant materials in large veins, but also reduces the ability of the blood to circulate through the microvasculature where contact with anticoagulants is highest[66]. Elderly individuals are at increased risk of immobility, and therefore stasis, due to an age-related reduction in activity and increased susceptibility to frailty and infection[4].

1.10 Conclusions.

The increased risk of VTE with age can be due to a variety of alterations in the hemostatic system. VTE itself is a multifaceted disease, triggered by a complex interplay of risk factors. We can expect the healthcare burden associated with VTE to increase exponentially as the population ages. More research in this field is critical for further defining and understanding how physiologic aging affect coagulation in the venous circulation.

1.11 References

1. Branchford BR, Mourani P, Bajaj L, et al. Risk factors for in-hospital venous thromboembolism in children: a case-control study employing diagnostic validation. *Haematologica*. 2012;97(4):509-515.

2. Galson S. The Surgeon Generals Call to Action to Prevent Deep Vein Thrombosis and Pulmonary Embolism. Available at: http://www.surgeongeneral.gov/topics/deepvein/calltoaction/call-to-action-on-dvt-2008.pdf. Accessed April 20, 2012.

3. Wong P, Baglin T. Epidemiology, risk factors and sequelae of venous thromboembolism. *Phlebology*. 2012;27 Suppl 2:2-11.

4. Silverstein RL, Bauer KA, Cushman M, et al. Venous thrombosis in the elderly: more questions than answers. *Blood*. 2007;110(9):3097-3101.

5. Spyropoulos AC, Hurley JS, Ciesla GN, de Lissovoy G. Management of acute proximal deep vein thrombosis: pharmacoeconomic evaluation of outpatient treatment with enoxaparin vs inpatient treatment with unfractionated heparin. *Chest*. 2002;122(1):108-114.

6. Wilkerson WR, Sane DC. Aging and thrombosis. *Semin. Thromb. Hemost*. 2002;28(6):555-568.

7. Franchini M. Hemostasis and aging. *Crit. Rev. Oncol. Hematol*. 2006;60(2):144-151.

8. Engbers MJ, van Hylckama Vlieg A, Rosendaal FR. Venous thrombosis in the elderly: incidence, risk factors and risk groups. *J. Thromb. Haemost*. 2010;8(10):2105-2112.

9. Tofler GH, Massaro J, Levy D, et al. Relation of the prothrombotic state to increasing age (from the Framingham Offspring Study). *Am. J. Cardiol*. 2005;96(9):1280-1283.

10. Mari D, Coppola R, Provenzano R. Hemostasis factors and aging. *Exp. Gerontol*. 2008;43(2):66-73.

11. Meade TW, North WR, Chakrabarti R, Haines AP, Stirling Y. Population-based distributions of haemostatic variables. *Br. Med. Bull*. 1977;33(3):283-288.

12. Koster T, Blann AD, Briët E, Vandenbroucke JP, Rosendaal FR. Role of clotting factor VIII in effect of von Willebrand factor on occurrence of deep-vein thrombosis. *Lancet*. 1995;345(8943):152-155.

13. van Hylckama Vlieg A, Rosendaal FR. High levels of fibrinogen are associated with the risk of deep venous thrombosis mainly in the elderly. *J. Thromb. Haemost*. 2003;1(12):2677-2678.

14. Machlus KR, Cardenas JC, Church FC, Wolberg AS. Causal relationship between hyperfibrinogenemia, thrombosis, and resistance to thrombolysis in mice. *Blood*. 2011;117(18):4953-4963.

15. Conlan MG, Folsom AR, Finch A, et al. Associations of factor VIII and von Willebrand factor with age, race, sex, and risk factors for atherosclerosis. The Atherosclerosis Risk in Communities (ARIC) Study. *Thromb. Haemost*. 1993;70(3):380-385.

16. Jeremic M, Weisert O, Gedde-Dahl TW. Factor VIII (AHG) levels in 1016 regular blood donors. The effects of age, sex, and ABO blood groups. *Scand. J. Clin. Lab. Invest*. 1976;36(5):461-466.

17. Tracy RP, Bovill EG, Yanez D, et al. Fibrinogen and factor VIII, but not factor VII, are associated with measures of subclinical cardiovascular disease in the elderly. Results from The Cardiovascular Health Study. *Arterioscler. Thromb. Vasc. Biol*. 1995;15(9):1269-1279.

18. Machlus KR, Lin F, Wolberg AS. Procoagulant activity induced by vascular injury determines contribution of elevated factor VIII to thrombosis and thrombus stability in mice. *Blood*. 2011;118(14):3960-3968.

19. Kyrle PA, Minar E, Hirschl M, et al. High plasma levels of factor VIII and the risk of recurrent venous thromboembolism. *N. Engl. J. Med*. 2000;343(7):457-462.

20. Koster T, Rosendaal FR, Reitsma PH, et al. Factor VII and fibrinogen levels as risk factors for venous thrombosis. A case-control study of plasma levels and DNA polymorphisms--the Leiden Thrombophilia Study (LETS). *Thromb. Haemost*. 1994;71(6):719-722.

21. Tsai AW, Cushman M, Rosamond WD, et al. Coagulation factors, inflammation markers, and venous thromboembolism: the longitudinal investigation of thromboembolism etiology (LITE). *Am. J. Med*. 2002;113(8):636-642.

22. Chauhan AK, Kisucka J, Lamb CB, Bergmeier W, Wagner DD. von Willebrand factor and factor VIII are independently required to form stable occlusive thrombi in injured veins. *Blood*. 2007;109(6):2424-2429.

23. Balleisen L, Bailey J, Epping PH, Schulte H, van de Loo J. Epidemiological study on factor VII, factor VIII and fibrinogen in an industrial population: I. Baseline data on the relation to age, gender, body-weight, smoking, alcohol, pill-using, and menopause. *Thromb. Haemost*. 1985;54(2):475-479.

24. Lowe G, Woodward M, Vessey M, et al. Thrombotic variables and risk of idiopathic venous thromboembolism in women aged 45-64 years. Relationships to hormone replacement therapy. *Thromb. Haemost*. 2000;83(4):530-535.

25. Yamamoto K, Shimokawa T, Yi H, et al. Aging and obesity augment the stress-induced

expression of tissue factor gene in the mouse. *Blood*. 2002;100(12):4011-4018.

26. Sweeney JD, Hoernig LA. Age-dependent effect on the level of factor IX. *Am. J. Clin. Pathol*. 1993;99(6):687-688.

27. van Hylckama Vlieg A, van der Linden IK, Bertina RM, Rosendaal FR. High levels of factor IX increase the risk of venous thrombosis. *Blood*. 2000;95(12):3678-3682.

28. Deguchi K, Deguchi A, Wada H, Murashima S. Study of cardiovascular risk factors and hemostatic molecular markers in elderly persons. *Semin. Thromb. Hemost*. 2000;26(1):23-27.

29. Scarabin PY, Aillaud MF, Amouyel P, et al. Associations of fibrinogen, factor VII and PAI-1 with baseline findings among 10,500 male participants in a prospective study of myocardial infarction--the PRIME Study. Prospective Epidemiological Study of Myocardial Infarction. *Thromb. Haemost*. 1998;80(5):749-756.

30. Sagripanti A, Carpi A. Natural anticoagulants, aging, and thromboembolism. *Exp. Gerontol*. 1998;33(7-8):891-896.

31. Abbate R, Prisco D, Rostagno C, Boddi M, Gensini GF. Age-related changes in the hemostatic system. *Int. J. Clin. Lab. Res*. 1993;23(1):1-3.

32. Ariëns RA, Coppola R, Potenza I, Mannucci PM. The increase with age of the components of the tissue factor coagulation pathway is gender-dependent. *Blood Coagul. Fibrinolysis*. 1995;6(5):433-437.

33. Hemmeryckx B, Emmerechts J, Bovill EG, Hoylaerts MF, Lijnen HR. Effect of ageing on the murine venous circulation. *Histochem. Cell Biol*. 2012;137(4):537-546.

34. Starr ME, Ueda J, Takahashi H, et al. Age-dependent vulnerability to endotoxemia is associated with reduction of anticoagulant factors activated protein C and thrombomodulin. *Blood*. 2010;115(23):4886-4893.

35. Xu Z, Castellino FJ, Ploplis VA. Plasminogen activator inhibitor-1 (PAI-1) is cardioprotective in mice by maintaining microvascular integrity and cardiac architecture. *Blood*. 2010;115(10):2038-2047.

36. Ghosh AK, Bradham WS, Gleaves LA, et al. Genetic deficiency of plasminogen activator inhibitor-1 promotes cardiac fibrosis in aged mice: involvement of constitutive transforming growth factor-beta signaling and endothelial-to-mesenchymal transition. *Circulation*. 2010;122(12):1200-1209.

37. Prisco D, Chiarantini E, Boddi M, et al. Predictive value for thrombotic disease of plasminogen activator inhibitor-1 plasma levels. *Int. J. Clin. Lab. Res*. 1993;23(2):78-82.

38. Hamsten A, de Faire U, Walldius G, et al. Plasminogen activator inhibitor in plasma: risk

factor for recurrent myocardial infarction. *Lancet*. 1987;2(8549):3-9.

39. Stegnar M, Pentek M. Fibrinolytic response to venous occlusion in healthy subjects: relationship to age, gender, body weight, blood lipids and insulin. *Thromb. Res*. 1993;69(1):81-92.

40. Bucciarelli P, Mannucci PM. The hemostatic system through aging and menopause. *Climacteric*. 2009;12 Suppl 1:47-51.

41. Morange PE, Bickel C, Nicaud V, et al. Haemostatic factors and the risk of cardiovascular death in patients with coronary artery disease: the AtheroGene study. *Arterioscler. Thromb. Vasc. Biol*. 2006;26(12):2793-2799.

42. Daly ME. Determinants of platelet count in humans. *Haematologica*. 2011;96(1):10-13.

43. Biino G, Gasparini P, D'Adamo P, et al. Influence of age, sex and ethnicity on platelet count in five Italian geographic isolates: mild thrombocytopenia may be physiological. *Br J Haematol*. 2012;157(3):384-387.

44. Segal JB, Moliterno AR. Platelet counts differ by sex, ethnicity, and age in the United States. *Ann Epidemiol*. 2006;16(2):123-130.

45. Kasjanovová D, Baláz V. Age-related changes in human platelet function in vitro. *Mech. Ageing Dev*. 1986;37(2):175-182.

46. Vilén L, Jacobsson S, Wadenvik H, Kutti J. ADP-induced platelet aggregation as a function of age in healthy humans. *Thromb. Haemost*. 1989;61(3):490-492.

47. Gleerup G, Winther K. The effect of ageing on platelet function and fibrinolytic activity. *Angiology*. 1995;46(8):715-718.

48. Winther K, Naesh O. Aging and platelet beta-adrenoceptor function. *Eur. J. Pharmacol*. 1987;136(2):219-223.

49. Yokoyama M, Kusui A, Sakamoto S, Fukuzaki H. Age-associated increments in human platelet alpha-adrenoceptor capacity. Possible mechanism for platelet hyperactivity to epinephrine in aging man. *Thromb. Res*. 1984;34(4):287-295.

50. Suehiro A, Uedaa M, Suehiroh M, Ohe Y, Kakishitaa E. Evaluation of platelet hyperfunction in aged subjects using spontaneous platelet aggregation in whole blood. *Arch Gerontol Geriatr*. 1995;21(3):277-283.

51. Gremmel T, Steiner S, Seidinger D, et al. Adenosine diphosphate-inducible platelet reactivity shows a pronounced age dependency in the initial phase of antiplatelet therapy with clopidogrel. *J. Thromb. Haemost*. 2010;8(1):37-42.

52. Müller AM, Skrzynski C, Nesslinger M, Skipka G, Müller K. Correlation of age with in vivo expression of endothelial markers. *Exp. Gerontol*. 2002;37(5):713-719.

53. Matsushita H, Chang E, Glassford AJ, et al. eNOS activity is reduced in senescent human endothelial cells: Preservation by hTERT immortalization. *Circ. Res*. 2001;89(9):793-798.

54. Yoon HJ, Cho SW, Ahn BW, Yang SY. Alterations in the activity and expression of endothelial NO synthase in aged human endothelial cells. *Mech. Ageing Dev*. 2010;131(2):119-123.

55. Lum H, Roebuck KA. Oxidant stress and endothelial cell dysfunction. *Am. J. Physiol., Cell Physiol*. 2001;280(4):C719-741.

56. Comi P, Chiaramonte R, Maier JA. Senescence-dependent regulation of type 1 plasminogen activator inhibitor in human vascular endothelial cells. *Exp. Cell Res*. 1995;219(1):304-308.

57. Csiszar A, Ungvari Z, Koller A, Edwards JG, Kaley G. Aging-induced proinflammatory shift in cytokine expression profile in coronary arteries. *FASEB J*. 2003;17(9):1183-1185.

58. Scarpati EM, Sadler JE. Regulation of endothelial cell coagulant properties. Modulation of tissue factor, plasminogen activator inhibitors, and thrombomodulin by phorbol 12-myristate 13-acetate and tumor necrosis factor. *J. Biol. Chem*. 1989;264(34):20705-20713.

59. Campbell RA, Overmyer KA, Selzman CH, Sheridan BC, Wolberg AS. Contributions of extravascular and intravascular cells to fibrin network formation, structure, and stability. *Blood*. 2009;114(23):4886-4896.

60. Paolisso G, Rizzo MR, Mazziotti G, et al. Advancing age and insulin resistance: role of plasma tumor necrosis factor-alpha. *Am. J. Physiol*. 1998;275(2 Pt 1):E294-299.

61. Bruunsgaard H, Andersen-Ranberg K, Jeune B, et al. A high plasma concentration of TNF-alpha is associated with dementia in centenarians. *J. Gerontol. A Biol. Sci. Med. Sci*. 1999;54(7):M357-364.

62. Wei J, Xu H, Davies JL, Hemmings GP. Increase of plasma IL-6 concentration with age in healthy subjects. *Life Sci*. 1992;51(25):1953-1956.

63. Matsuda S, Yamashita A, Sato Y, et al. Human C-reactive protein enhances thrombus formation after neointimal balloon injury in transgenic rabbits. *J. Thromb. Haemost*. 2011;9(1):201-208.

64. van Aken BE, den Heijer M, Bos GM, van Deventer SJ, Reitsma PH. Recurrent venous thrombosis and markers of inflammation. *Thromb. Haemost*. 2000;83(4):536-539.

65. Perez A, Bartholomew JR. Interpreting the JUPITER trial: statins can prevent VTE, but

more study is needed. *Cleve Clin J Med*. 2010;77(3):191-194.

66. Esmon CT. Basic mechanisms and pathogenesis of venous thrombosis. *Blood Rev*. 2009;23(5):225-229.

Chapter 2

Introduction

The Role of $p16^{INK4a}$ Expression in Aging and Cardiovascular Disease

2.1 Introduction.

The gene products encoded by the *INK4b-ARF-INK4a* locus play a critical role in regulating cell cycle progression and are thus important for inhibiting malignant transformation[1,2]. Of the two cyclin-dependent kinase inhibitors encoded on this locus, expression of $p16^{INK4a}$ increases in an age-dependent manner. A known biomarker of human and murine aging[3,4], the contribution of $p16^{INK4a}$ to age-related diseases is the focus of many recent reports. Genome-wide association studies suggest $p16^{INK4a}$ plays a protect role in many cardiovascular diseases affecting the arteries, likely through its anti-proliferative function[5,6]. Conversely, $p16^{INK4a}$ expression may contribute to diseases of the venous circulation by promoting endothelial dysfunction upon induction of senescence in the vasculature[7-9]. This review focuses on the structure, function, and regulation of the *INK4b-ARF-INK4a* locus and recent publications that offer insight into how $p16^{INK4a}$ may promote or protect from age-related pathologies.

2.2 *INK4b-ARF-INK4a* structure and function.

The *INK4b-ARF-INK4a* locus, located on chromosome 9p21, is approximately 35kb in length and encodes for three proteins critical in regulating cellular proliferation. Two of

these proteins are the cyclin-dependent kinase inhibitors $p15^{INK4b}$ and $p16^{INK4a}$ while the third, $p14^{ARF}$ (ARF), is involved in stabilizing p53[1,2]. In terms of genomic structure, $p15^{INK4b}$ lies upstream of $p16^{INK4a}$ and ARF, and utilizes its own coding region. Downstream of $p15^{INK4b}$ lies the shared coding region for $p16^{INK4a}$ and ARF. This region contains two alternatively spliced first exons: exon 1α and exon 1β, each containing their own promoter. In the case of ARF, exon 1α is spliced to exons 2 and 3 to produce the ARF transcript. In the case of $p16^{INK4a}$, exon 1β is spliced to exons 2 and 3, producing the $p16^{INK4a}$ transcript. Together, these genes are referred to as *CDKN2A* (Figure 2.1)[1,2]. Interestingly, the *INK4b-ARF-INK4a* locus also encodes a non-coding RNA called antisense non-coding RNA in the INK4 locus (ANRIL) (Figure 2.1). Although its function is not yet fully understood, it likely plays an important role in regulating gene expression from this locus[1,2,10].

Functionally, both $p15^{INK4b}$ and $p16^{INK4a}$ are cyclin-dependent kinase (CDK) inhibitors. They bind to CDK4 and CDK6 causing an allosteric conformational change, disrupting the ability of these CDKs to bind to D-type cyclins. In cycling cells, CDK/cyclin complexes regulate the cell cycle through interaction with the retinoblastoma protein (Rb)[1,2,11]. Unmodified, Rb is bound to the transcription factor, E2F, which remains inactive while bound to Rb. Upon phosphorylation of Rb by the CDK/cyclin complex during cell cycle progression, Rb dissociates from E2F which can now bind to DNA and initiate transcription of genes involved in promoting cell cycle progression (Figure 2.2). Therefore, $p15^{INK4b}$ and $p16^{INK4a}$ inhibit cell cycle progression by blocking the phosphorylation of Rb by CDK/cyclin complexes, causing cell cycle arrest in G1 phase[1,2,11].

The ARF gene product can also regulate cell cycle progression or induce apoptosis through its effects on p53. ARF interacts with MDM2, an inhibitor of p53 transcriptional

activation and therefore negative regulator of p53 activity. ARF binds to MDM2 and keeps it sequestered in the nucleolus, making MDM2 unable to inhibit p53-mediated transcription. This, in turn leads to activation of p53 and either apoptosis or cell cycle arrest through upregulation of p21, a CDK4 and CDK2 inhibitors[1,2,12-14].

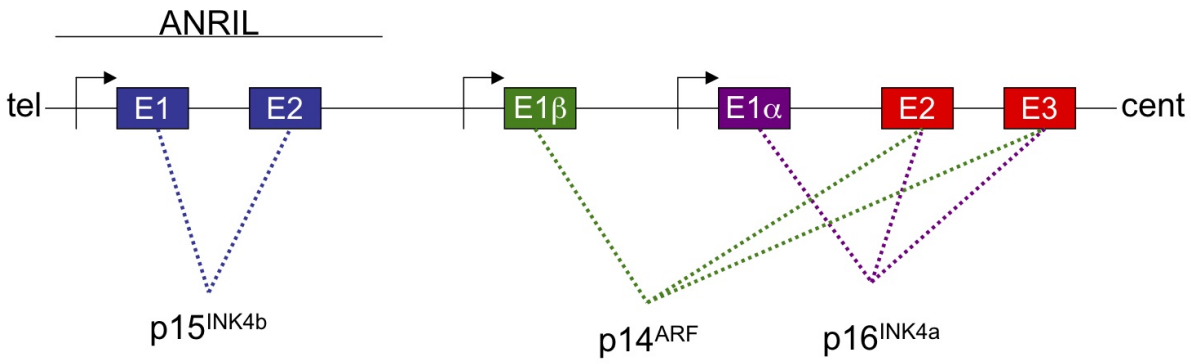

Figure 2.1. Genomic structure of the *INK4b-ARF-INK4a* gene locus. Exons are color coded to represent the gene product they are spliced into. Arrows represent promoters and direction of transcription. ANRIL is encoded on the *INK4a-ARF* locus although the exact position is not known. Schematic is not drawn to scale and positions are approximate.

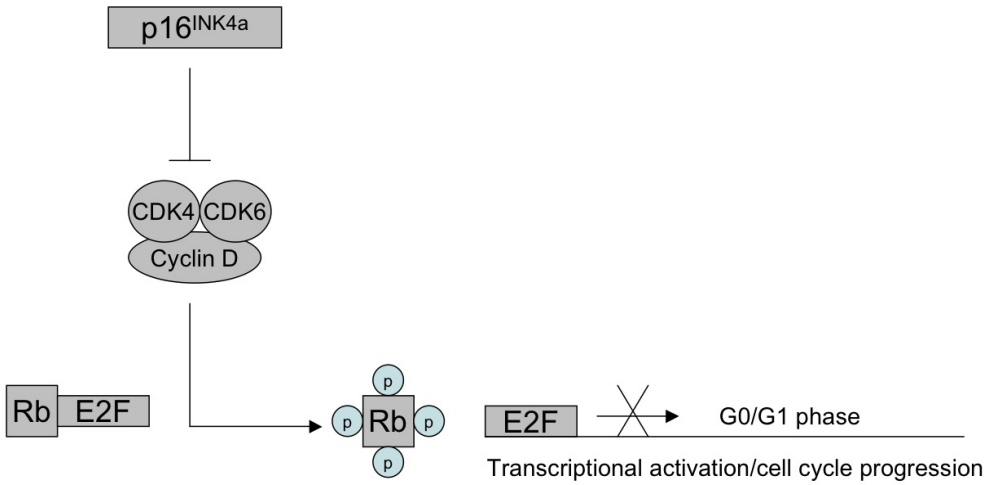

Figure 2.2. Mechanism by which p16^{INK4a} regulates cell cycle progression through hypophosphorylation of Rb. p16^{INK4a} binds to CDK4 and 6 to disable interaction of D-type cyclins. This maintains Rb in a hypophosphorylated state with E2F repressionally bound and thus inhibiting cell cycle progression and arrest in G0/G1 phase.

2.3 *INK4b-ARF-INK4a* regulation.

The INK4b-ARF-INK4a locus encodes proteins which perform important tumor suppressor functions; most notably $p16^{INK4a}$. Loss of $p16^{INK4a}$, in the absence of inactivation of $p15^{INK4b}$ or ARF, is observed in several human cancers[15-18]. $p16^{INK4a}$ is activated in response to oncogenic signaling (i.e. RAS or RAF) or aberrant cellular proliferation and functionally inhibits tumor progression through negative regulation of the cell cycle[1,19,20]. $p16^{INK4a}$ is also activated during normal physiologic aging. This is likely in response to the accumulation of low-level oncogenic signals and cellular stresses over time and evolved as a mechanism to prevent, or as a pre-emptive strike against malignant transformation[21,22].

Conversely, several negative regulators repress $p16^{INK4a}$ expression. Among these is the DNA-binding protein ID-1. ID-1 binds to and inhibits Ets-2, a transcription factor that activates the $p16^{INK4a}$ promoter, thus downregulating $p16^{INK4a}$ transcription[23]. Additionally, $p16^{INK4a}$ and other parts of the *INK4b-ARF-INK4a* locus are repressed through negative regulation by Polycomb group (PcG) proteins. Members of the PcG work cooperatively to form Polycomb repressive complex (PRC) 1 and 2, which functions by ubiquitinylation of histone H2A and methylation of histone H3 followed by transcriptional shut down of the epigenetically tagged chromatin. A critical member of the PRC1 complex is Bmi-1, the only known PcG protein involved in repressing all three products of the *INK4b-ARF-INK4b* locus. Bmi-1 is involved in stabilizing the PRC1 complex[24,25]. Although the mechanism is not completely understood, knocking down Bmi-1 in cell culture results in premature senescence and increased proteins levels of $p15^{INK4b}$, $p16^{INK4a}$ and ARF[26]. It is also thought that ANRIL, the non-coding RNA present on the *CDKN2A* locus, is also a negative regulator of $p16^{INK4a}$ expression. ANRIL recruits PRCs to the coding region on this locus, thus inducing

transcription repression of $p16^{INK4a}$ [25]. Thus a reduction in ANRIL expression is associated with increased $p16^{INK4a}$ expression[27].

2.4 Role of *INK4b-ARF-INK4a* in cellular senescence.

Cellular senescence is an irreversible growth arrest or terminal differentiation induced by a variety of stimuli. There are two broad categories of cellular senescence: replicative and stress-induced senescence[28]. Replicative senescence results from telomere attrition. Telomeres are nucleotide repeat 'caps' present at the chromosome ends and protect the last gene on the chromosome arm from deteriorating upon multiple divisions. Inevitably, chromosomes shorten after each mitotic event due to the inability to copy the farthest ends of the DNA strand, called the "end-replication problem". A cell can only divide as many times as the telomeres will still be present to protect the coding regions. This number is called the Hayflick Limit, or the number of times a cell can divide before sensing telomore attrition, triggering a DNA damage response and undergoing senescence in response to p53 signaling[28-31,7]. Interestingly, $p16^{INK4a}$ accumulates in fibroblasts with shortening telomeres, suggesting it may also play a role in promoting replicative senescence[32].

Alternatively, a cell can undergo senescence prior to reaching this limit and independent of telomere length in response to oncogenic or other environmental stresses. This is called stress-induced senescence and is mediated by CDK inhibitors to promote cell cycle arrest[28,31]. While each product of the *INK4b-ARF-INK4a* locus causes an irreversible cell cycle arrest, the most important effector of senescence in human cells is $p16^{INK4a}$. Studies have shown that activation of the Ras/Raf/Mek oncogenic pathway leads to constitutive activation of the Ets1/2 transcription factor promoting $p16^{INK4a}$ expression and subsequent

down-regulation of the Ets1/2 inhibitor, Id-1[30]. In addition to oncogene expression, stress-induced senescence can be induced by reactive oxygen species, ionizing radiation, inflammation and a variety of other environmental pressures that could promote malignant transformation[7]. Although the mechanisms driving stress-induced senescence are not entirely understood, induction of $p16^{INK4a}$ and hypophosphorylation of Rb are commonly observed upon treatment of fibroblasts and endothelial cells with these environmental stressors[33].

2.5 Role of $p16^{INK4a}$ in aging.

There are 4 members of the INK4 class of CDK inhibitors. Two of them, $p18^{INK4c}$ and $p19^{INK4d}$, are highly expressed during development. However, both $p15^{INK4b}$ and $p16^{INK4a}$ are undetectable during early life, suggesting they likely have no role in fetal development and rather function solely as tumor suppressors in adult tissues[2,34]. As previously mentioned, $p16^{INK4a}$ expression increases during normal, physiologic aging in many different tissues. In fact, $p16^{INK4a}$ has recently been proposed as a biomarker of physiologic, as opposed to chronologic, aging[3]. How $p16^{INK4a}$ is regulated during aging, what signals promote age-dependent expression and whether $p16^{INK4a}$ plays a causative role in aging or is just a marker of aging have not been fully elucidated.

Our body relies on self-renewing cell compartments to replace damaged or healing tissue throughout a lifetime of "wear and tear". Stem cells exist normally in a quiescent state, but can be prompted to proliferate in response to the need to repopulate damaged tissue[35,36]. While most mature organs utilize non-self renewing strategies to replace damaged or dead cells, self-renewing stem cells exists in certain "high-turnover" organ compartments like the

bone marrow or intestines to provide undifferentiated, multipotent daughter cells with the same renewing potential as the parent cell[36]. The clinical observation that donor age is an important determinant of successful long-term transplantation of certain organs such as bone marrow would suggest that self-renewing stem cells do age, and become functionally limited as they age[36,37]. It was recently shown that $p16^{INK4a}$ expression increases in an age-dependent manner in peripheral blood leukocytes, a cell type that originates in the hematopoietic compartment[4]. Additionally, Krishnamurthy et al demonstrated that aged, $p16^{INK4a}$ deficient mice display enhanced islet cell proliferation following streptozotocin treatment compared to age-matched wild-type controls. Conversely, $p16^{INK4a}$ transgenic mice display reduced islet cell proliferation following the same cellular ablation, suggesting that $p16^{INK4a}$ expression in certain cell compartments contributes to the age-related decline in proliferation and tissue repair[38]. These data suggest that $p16^{INK4a}$ is not only a biomarker of aging, but also contributes to organismal aging by limiting the capacity for cellular self-renewal.

Expression of $p16^{INK4a}$ as a biomarker of aging is not only true in humans, but rodents as well, as established by Krishnamurthy *et al*[3] and also tested in our lab (Figure 2.3). In mice, the *CDKN2A* locus is present on chromosome 4. It shares a high level of sequence homology with humans and although the ARF gene product is slightly smaller than in humans (thus called $p14^{ARF}$ rather than $p19^{ARF}$), the $p16^{INK4a}$ proteins are orthologous between mice and humans[39]. Therefore, mice are a useful tool for studying $p16^{INK4a}$ expression during aging.

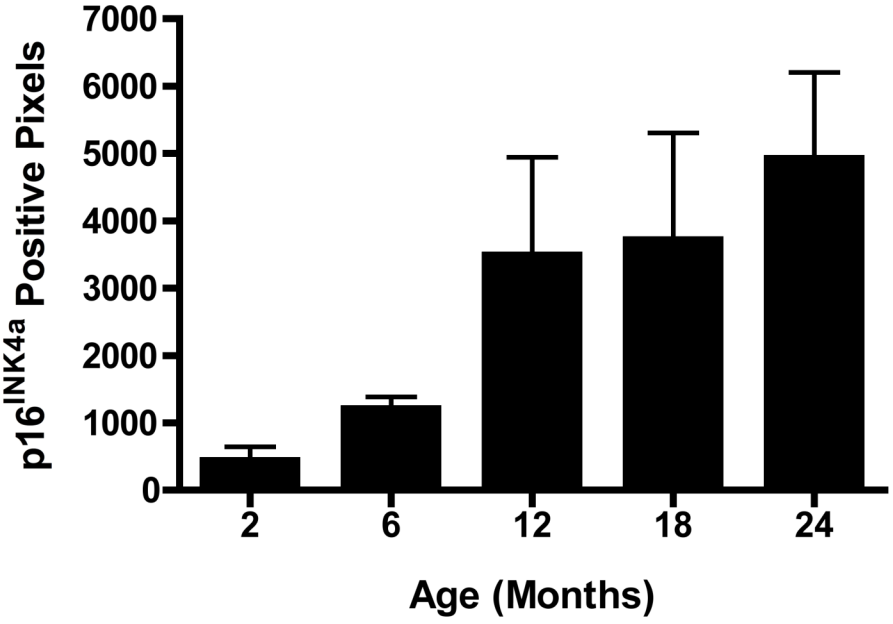

Figure 2.3: Expression of p16^{INK4a} in mouse kidneys with age. Expression of p16^{INK4a} in the kidneys of mice aged 2-24 months was measured by immunhistochemistry. Quantification was performed in Adobe Photoshop to count the number of positively stained pixels.

2.6 Role of Role of $p16^{INK4a}$ in cardiovascular disease.

While there is no doubt that $p16^{INK4a}$ plays an absolutely pivotal role in preventing tumorigenesis, the role of $p16^{INK4a}$ in age-related diseases is less well understood. A series of recent studies have identified several single nucleotide polymorphisms (SNPs) clustered around the *INK4b-ARF-INK4a* locus that are associated with Alzheimer's disease, type 2 diabetes, frailty, and coronary artery disease[1,40-44].

Age is one of the greatest risk factors for cardiovascular disease. How the *CDKN2A* locus may contribute to cardiovascular disease has recently been widely explored. Given its physiologic function as a cell cycle inhibitor, a role for $p16^{INK4a}$ expression in protecting against cardiovascular diseases associated with aberrant cellular proliferation, such as atherosclerosis, would seem intuitive. However, studies looking at the effect of $p16^{INK4a}$ on atherosclerosis have not had totally uniform findings.

The chromosome 9p21 locus was first identified in a large genome-wide association study (GWAS) looking for genetic variants associated with coronary artery disease (CAD)[45]. A common risk allele was discovered with several SNPs mapping to a narrow DNA sequence on this locus. Positioned only a short distance away are the *CDKN2B* and *CDKN2A* loci, the closest coding regions to the CAD risk segment[45,5]. Several groups have independently confirmed this finding and have also mapped high-risk regions on this chromosome in GWAS analysis of other types of cardiovascular disease such as stroke, aneurysm, carotid artery disease, and heart failure[5]. A recent publication from Liu *et al* reports that the individuals with SNP genotypes associated with CAD risk actually display a significant reduction in expression of $p16^{INK4a}$ [6]. Also, SNPs resulting in alterations in expression of ANRIL, a negative regulator of $p16^{INK4a}$ expression, also confer increased risk of CAD[46].

Collectively, human studies overwhelmingly suggest that $p16^{INK4a}$ plays a role in protecting individuals from arterial disease.

These findings prompted a number of genetic mouse model studies to look at how genes encoded by these loci affect cardiovascular disease. A recent study by Gonzalez-Navarro *et al* demonstrated that the $p19^{ARF-/-}$ mouse crossed to the $ApoE^{-/-}$ displayed increased atherosclerosis[47]. Similarly, an independent report by Kuo et al showed that bone marrow transplantation from mice with heterozygous deficiency for both $p19^{ARF}$ and $p16^{INK4a}$ into $Ldlr^{-/-}$ mice results in increased atherosclerosis[48].

Conversely, Visel et al deleted a specific non-coding region on the *CDKN2A* locus thought to be orthologous to the human ANRIL non-coding RNA, which functionally represses $p16^{INK4a}$ expression. While deletion of this region resulted in significant down-regulation of both *CDKN2B* and *CDKN2A* with subsequent increases in cellular proliferation, it had no effect on atherosclerotic plaque formation[49]. Additionally, a recent report demonstrated that bone marrow transplantation from $p16^{INK4a}$ deficient mice into $Ldlr^{-/-}$ mice on a high fat diet did not affect atherosclerotic plaque formation[39].

Although $p16^{INK4a}$ expression may be protective in early atherogenesis according to some studies, its role in promoting vascular cell senescence and dysfunction may have deleterious effects on already formed plaques. Holdt *et al* demonstrated marked positive staining of $p16^{INK4a}$ and other CDK inhibitors in human atherosclerotic plaques. They were able to estimate plaque stability by measuring expression levels of methylthioadenosine phosphorylase (MTAP), an enzyme involved in synthesizing polyamines critical for plaque stabilization. Plaques with the lowest expression of MTAP exhibited the highest levels of

$p16^{INK4a}$ expression, suggesting that $p16^{INK4a}$ may play a role in plaque instability and rupture[50].

Given these observations, data in *in vivo* models supporting a role for *CDKN2A* in atherosclerosis has been somewhat controversial. However, an important limitation to using mice to study this phenomenon is the possibility that the mouse *CDKN2A* locus, although very similar to that of humans, may be regulated differently. Also, mice are not susceptible to atherosclerosis without being crossed to an $ApoE^{-/-}$ or $Ldlr^{-/-}$ strain and fed a high fat diet. Therefore, studying the pathophysiology of atherosclerotic plaque formation may not offer a completely representative picture, or always correspond with genetic data in humans.

2.7 $p16^{INK4a}$ expression in vascular endothelial cells.

Although $p16^{INK4a}$ may play a protective role against proliferative arterial diseases such as atherosclerosis by limiting aberrant cellular proliferation, there are a number of physiologic changes that are associated with $p16^{INK4a}$ expression in other vascular compartments that may promote age-related diseases. One tissue that responds to $p16^{INK4a}$ expression and undergoes senescence is the vascular endothelium[51,52]. Endothelial cells provide a barrier between the luminal blood and highly procoagulant sub-endothelial proteins and are thus critical regulators of coagulation in both the arterial and venous circulation. Cellular senescence induced by $p16^{INK4a}$ expression is thought to promote vascular dysfunction by mediating phenotypic changes in endothelial cells[31]. Similar to other cell types, endothelial cell senescence is marked by characteristic changes that distinguish it from quiescence, a non-terminal, reversible resting state. First, senescent endothelial cells undergo a marked change in morphology adopting an enlarged, flattened shape compared to

proliferating cells which have a cobble-stone morphology *in vitro*[53]. Another tell-tale signature of endothelial cell senescence is the expression of senescence-associated (SA) β-galactosidase. The detection of β-galactosidase at a pH of 6.0 is a common biomarker of senescence in many cell types. Although the mechanism is not fully understood, it is thought that expression of acidic β-galactosidase is due to the presence of enlarged lysosomes and the accumulation of this enzyme in autophagic vacuoles within those lysosomes[52].

In addition to these distinct morphologic features that, in the presence of $p16^{INK4a}$ or p21 overexpression, define endothelial cell senescence, other phenotypic changes have been reported that could have pathophysiologic consequences[7]. *In vitro*, senescent endothelial cells secrete a variety of pro-inflammatory cytokines such as interleukin (IL)-6, IL-1α, IL-1β, and IL-8[54]. Cytokine upregulation results in increased recruitment and binding of leukocytes to the vessel wall, which could support and sustain low level blood coagulation, particularly in the presence of tissue factor (TF)-bearing leukocytes. Senescent endothelial cells also secrete more matrix metalloproteases (MMPs)[8], which are involved in extracellular matrix degredation and are also able to cleave several chemokines and cytokines. Another hallmark of vascular aging and endothelial cell senescence is reduced endothelial nitric oxide synthase (eNOS) production. eNOS is critical for catalyzing the nitric oxide (NO)-generating reaction in blood vessels. NO is an important vasodilator and also potent inhibitor of platelet aggregation and leukocyte binding. Loss of eNOS production during endothelial cell senescence results in reduced vasodilation, increased vessel rigidity, and increased platelet and leukocyte activation as a result of reduced NO bioavailability[55-57]. Lastly and very importantly, increased expression of antifibrinolytic plasminogen activator inhibitor-1 (PAI-1) is a biomarker of both replicative and stress-induced senescence[8,9]. PAI-1 is a

powerful regulator of clot dissolution through inhibition of fibrinolytic proteases tissue and urokinase plasminogen activator (tPA and uPA, respectively) and is also an acute phase reactant and pro-inflammatory in nature[58]. Therefore, increased production of PAI-1 by senescent vascular endothelial cells can lead to increased inflammation and the sustained presence of venous and arterial thrombi.

2.8 $p16^{INK4a}$ expression in leukocytes.

One of the initial reports establishing $p16^{INK4a}$ as a biomarker of physiologic aging came from data on $p16^{INK4a}$ expression in peripheral blood lymphocytes from humans of various ages[4]. Expression of $p16^{INK4a}$ has also been found in other leukocytes, including monocytes and macrophages[59]. One of the earliest phases of atherosclerotic plaque formation is the adherence of circulating monocytes to the vessel wall where they migrate into the sub-endothelial spaces, differentiate in macrophages and ultimately consume oxidized low density lipoproteins and subsequently become foam cells[60]. Monocytes and macrophages are also key players in the formation and resolution of venous thrombi through production of procoagulant TF and antifibrinolytic PAI-1, as well as phagocytosis of dead cells and promotion of proteolysis during thrombus resolution[61]. Therefore, dysfunction of these cell types has important cardiovascular implications.

Interestingly, two recent reports highlight the effects of cellular senescence on monocyte and macrophage function. Merino *et al* demonstrated that elderly and chronically ill patients display a shift in their circulating monocyte immunophenotype from a $CD14^{++}CD16^{-}$ predominant population to a $CD14^{+}CD16^{+}$ population[62]. This expanded sub-population of monocytes were found to have increased SA β-galactosidase expression and reduced

telomere length compared to those from young and healthy controls, indicating that these cells had undergone senescence. Additionally, the $CD14^{+}CD16^{+}$ sub-population of monocytes expressed increased vascular adhesion molecules and demonstrated increased adhesion to vascular endothelial cells. They also were more sensitive to antigenic stimulation compared to controls and released more pro-inflammatory cytokines[62]. These data suggest that senescent circulating monocytes are more pro-inflammatory and pro-atherogenic compared to non-senescent monocytes.

Further support for the idea that leukocyte senescence can modulate inflammatory responses comes from a recent report from Cudejko *et al*[63]. This group found that macrophages from $p16^{INK4a}$ deficient mice displayed reduced expression of inflammatory cytokines IL-6 and TNF-α with increased expression of anti-inflammatory IL-R1. These data suggest that $p16^{INK4a}$ expression has the ability to regulate monocyte and macrophage immunophenotyes and inflammatory function.

2.9 Focus of this dissertation.

While the anti-proliferative effects of $p16^{INK4a}$ may be important for reducing the risk of atherosclerotic disease, expression of $p16^{INK4a}$ in endothelial cells and leukocytes and the associated phenotypic changes discussed here could play a role in promoting other age-related diseases in the vasculature. Currently, there are virtually no publications studying the role of $p16^{INK4a}$ expression in the pathophysiology of venous thrombosis. The upregulation of $p16^{INK4a}$ in the vasculature could be an important factor in the increased risk of venous thromoboembolism in the elderly.

2.10 References

1. Popov N, Gil J. Epigenetic regulation of the INK4b-ARF-INK4a locus: in sickness and in health. *Epigenetics*. 2010;5(8):685-690.

2. Gil J, Peters G. Regulation of the INK4b-ARF-INK4a tumour suppressor locus: all for one or one for all. *Nat. Rev. Mol. Cell Biol*. 2006;7(9):667-677.

3. Krishnamurthy J, Torrice C, Ramsey MR, et al. Ink4a/Arf expression is a biomarker of aging. *J. Clin. Invest*. 2004;114(9):1299-1307.

4. Liu Y, Sanoff HK, Cho H, et al. Expression of p16(INK4a) in peripheral blood T-cells is a biomarker of human aging. *Aging Cell*. 2009;8(4):439-448.

5. Jarinova O, Stewart AFR, Roberts R, et al. Functional analysis of the chromosome 9p21.3 coronary artery disease risk locus. *Arterioscler. Thromb. Vasc. Biol*. 2009;29(10):1671-1677.

6. Liu Y, Sanoff HK, Cho H, et al. INK4/ARF transcript expression is associated with chromosome 9p21 variants linked to atherosclerosis. *PLoS ONE*. 2009;4(4):e5027.

7. Erusalimsky JD. Vascular endothelial senescence: from mechanisms to pathophysiology. *J. Appl. Physiol*. 2009;106(1):326-332.

8. Erusalimsky JD, Kurz DJ. Cellular senescence in vivo: its relevance in ageing and cardiovascular disease. *Exp. Gerontol*. 2005;40(8-9):634-642.

9. Comi P, Chiaramonte R, Maier JA. Senescence-dependent regulation of type 1 plasminogen activator inhibitor in human vascular endothelial cells. *Exp. Cell Res*. 1995;219(1):304-308.

10. Pasmant E, Sabbagh A, Vidaud M, Bièche I. ANRIL, a long, noncoding RNA, is an unexpected major hotspot in GWAS. *FASEB J*. 2011;25(2):444-448.

11. Stein GH, Dulić V. Molecular mechanisms for the senescent cell cycle arrest. *J. Investig. Dermatol. Symp. Proc*. 1998;3(1):14-18.

12. Ozenne P, Eymin B, Brambilla E, Gazzeri S. The ARF tumor suppressor: structure, functions and status in cancer. *Int. J. Cancer*. 2010;127(10):2239-2247.

13. Dominguez-Brauer C, Brauer PM, Chen Y, Pimkina J, Raychaudhuri P. Tumor suppression by ARF: gatekeeper and caretaker. *Cell Cycle*. 2010;9(1):86-89.

14. Matheu A, Maraver A, Serrano M. The Arf/p53 pathway in cancer and aging. *Cancer Res*. 2008;68(15):6031-6034.

15. Matsuda Y. Molecular mechanism underlying the functional loss of cyclindependent

kinase inhibitors p16 and p27 in hepatocellular carcinoma. *World J. Gastroenterol*. 2008;14(11):1734-1740.

16. Williams RT, Sherr CJ. The INK4-ARF (CDKN2A/B) locus in hematopoiesis and BCR-ABL-induced leukemias. *Cold Spring Harb. Symp. Quant. Biol*. 2008;73:461-467.

17. Yang J, Du X, Lazar AJF, et al. Genetic aberrations of gastrointestinal stromal tumors. *Cancer*. 2008;113(7):1532-1543.

18. Kim WY, Sharpless NE. The regulation of INK4/ARF in cancer and aging. *Cell*. 2006;127(2):265-275.

19. Lin AW, Barradas M, Stone JC, et al. Premature senescence involving p53 and p16 is activated in response to constitutive MEK/MAPK mitogenic signaling. *Genes Dev*. 1998;12(19):3008-3019.

20. Serrano M, Lin AW, McCurrach ME, Beach D, Lowe SW. Oncogenic ras provokes premature cell senescence associated with accumulation of p53 and p16INK4a. *Cell*. 1997;88(5):593-602.

21. Jeyapalan JC, Sedivy JM. Cellular senescence and organismal aging. *Mech. Ageing Dev*. 2008;129(7-8):467-474.

22. Adams PD. Healing and hurting: molecular mechanisms, functions, and pathologies of cellular senescence. *Mol. Cell*. 2009;36(1):2-14.

23. Ohtani N, Zebedee Z, Huot TJ, et al. Opposing effects of Ets and Id proteins on p16INK4a expression during cellular senescence. *Nature*. 2001;409(6823):1067-1070.

24. Dhawan S, Tschen S, Bhushan A. Bmi-1 regulates the Ink4a/Arf locus to control pancreatic beta-cell proliferation. *Genes Dev*. 2009;23(8):906-911.

25. Aguilo F, Zhou M, Walsh MJ. Long noncoding RNA, polycomb, and the ghosts haunting INK4b-ARF-INK4a expression. *Cancer Res*. 2011;71(16):5365-5369.

26. Jacobs JJ, Kieboom K, Marino S, DePinho RA, van Lohuizen M. The oncogene and Polycomb-group gene bmi-1 regulates cell proliferation and senescence through the ink4a locus. *Nature*. 1999;397(6715):164-168.

27. Yap KL, Li S, Muñoz-Cabello AM, et al. Molecular interplay of the noncoding RNA ANRIL and methylated histone H3 lysine 27 by polycomb CBX7 in transcriptional silencing of INK4a. *Mol. Cell*. 2010;38(5):662-674.

28. Kuilman T, Michaloglou C, Mooi WJ, Peeper DS. The essence of senescence. *Genes Dev*. 2010;24(22):2463-2479.

29. Campisi J. The biology of replicative senescence. *Eur. J. Cancer*. 1997;33(5):703-709.

30. Ohtani N, Yamakoshi K, Takahashi A, Hara E. The p16INK4a-RB pathway: molecular link between cellular senescence and tumor suppression. *J. Med. Invest*. 2004;51(3-4):146-153.

31. Erusalimsky JD, Skene C. Mechanisms of endothelial senescence. *Exp. Physiol*. 2009;94(3):299-304.

32. Alcorta DA, Xiong Y, Phelps D, et al. Involvement of the cyclin-dependent kinase inhibitor p16 (INK4a) in replicative senescence of normal human fibroblasts. *Proc. Natl. Acad. Sci. U.S.A*. 1996;93(24):13742-13747.

33. Campisi J, d'Adda di Fagagna F. Cellular senescence: when bad things happen to good cells. *Nat. Rev. Mol. Cell Biol*. 2007;8(9):729-740.

34. Sharpless NE. Ink4a/Arf links senescence and aging. *Exp. Gerontol*. 2004;39(11-12):1751-1759.

35. Li J. Quiescence regulators for hematopoietic stem cell. *Exp. Hematol*. 2011;39(5):511-520.

36. Sharpless NE, DePinho RA. How stem cells age and why this makes us grow old. *Nat. Rev. Mol. Cell Biol*. 2007;8(9):703-713.

37. Kollman C, Howe CW, Anasetti C, et al. Donor characteristics as risk factors in recipients after transplantation of bone marrow from unrelated donors: the effect of donor age. *Blood*. 2001;98(7):2043-2051.

38. Krishnamurthy J, Ramsey MR, Ligon KL, et al. p16INK4a induces an age-dependent decline in islet regenerative potential. *Nature*. 2006;443(7110):453-457.

39. Wouters K, Cudejko C, Gijbels MJJ, et al. Bone marrow p16INK4a-deficiency does not modulate obesity, glucose homeostasis or atherosclerosis development. *PLoS ONE*. 2012;7(3):e32440.

40. Melzer D, Frayling TM, Murray A, et al. A common variant of the p16(INK4a) genetic region is associated with physical function in older people. *Mech. Ageing Dev*. 2007;128(5-6):370-377.

41. McPherson R, Pertsemlidis A, Kavaslar N, et al. A common allele on chromosome 9 associated with coronary heart disease. *Science*. 2007;316(5830):1488-1491.

42. Helgadottir A, Thorleifsson G, Manolescu A, et al. A common variant on chromosome 9p21 affects the risk of myocardial infarction. *Science*. 2007;316(5830):1491-1493.

43. Zeggini E, Weedon MN, Lindgren CM, et al. Replication of genome-wide association signals in UK samples reveals risk loci for type 2 diabetes. *Science*. 2007;316(5829):1336-1341.

44. Züchner S, Gilbert JR, Martin ER, et al. Linkage and association study of late-onset Alzheimer disease families linked to 9p21.3. *Ann. Hum. Genet*. 2008;72(Pt 6):725-731.

45. Holdt LM, Teupser D. Recent studies of the human chromosome 9p21 locus, which is associated with atherosclerosis in human populations. *Arterioscler. Thromb. Vasc. Biol*. 2012;32(2):196-206.

46. Burd CE, Jeck WR, Liu Y, et al. Expression of linear and novel circular forms of an INK4/ARF-associated non-coding RNA correlates with atherosclerosis risk. *PLoS Genet*. 2010;6(12):e1001233.

47. González-Navarro H, Abu Nabah YN, Vinué A, et al. p19(ARF) deficiency reduces macrophage and vascular smooth muscle cell apoptosis and aggravates atherosclerosis. *J. Am. Coll. Cardiol*. 2010;55(20):2258-2268.

48. Kuo C, Murphy AJ, Sayers S, et al. Cdkn2a is an atherosclerosis modifier locus that regulates monocyte/macrophage proliferation. *Arterioscler. Thromb. Vasc. Biol*. 2011;31(11):2483-2492.

49. Visel A, Zhu Y, May D, et al. Targeted deletion of the 9p21 non-coding coronary artery disease risk interval in mice. *Nature*. 2010;464(7287):409-412.

50. Holdt LM, Sass K, Gäbel G, et al. Expression of Chr9p21 genes CDKN2B (p15(INK4b)), CDKN2A (p16(INK4a), p14(ARF)) and MTAP in human atherosclerotic plaque. *Atherosclerosis*. 2011;214(2):264-270.

51. Chen J, Huang X, Halicka D, et al. Contribution of p16INK4a and p21CIP1 pathways to induction of premature senescence of human endothelial cells: permissive role of p53. *Am. J. Physiol. Heart Circ. Physiol*. 2006;290(4):H1575-1586.

52. Chen J, Goligorsky MS. Premature senescence of endothelial cells: Methusaleh's dilemma. *Am. J. Physiol. Heart Circ. Physiol*. 2006;290(5):H1729-1739.

53. Rosen EM, Mueller SN, Noveral JP, Levine EM. Proliferative characteristics of clonal endothelial cell strains. *J. Cell. Physiol*. 1981;107(1):123-137.

54. Davalos AR, Coppe J, Campisi J, Desprez P. Senescent cells as a source of inflammatory factors for tumor progression. *Cancer Metastasis Rev*. 2010;29(2):273-283.

55. Yoon HJ, Cho SW, Ahn BW, Yang SY. Alterations in the activity and expression of endothelial NO synthase in aged human endothelial cells. *Mech. Ageing Dev*. 2010;131(2):119-123.

56. Arnal JF, Dinh-Xuan AT, Pueyo M, Darblade B, Rami J. Endothelium-derived nitric oxide and vascular physiology and pathology. *Cell. Mol. Life Sci*. 1999;55(8-9):1078-1087.

57. Matsushita H, Chang E, Glassford AJ, et al. eNOS activity is reduced in senescent human endothelial cells: Preservation by hTERT immortalization. *Circ. Res*. 2001;89(9):793-798.

58. Nicholl SM, Roztocil E, Davies MG. Plasminogen activator system and vascular disease. *Curr Vasc Pharmacol*. 2006;4(2):101-116.

59. Randle DH, Zindy F, Sherr CJ, Roussel MF. Differential effects of p19(Arf) and p16(Ink4a) loss on senescence of murine bone marrow-derived preB cells and macrophages. *Proc. Natl. Acad. Sci. U.S.A*. 2001;98(17):9654-9659.

60. Whalin MK, Taylor WR. Rounding up the usual suspects in atherosclerosis. Focus on "Growth factors induce monocyte binding to vascular smooth muscle". *Am. J. Physiol., Cell Physiol*. 2004;287(3):C592-593.

61. Saha P, Humphries J, Modarai B, et al. Leukocytes and the natural history of deep vein thrombosis: current concepts and future directions. *Arterioscler. Thromb. Vasc. Biol*. 2011;31(3):506-512.

62. Merino A, Buendia P, Martin-Malo A, et al. Senescent CD14+CD16+ monocytes exhibit proinflammatory and proatherosclerotic activity. *J. Immunol*. 2011;186(3):1809-1815.

63. Cudejko C, Wouters K, Fuentes L, et al. p16INK4a deficiency promotes IL-4-induced polarization and inhibits proinflammatory signaling in macrophages. *Blood*. 2011;118(9):2556-2566.

Chapter 3.

Overexpression of the Cell Cycle Inhibitor $p16^{INK4a}$ Promotes a Prothrombotic Phenotype Following Vascular Injury in Mice[1]

3.1 Introduction

Aging is an important risk fact[1]or for developing cardiovascular disease, and also the least understood[1,2]. Venous thromboembolism (VTE) is characterized by the development of thrombi in the deep veins of the legs, which are prone to dislodging and embolizing to the lungs. This condition accounts for 140,000-200,000 deaths each year in the U.S[3,4]. The risk of developing VTE substantially increases with age and individuals over the age of 55 years have an annual incidence 5-7 times higher than young adults[5]. While VTE in the younger population is often explained by mutations in hemostatic genes, mechanisms behind the increased risk of VTE in the elderly are less well understood.

Senescence is one cellular phenomenon known to be associated with aging. Cellular senescence is a stress-induced process, controlled by cell cycle inhibitors, which promotes an irreversible growth arrest[6-9]. $p16^{INK4a}$, a cell cycle inhibitor that promotes senescence, binds to cyclin-dependent kinases 4 and 6 to disrupt phosphorylation of the retinoblastoma protein, causing a G1 cell cycle arrest[10]. Expression of $p16^{INK4a}$ increases with age in many tissues

---

[1] Cardenas JC, Owens AP, Krishnamurthy J, et al. Overexpression of the cell cycle inhibitor p16INK4a promotes a prothrombotic phenotype following vascular injury in mice. *Arterioscler. Thromb. Vasc. Biol*. 2011;31(4):827-833

and is a biomarker of aging[11-14]. Furthermore, $p16^{INK4a}$ expression correlates with biomarkers of senescence, such as senescence-associated β-galactosidase expression, and expression is associated with gerontogenic activities such as smoking, physical inactivity and *ad libitum* feeding in humans or mice[11,14]. In some tissues such as pancreatic beta cells, neural stem cells, and hematopoietic stem or progenitor cells, the age-induced increase in $p16^{INK4a}$ expression is associated with reduced cellular proliferation coupled with an impaired tissue response to injury[15-17]. Additionally, senescent cells are thought to contribute to aging pathology through the production of cytokines (IL-6) that further promote inflammation and cellular dysfunction[18].

The contribution of senescence to disease in the venous circulation, and how this may be involved in age-related VTE or a possible prothrombotic phenotype, remains largely uncharacterized. The aim of this study was to ascertain whether overexpression of $p16^{INK4a}$ modified venous thrombus formation in several well-defined animal models. Our results demonstrate that $p16^{INK4a}$ overexpression augments vascular occlusion and delayed thrombus resolution relative to wild-type controls. Furthermore, $p16^{INK4a}$ transgenic mice display enhanced thrombin generation, increased thrombin-antithrombin (TAT), and increased PAI-1 levels when exposed to low-dose lipopolysaccharide (LPS). Additionally, bone marrow transplantation between wild-type and $p16^{INK4a}$ transgenic mice demonstrated a substantial contribution of hematopoietic cells to this phenotype. Overall, these results show that expression of $p16^{INK4a}$ is involved in promoting a prothrombotic environment in the venous vasculature.

3.2 Materials and Methods

Mice

All animal procedures were performed in accordance with protocols approved by the Institutional Animal Care and Use Committee, UNC-Chapel Hill. The bacterial artificial chromosome (BAC) transgenic mice overexpressing $p16^{INK4a}$ used in this study have been previously described[15]. These animals harbor a single copy integration of 60 kb of the murine $p16^{INK4a}$ locus, and exhibit a 3-8 fold increase in $p16^{INK4a}$ expression in all tissues examined to date. These animals do not overexpress other transcripts from the Ink4/Arf locus (i.e., $p15^{INK4b}$ and Arf) (data not included). Mice were backcrossed to the C57BL/6 background. Experiments were done on male and female littermate progeny of indicated genotypes. In all cases the mice were 6-8 weeks of age. No differences were detected between males and females in the experiments performed.

Real-Time PCR

Quantitative Real-time PCR analysis was performed as previously described[15]. Briefly, representative tissues were collected from transgenic and wild-type littermates used in thrombosis models for PCR analysis with the following primers. Forward primer sequence: CGGTCGTACCCCGATTCAG. Reverse primer sequence: GCACCGTAGTTGAGCAGAAGAG. Expression of ARF was also quantified as a control with the following primers: Forward primer sequence: TGAGGCTAGAGAGGATCTTGAGAAG. Reverse primer sequence: GTGAACGTTGCCCATCATCATC.

Complete Blood Count

Whole blood collected by cardiac puncture into EDTA tubes was analyzed for complete blood counts (CBC) by the UNC-CH Division of Lab Animal Medicine. Blood samples were submitted from three mice per group.

Prothrombin Time (PT)

Prothrombin times were measured using a STart®4 semi-automated hemostasis analyzer (Diagnostica Stago – Parispanny, NJ) by mixing equal volumes platelet poor plasma, calcium chloride (25 mM), and tissue factor (Innovin, 400 pM). Data represents pooled plasma from three mice per group.

Hemostasis Model

Hemostasis was assessed as previously described[19]. Briefly, wild-type and $p16^{INK4a}$ transgenic mice at 8 weeks of age were anesthetized with 2.5% tribromoethanol (Sigma Aldrich – St. Louis, MO, T48402) at 0.1 mL/g body weight. The saphenous vein of anesthetized mice was exposed and transected with a 23-G needle. Once bleeding stopped, a longitudinal cut was made in the vessel and the blood gently wiped away with kimwipes (Kimberly – Clark - Roswell, GA) until clotted. The blood clot was disrupted using a 30-G needle and the blood gently wiped away. Clot disruption was repeated every time hemostasis occurred and each hemostatic event was recorded using Chart software for 20 minutes.

For carotid artery thrombosis, the right common carotid artery was exposed after midline cervical incision. A Doppler transonic flow probe (Transonic Systems, Ithaca, NY) was applied and connected to a flow meter (model T206, Transonic Systems, Ithaca, NY)

supplying a data acquisition system (PowerLab 4/30 model ML866, AD Instruments, Australia). The carotid artery was dried and 10% $FeCl_3$ (0.62 M $FeCl_3$ on 0.5x0.5 mm filter paper) placed on the artery for 3 minutes, removed, and tissues washed 3 times with warm saline. Following injury, blood flow was continuously monitored. For saphenous vein thrombosis, the saphenous vein of the right leg was dissected and exposed, 5% $FeCl_3$ (0.31 M $FeCl_3$ on 0.5x2 mm filter paper) placed on the vein for 3 minutes, removed, and tissues washed 3 times with warm saline. Blood flow was monitored auditorily by Doppler ultrasonic flow probe. In both models, the TTO was the time between $FeCl_3$ administration and lack of flow for 60 consecutive seconds. Experiments were stopped at 45 minutes if no occlusion occurred. Occluded vessels were excised and fixed in 10% formalin.

Thrombolysis was assessed in mice subject to $FeCl_3$ carotid artery thrombosis. After 5 consecutive minutes of blood flow below 0.1 mL/min, mice were infused with TNKase (0.5–5 mg/kg) through the saphenous vein intravenous catheter while continuously monitoring carotid blood flow.

$FeCl_3$ Vascular Injury

The saphenous vein thrombosis model was performed as previously described[19]. Briefly, the saphenous veins of anesthetized mice was exposed and dissected away from the saphenous artery. A 0.5 x 2 mm piece of filter paper was soaked in 2.5% (N=4), 5% (N=5) or 10% (N=4) $FeCl_3$ (Sigma Aldrich – F7134), and laid over the saphenous vein for 3 minutes. The filter paper was then removed and the tissue was washed 3 times with warm saline. Blood flow was monitored using a 20-MHz Doppler flow probe (Indus Instruments – Webster, TX).

Occlusion is defined as the absence of blood flow for one minute. The time to flow restriction was defined as the time after injury at first cessation of blood flow.

Rose Bengal Photochemical Vascular Injury

Photochemical injury was performed as previously described[20]. Briefly, both right and left saphenous veins of anesthetized mice were exposed. The left saphenous vein was catheterized using catheters made in-house using pulled PE-10 tubing (Braintree Scientific - Braintree, MA). Rose Bengal (Sigma Aldrich – R-3877), diluted to 30 mg/mL in normal saline, was infused through the catheter at a dose of 75 mg/kg through a gastight syringe (Hamilton Co. - Reno,NV). Prior to infusion of Rose Bengal, a 1.75 mW green light (540 nm) (Prizmatix – Southfield, MI) was directed 0.5 cm over the injury site on the right saphenous vein. Light was applied to the vessel until a stable thrombus (defined as the absence of blood flow for 1 minute) was achieved.

Thrombus resolution

We developed a new method to measure thrombus resolution using the saphenous vein. Wild-type and $p16^{INK4a}$ transgenic mice (n=3 per genotype at each time point) were subjected to 10% $FeCl_3$ injury to the saphenous vein. The tissue was then washed 3 times with warm saline and a single ligature was placed upstream of the thrombus using a 8-0 monofilament polypropylene suture to prevent embolization and the leg was sutured closed. Mice were sacrificed at various time points and the saphenous neurovascular bundle was removed and fixed overnight in 4% paraformaldehyde and paraffin embedded. Five micron sections were cut and hematoxylin and eosin (H&E) stained to visualize the presence of a thrombus under

light microscopy. Vessels were sectioned through and those sections showing the greatest area of occlusion were chosen for analysis. Such sections typically occurred near the center of the injured vessel. Images were analyzed using ImageJ software to calculate the percent of the vessel lumen that remained occluded by a thrombus.

Low Dose Lipopolysaccharide (LPS) Treatment

Wild-type and $p16^{INK4a}$ transgenic mice were treated with 2mg/kg intraperitoneal injection of LPS (Sigma L3012). At various times (1, 3, and 5 hours), the mice (n=5 per genotype each time point) were anesthetized and 1mL of blood was collected from the inferior vena cava (IVC) into 3.8% sodium citrate at a ratio of 1:9 using a 25 gauge needle. Whole blood was spun at 4,000 x g for 15 minutes and the platelet poor plasma was collected and stored at -80°C until analyzed.

Thrombin Generation

Thrombin generation was measured by calibrated automated thrombography (CAT) using Z-Gly-Gly-Arg-AMC fluorogenic substrate for thrombin (Diagnostica Stago, Parsippany, NJ) on a Fluoroskan Ascent fluorometer (ThermoLabsystem, Helsinki, Finland). Mouse plasma was analyzed as previously described[21]. Briefly, mouse plasma samples were pooled, diluted 1:4 in phosphate buffered saline and 80 μL of plasma was added to 20 μL low tissue factor (1 pM) reagent to initiate the reaction. Variations in plasma color were accounted for using a α2-macroglobulin/thrombin calibrator reagent (Diagnostica Stago, Parsippany, NJ). Parameters were calculated by Thrombinoscope software version 3.0.0.29 (Thrombinoscope BV, Maastricht, Netherlands).

ELISAs

TAT complexes were detected in mouse plasma using an Enzygnost TAT complex ELISA (Siemens – New York, NY, USA). Plasma samples were diluted 1:10 in Enzygnost ELISA sample buffer. PAI-1 was measured using an ELISA for mouse total PAI-1 from Molecular Innovations. Fibrinogen was measured using an ELISA for mouse fibrinogen from Molecular Innovations (Novi, MI, USA). Plasma samples from mice treated with LPS were diluted 1:40 and 1:160 for the PAI-1 and fibrinogen ELISAs, respectively. Plasma samples from control mice were diluted 1:5 for both ELISAs. All ELISAs were performed according to the company protocols and standard curves were generated using proteins supplied by the company.

Immunohistochemistry

Tissues were extracted and fixed overnight in 4% paraformadehyde. Tissue embedding and cutting was performed in the UNC Linberger Comprehensive Cancer Center Animal Histopathology Core Facility. Briefly, 5 micron sections were cut from paraffin blocks and antigen retrieval was performed in Target Retrieval Solution (Dako – Capinteria, CA, S1699) in a 95°C water bath. Slides were blocked for 1 hour in 1% BSA and stained with antibodies against $p16^{INK4a}$ (Santa Cruz Biotechnology - Santa Cruz, CA, sc-1661, 1:200 dilution), Ki67 (Dako – M7249, 1:500 dilution), or PAI-1 (Santa Cruz Biotechnology – sc-8979, 1:250 dilution) for 1 hour at room temperature in a humidity-controlled chamber. Biotinylated secondary antibodies were obtained from Vector Laboratories. Tissue slides were developed using the avidin-biotin complex (ABC) method using reagents and protocols obtained from Dako. Negative control slides were stained simultaneously in the absence of primary

antibody. Images were analyzed by taking a representative digital photograph of tissue from each mouse. A grid was laid over the images using ImageJ software and percent positive grid boxes were calculated by counting the number of grid boxes containing a positively stained cell and dividing it by the total number of grid boxes on the image.

Bone marrow transplantation

This procedure was performed as described previously[22]. Briefly, mice were irradiated using a Cesium^{137} irradiator (JL Shepherd, San Fernando, CA) with a total of 11 Gy (two doses of 550 rad, with a 4 hour rest) to abolish endogenous hematopoietic cells. Bone marrow cells were isolated from donor mice[22] and 1 x 10^7 cells were injected (100 μL) into the retro-orbital sinus. Four weeks after irradiation, recipient mice underwent $FeCl_3$ injury to the saphenous vein to determine vascular occlusion times. At termination, recipient mouse bone marrow was genotyped to verify successful repopulation of donor cells by polymerase chain reaction. Expression of $p16^{INK4a}$ was compared to an IL-2 loading control.

Statistics

All statistical analyses were performed with Graphpad Prism. All measurements are respresented as the mean ± standard error of the mean (SEM). One-way ANOVA or Students T-test was performed where indicated. One-way ANOVA was performed with a Tukey's post-hoc test on measurements were indicated. For two group comparison of parametric data, a student's t-test was performed where indicated. Values of $p<0.05$ were considered statistically significant.

3.3 Results

$p16^{INK4a}$ transgenic and wild-type mice respond similarly in a hemostasis model.

To determine the contribution of $p16^{INK4a}$ overexpression on potential hemostatic defects, mice initially underwent a model of saphenous vein hemostasis. No difference was observed in the number of hemostatic clots formed over 20 minutes between transgenic (25.8 ± 3.4) and wild-type mice (25.8 ± 2.1, Figure 3.1A) or in the average time to hemostasis (33.5 ± 3.7 sec and 36.6 ± 2.6 sec, respectively, Figure 3.1B). Furthermore, no significant differences were observed in body weight, venous blood flow velocity, plasma prothrombin time (PT) and complete blood count (CBC) between the two groups of mice (Table 3.1). These results suggest there is no obvious physical or hematologic phenotype in the $p16^{INK4a}$ transgenic mice at the ages studied.

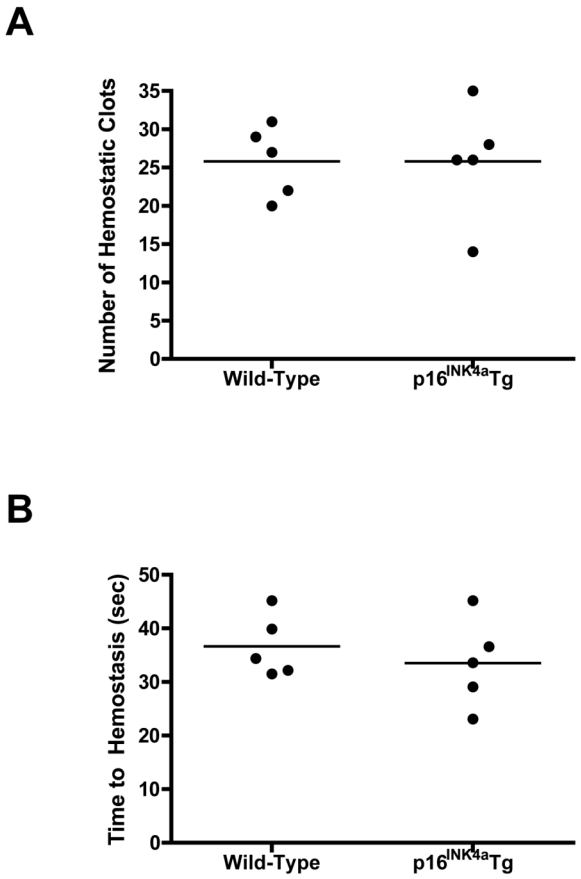

Figure 3.1. Hemostatic parameters in saphenous vein hemostasis model. Hemostatic measurements were compared between wild-type and $p16^{INK4a}$ transgenic mice following blunt injury to the saphenous vein. (A) The number of hemostatic clots formed and (B) the average time to stoppage of bleeding following serial clot disruption over 30 minutes. Data not statistically significant.

Table 3.1. Baseline parameters in wild-type vs. $p16^{INK4a}$ transgenic mice

General Parameters	**Wild-Type C57Bl/6**	**$p16^{INK4a}$ Transgenic**
Body Weight (g)	22.9 ± 0.6	22.7 ± 1.7
Venous Flow Velocity (mm/s)	35.88 ± 4.11	38.85 ± 4.78
Hemostasis Parameters		
Prothrombin Time (PT)	52.3 ± 0.5	52.4 ± 0.8
Fibrinogen (μg/ml)	29.2 ± 3.7	34.1 ± 10.4
PAI-1 (ng/ml)	0.012 ± 0.004	0.014 ± 0.004
TAT (ng/ml)	7.2 ± 3.0	9.2 ± 1.8
Complete Blood Count		
White Blood Cells (x 10^6/μL)	3.3 ± 1.3	2.1 ± 1.8
Red Blood Cells (x 10^3/μL)	8.82 ± 0.3	8.87 ± 1.1
Hemoglobin (g/dL)	13.7 ± 0.3	14.5 ± 0.9
Hematocrit (Vol %)	40.0 ± 1.3	42.2 ± 1.5
Mean Corpuscular Volume (fL)	45.3 ± 0.1	47.6 ± 1.0
Mean Corpuscular Hemoglobin (pg)	15.6 ± 0.2	16.3 ± 0.4
Mean Corpuscular Hemoglobin Concentration (g/dL)	34.3 ± 0.4	34.3 ± 0.8
Platelets (x 10^3/μL)	1294 ± 31.1	1406 ± 21.9

Baseline parameters that could potentially affect thrombosis were compared in wild-type and $p16^{INK4a}$ transgenic mice (± SD), as described in the Materials and Methods.

$p16^{INK4a}$ transgenic mice show increased $p16^{INK4a}$ expression and decreased cellular proliferation compared to wild-type.

In order to determine the utility of this model for vascular studies, saphenous veins and other tissues from mice were characterized by real-time PCR and immunohistochemistry as to $p16^{INK4a}$ mRNA and protein expression, respectively. In accord with prior results, mRNA analysis showed between 2- and 6 -fold increased expression of $p16^{INK4a}$ over wild-type littermates in heart, lung and spleen (Figure 3.2A). Additionally, a six-fold increase in expression was noted in saphenous vein (Figure 3.2A). Immunohistochemical staining showed ~30% positive staining for $p16^{INK4a}$ in kidney cells of transgenic mice, and ~3% positive staining for $p16^{INK4a}$ in wild-type mice (Figure 3.2B). These results indicate that $p16^{INK4a}$ expression is elevated in most tissues, including larger veins, of the transgenic mice compared to littermate controls, and that this increased expression is associated with decreased proliferation, as determined by staining for the proliferation marker Ki67 (data not shown).

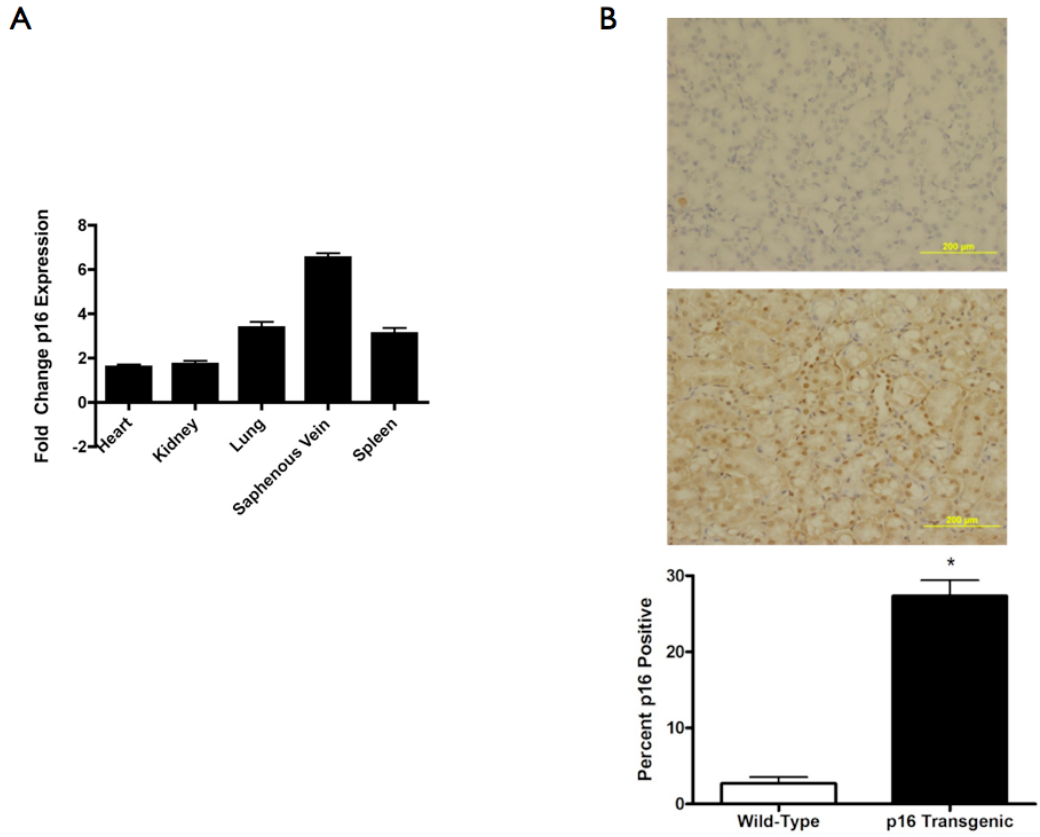

Figure 3.2. $p16^{INK4a}$ mRNA and protein levels in transgenic vs. wild-type mice. (A) Real-time quantitative PCR was performed on organs collected from transgenic and wild-type littermates. Data are expressed as fold change in transgenic mice over wild-type, as described in Materials and Methods. (B) $p16^{INK4a}$ protein was measured in kidneys of wild-type (top panel) and transgenic (middle panel) mice by immunostaining as described in the Supplemental Materials and Methods. Images were quantified in ImageJ and expressed as percent positive staining for $p16^{INK4a}$ (bottom panel). *denotes $p<0.05$ versus wild-type control by student t-test.

$p16^{INK4a}$ transgenic mice display a prothrombotic phenotype in a $FeCl_3$ injury model.

$FeCl_3$ injury is a well-established mechanism for inducing thrombus formation *in vivo*[23-25]. We first demonstrated a dose-dependent effect of $FeCl_3$ on the occlusion time in the saphenous vein, exposing wild-type mice to 2.5, 5, and 10% $FeCl_3$ injuries to the saphenous vein (Figure 3.3A).

Wild-type and $p16^{INK4a}$ transgenic mice were then subjected to $FeCl_3$ (5%) injury to the saphenous vein. The $p16^{INK4a}$ transgenic mice showed a significantly faster time to occlusion (13.1 ± 0.4 min) compared to wild-type mice (19.7 ± 1.1 min, Figure 3.3B). Furthermore, the time to flow restriction was also measured. The $p16^{INK4a}$ transgenic mice demonstrated faster times to flow restriction (6.4 ± 0.91 min) compared to wild-type controls (8.7 ± 0.54 min, $p<0.05$, data not shown). These results indicate overexpression of $p16^{INK4a}$ results in a prothrombotic phenotype following vascular injury.

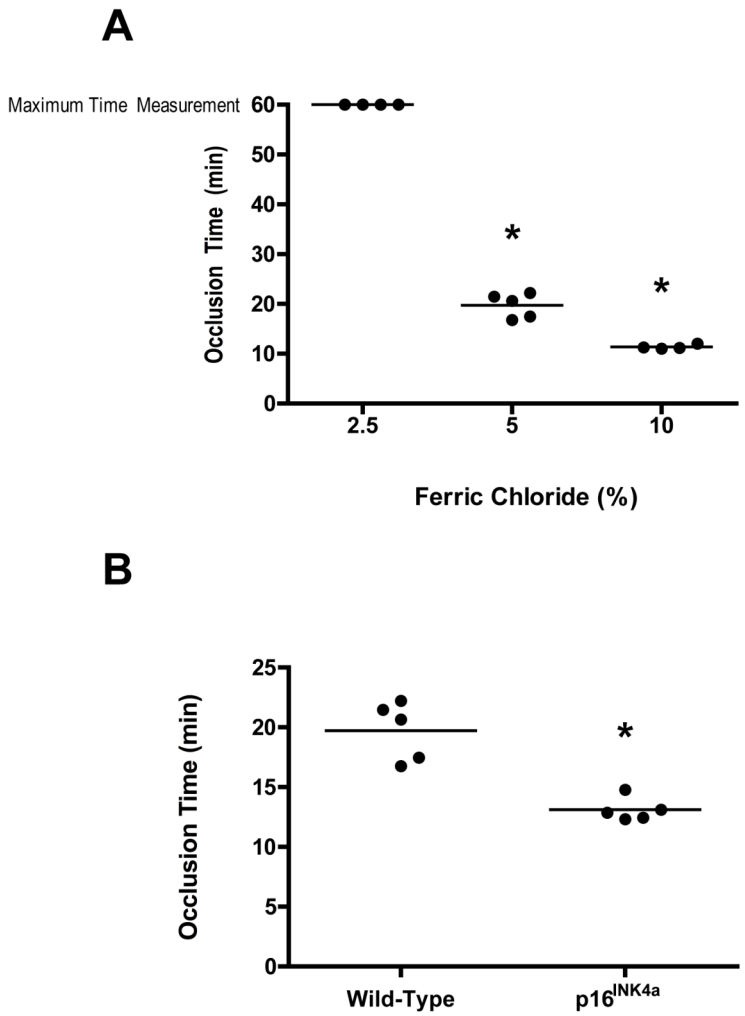

Figure 3.3. Overexpression of $p16^{INK4a}$ decreases time to occlusion in $FeCl_3$ vascular injury model. (A) Wild-type mice were subjected to increasing doses of $FeCl_3$ to the saphenous vein to determine a dose-dependent effect on the occlusion time as described in the Materials and Methods *$p<0.01$ versus 2.5% $FeCl_3$. (B) Vascular occlusion times were compared between wild-type and $p16^{INK4a}$ transgenic mice after 5% $FeCl_3$ injury to the saphenous vein. The occlusion time represents the amount of time required to form an occlusive thrombus as described in the Materials and Methods. * denotes $p<0.01$ versus wild-type control by student t-test.

$p16^{INK4a}$ transgenic mice display a prothrombotic phenotype in a photochemical injury model.

The excitation of Rose Bengal to induce photochemical injury is another well-established mechanism for inducing thrombus formation *in vivo*[26-28]. Upon photochemical injury to the saphenous vein, $p16^{INK4a}$ transgenic mice displayed a significantly faster time to occlusion (12.7 ± 2.0 min) when compared to wild-type mice (18.6 ± 1.9 min, Figure 3.4). These results suggest the prothrombotic phenotype in mice overexpressing $p16^{INK4a}$ can be recapitulated in other vascular injury models.

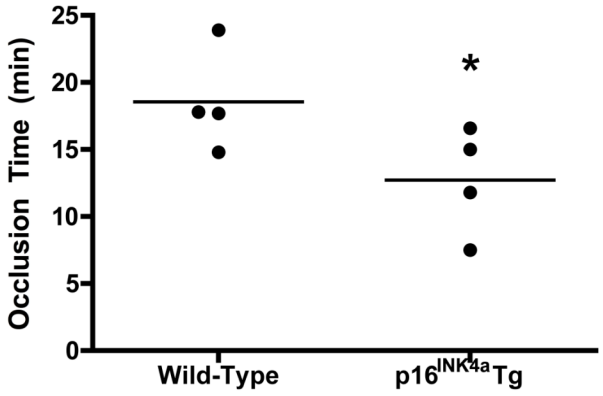

Figure 3.4. $p16^{INK4a}$ Transgenic mice have decreased time to occlusion in rose bengal photochemical vascular injury model. Vascular occlusion times between wild-type and $p16^{INK4a}$ transgenic mice were compared following saphenous vein injury with 75 mg/kg Rose Bengal excited with 1.75 mW green light at 540 nm. Occlusion times represent the amount of time required to form an occlusive thrombus. *denotes $p<0.05$ versus wild-type control by student t-test.

$p16^{INK4a}$ transgenic mice exhibit delayed thrombus resolution.

Venous thrombosis is characterized by the presence of unresolved thrombi in the lower extremities. In order to study the effect of overexpressing $p16^{INK4a}$ on thrombus resolution, thrombi formed post-$FeCl_3$ injury in wild-type and $p16^{INK4a}$ transgenic mice were monitored over time. Mice were euthanized from 1 hour to 15 days post-$FeCl_3$ injury and vascular ligation. No significant differences in thrombus resolution were observed until 7 days after vascular injury. By 10 days post-injury, all wild-type mice exhibited complete thrombus resolution, whereas $p16^{INK4a}$ transgenic mice maintained an average of 60% vessel occlusion. $p16^{INK4a}$ transgenic mice required additional time post-injury for thrombus resolution relative to wild-type controls (Figure 3.5 A). Representative images show little difference in percent occlusion at one day (Figure 3.5 B) between $p16^{INK4a}$ transgenic and wild-type mice. Black staining represents $FeCl_3$ trapped within the thrombus. At 10 days, we observed that residual $FeCl_3$ was mostly contained within inflammatory macrophages and was present in the perivascular space of wild-type mice. However, residual $FeCl_3$ contained within macrophages was still present in the intravascular space of $p16^{INK4a}$ transgenic mice at 10 days (Figure 3.5 B). These results demonstrate a defect in thrombus resolution with $p16^{INK4a}$ overexpression.

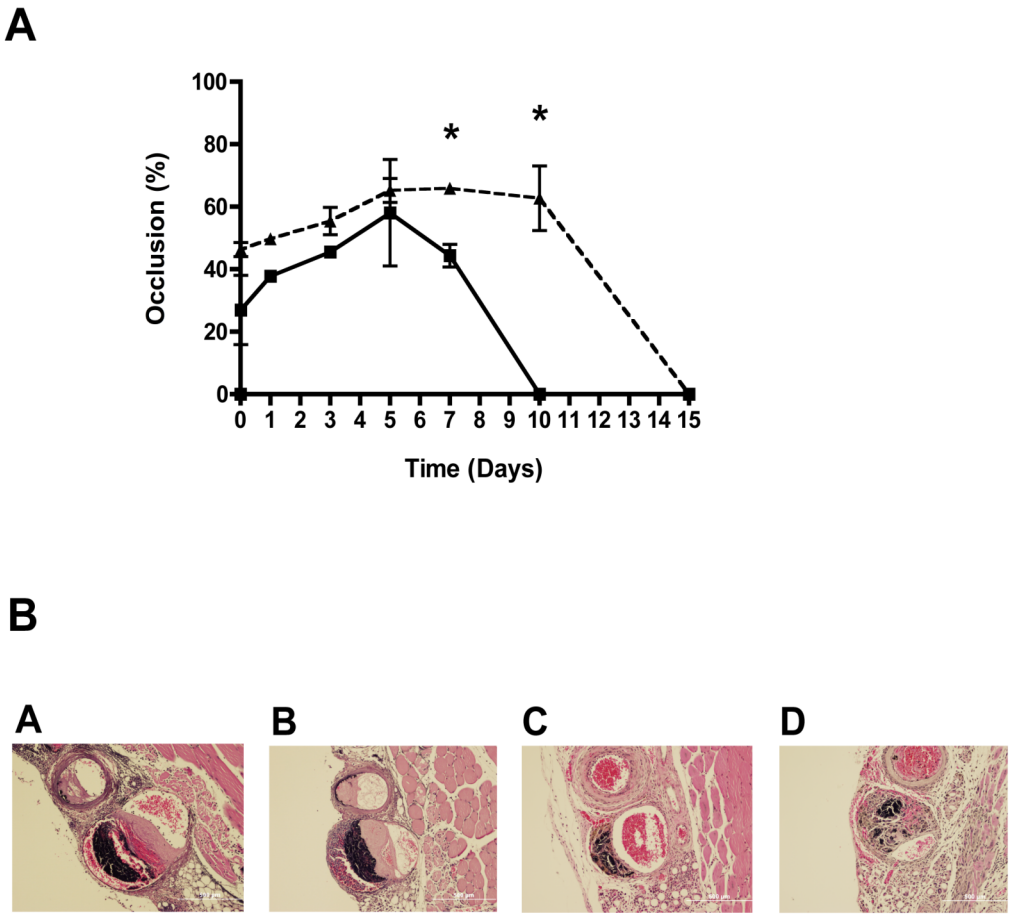

Figure 3.5. p16^{INK4a} transgenic mice display defective thrombus resolution. (A) Thrombus resolution was measured over time after 10% $FeCl_3$ injury to the saphenous vein and stasis induced by ligation as described in the Materials and Methods. *denotes $p<0.05$ versus respective wild-type control by student t-test. (B) Representative histologic images were analyzed using ImageJ software to determine percent occlusion (plotted in A). (a) Wild-type at 1 day, (b) p16 Transgenic at 1 day, (c) Wild-type at 10 days, (d) p16 Transgenic at 10 days. ■ - Wild-Type, ▲ - p16^{INK4a} Transgenic

$p16^{INK4a}$ transgenic mice display enhanced thrombin generation in response to LPS challenge.

Chronic inflammation and endothelial dysfunction have been linked to enhanced thrombin generation and the risk of venous thrombosis[29-31]. LPS is known to activate the vascular endothelium and promote the formation of spontaneous thrombi[32-35]. To study the effects of inflammation-induced coagulation, we exposed $p16^{INK4a}$ transgenic and wild-type mice to low dose LPS. When analyzed by calibrated automated thrombography (CAT), plasma from the $p16^{INK4a}$ transgenic mice showed significantly shorter lagtime to initiation of thrombin generation and time to peak amount of thrombin generated at all time points post LPS treatment (Table 3.2). The peak amount of thrombin generated was significantly higher in $p16^{INK4a}$ transgenic mice 3 and 5 hours after LPS treatment (Table 3.2). The observed differences in thrombin generation demonstrates $p16^{INK4a}$ transgenic mice are able to generate more thrombin and have a prothrombotic phenotype when challenged with LPS.

Mouse plasma was further analyzed to compare markers of coagulation and fibrinolysis. Fibrinogen was used as an acute phase reactant marker, no difference was detected by ELISA between wild-type and $p16^{INK4a}$ transgenic mice (Figure 3.6 A). Circulating TAT complexes peaked at 3 hours post LPS treatment and subsequently declined to untreated baseline in both wild-type and $p16^{INK4a}$ transgenic mice (Figure 3.6 B). While kinetic patterns were similar, transgenic mice had elevated TAT complex levels relative to wild-type at the 1 and 3 hour time points. Induction of PAI-1 following LPS treatment was similar in pattern to TAT complex formation between wild-type and transgenic mice. Peak PAI-1 levels were achieved at 3 hours post LPS treatment with a trending increase in PAI-1 in transgenic mice at this time point (Figure 3.6 C). Immunostaining of livers collected 3 hours post LPS

treatment showed increased PAI-1 nuclear staining in $p16^{INK4a}$ transgenic mice, but not in wild-type mice (Figure 3.6 D). These results suggest the altered thrombin generation parameters seen in the transgenic mice are not due to general differences in liver function, but to enhanced activation of specific coagulation proteins in $p16^{INK4a}$ transgenic mice.

Table 3.2. Thrombin generation in wild-type (WT) vs p16^{INK4a} transgenic (Tg) mouse plasma after LPS treatment

Time (hrs)	Lagtime (min)		Peak Height (nM)		Time to Peak (min)	
	WT	p16^{INK4a} Tg	WT	p16^{INK4a} Tg	WT	p16^{INK4a} Tg
0	2.17 ± 0.19	2.33 ± 0.24	46.16 ± 0.53	49.15 ± 1.98	5.33 ± 0.87	5.21 ± 0.62
1	3.4 ± 0.16	1.85 ± 0.12*	45.44 ± 9.45	44.21 ± 1.3	6.19 ± 0.27	4.52 ± 0.14*
3	2.85 ± 0.11	1.85 ± 0.09*	36.44 ± 0.43	51.26 ± 0.63*	6.07 ± 0.16	4.41 ± 0.16*
5	2.01 ± 0.17	2.51 ± 0.19*	32.06 ± 0.46	39.55 ± 0.67*	5.18 ± 0.23	5.52 ± 0.11*

Thrombin generation in plasma from mice treated with 2mg/kg LPS was measured using CAT, as described in the Supplemental Materials and Methods. Data represents experiments performed in duplicate with 5 mice per group per time point (± SD). *$p<0.05$

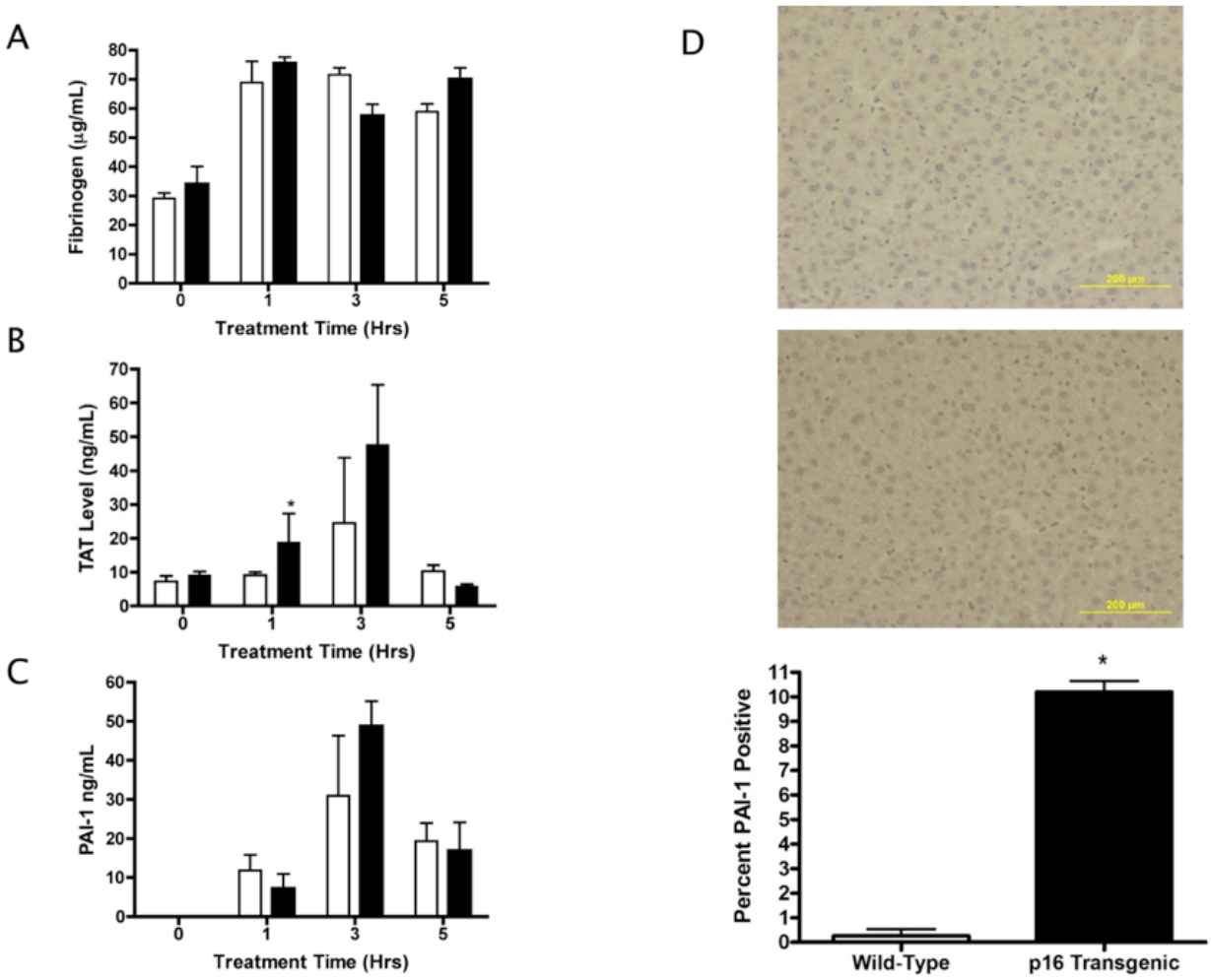

Figure 3.6. Plasma analysis (A-C) and PAI-1 levels in liver (D) after LPS treatment. Plasma collected from the IVC after LPS treatment was analyzed using ELISAs for fibrinogen (A) and circulating TAT complexes (B) and PAI-1 (C). *denotes $p<0.05$ versus respective wild-type control by student t-test. (D) PAI-1 protein levels were measured in wild-type (top panel) and transgenic (middle panel) livers by immunostaining as described in the Supplemental Materials and Methods. ❑ - Wild-Type, ■ - $p16^{INK4a}$ Transgenic

$p16^{INK4a}$ expression in hematopoietic cells contributes to the observed prothrombotic phenotype.

In order to determine the relative contribution of $p16^{INK4a}$ expression in the hematopoietic cell compartment to the observed prothrombotic phenotype, bone marrow transplants were performed between transgenic and wild-type mice. Following transplantation and recovery, mice were subjected to 10% $FeCl_3$ injury to the saphenous vein. Consistent with our previous results (Figure 3.2 B), transgenic mice receiving transgenic bone marrow had retained their significantly reduced occlusion time (8.4 ± 0.48 min) when compared to wild-type mice receiving wild-type bone marrow (13.0 ± 0.79 min, Figure 3.7). Interestingly, transgenic mice receiving wild-type bone marrow displayed occlusion times similar to wild-type mice (12.8 ± 1.3 min), whereas wild-type mice receiving transgenic bone marrow displayed occlusion times similar to transgenic mice (9.5 ± 0.61 min, Figure 3.7). PCR results confirmed successful reconstitution by donor bone marrow cells (Figure 3.8). These results demonstrate that the effects of $p16^{INK4a}$ overexpression are, at least in part, mediated by hematopoietic cells.

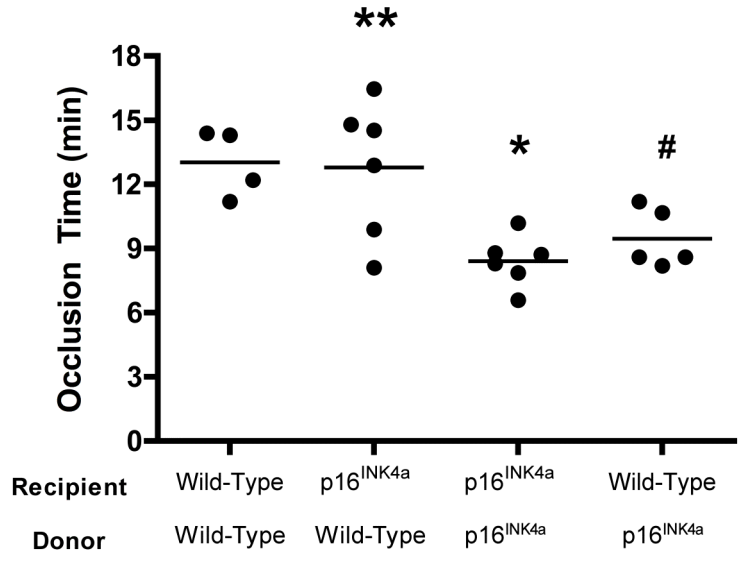

Figure 3.7. Vascular occlusion times are altered by bone marrow transplantation. Vascular occlusion times were compared between cohorts of bone marrow transplanted mice following injury of the saphenous vein with 10% $FeCl_3$. Occlusion time represent the amount of time required to form an occlusive thrombus. *denotes $p<0.05$ versus wild-type control cohort. ** denotes $p<0.05$ versus transgenic control cohort. # denotes $p=0.08$ versus wild type control cohort. Statistical relevance was determined by one-way ANOVA with Tukey's post-hoc analysis.

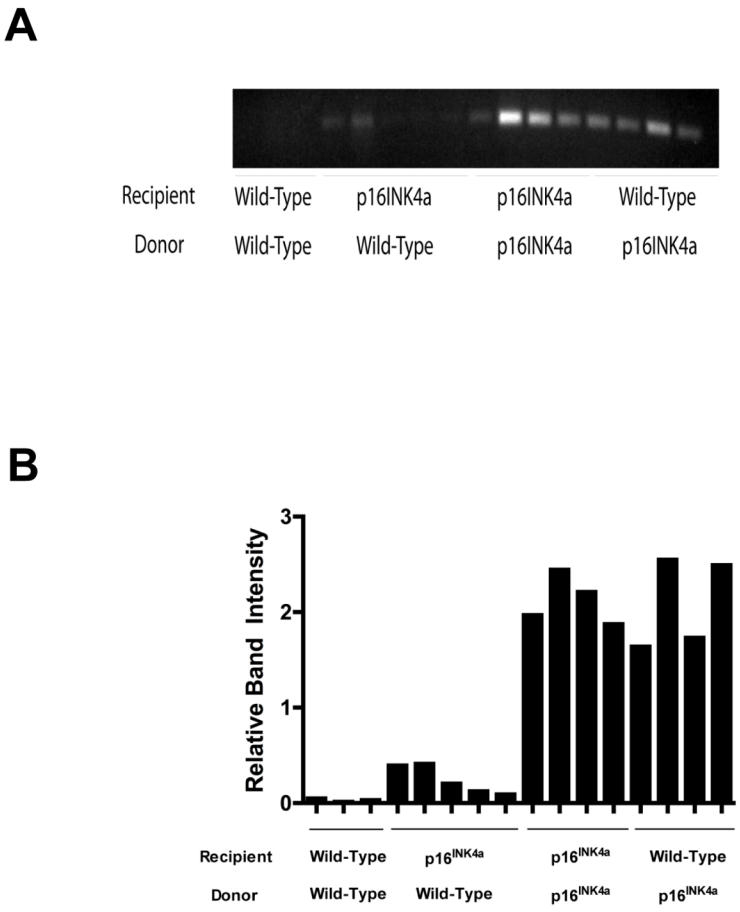

Figure 3.8. PCR analysis of bone marrow transplantation recipients. Quantitation of PCR performed on bone marrow collected from transplantation recipient mice to confirm successful repopulation with donor cells. $p16^{INK4a}$ levels were compared to IL-2 and quantified using Image J software from a representative gel.

3.4 Discussion

Senescence is a complex process that is thought to contribute to cardiovascular pathologies associated with aging. Despite several reviews describing prothrombotic changes in senescent vascular endothelial cells[36,37], no studies have described a venous thrombotic phenotype in mice overexpressing senescence-promoting genes. In the current study, we examined parameters that define venous thrombotic potential in a mouse model of premature senescence through transgenic overexpression of the cell cycle inhibitor $p16^{INK4a}$. As expected, the $p16^{INK4a}$ transgenic mouse exhibited increased expression of $p16^{INK4a}$ mRNA by real-time PCR analysis in all tissues tested. Mice overexpressing $p16^{INK4a}$ exhibit normal basal hemostatic parameters as tested by CBC, PT, and an *in vivo* hemostasis model. This suggests that in the absence of vascular injury, overexpression of $p16^{INK4a}$ has no overt hemostatic consequences. However, upon challenge in various vascular injury models, the $p16^{INK4a}$ transgenic mice displayed an obvious prothrombotic response.

We have demonstrated a prothrombotic phenotype using two different vascular injury models. Exposure of the vessel to $FeCl_3$ is a type of biochemical injury that results in endothelial denudation and exposure of the subendothelium following lipid peroxidation[38]. This type of oxidative damage produces thrombi that are rich in platelets, but also contain red blood cells both encased in a dense fibrin meshwork indicating a role for soluble plasma factors driving thrombus formation[39-41]. Rose Bengal is a fluorescein-based chemical that is excited to produce reactive oxygen species when exposed to green light at 540 nm. This results in endothelial activation, although there is very little denudation, and is accompanied by rapid platelet adhesion. Thrombi in this model are primarily composed of platelets and contain less fibrin implying this process is mostly platelet driven[39]. The observation that

$p16^{INK4a}$ transgenic mice exhibit faster occlusion times in both of these models suggests there is likely a contribution by both soluble plasma factors and circulating cells. The differences observed in the time to flow restriction may reflect altered rates of thrombus growth between wild-type and $p16^{INK4a}$ transgenic mice, which could be indicative of the potential to produce larger thrombi.

In addition to more rapid rates of venous occlusion, $p16^{INK4a}$ transgenic mice also display impaired thrombus resolution. The percent occlusion appears to be correlated with the sustaining of inflammatory infiltration. It is possible that the inability to clear residual $FeCl_3$ from the intravascular space could be involved in further promoting thrombus formation. The increased production of PAI-1 observed in $p16^{INK4a}$ transgenic mice could also partly explain the thrombus resolution defect (Figure 3.6). Evidence in the literature suggests increased circulating PAI-1 could have a negative impact on wound healing and fibrinolysis. Originally, Farrehi *et al* demonstrated enhanced fibrinolysis in PAI-1 deficient mice[42]. Eitzman *et al* found that transgenic mice overexpressing PAI-1 have more severe fibrosis following bleomycin-induced lung injury[43]. Zaman et al showed a profibrotic effect of PAI-1 overexpression in the heart following myocardial infarction[44]. Recently, McDonald *et al* demonstrated that aged mice display impaired thrombus resolution following stasis induced by inferior vena cava (IVC) ligation[45]. In addition, they reported differences in various plasma and venous endothelium-associated proteins between aged and young wild-type mice[45]. While an exact mechanism to account for the observed thrombus resolution defect in the aged mice is not yet known[45], it is possible that changes in both the vessel wall and soluble plasma factors contribute, which may also be true of $p16^{INK4a}$ overexpressing mice.

To better understand differences in thrombus formation between $p16^{INK4a}$ transgenic and wild-type mice, coagulation parameters in mouse plasma samples were analyzed by CAT after inducing endothelial dysfunction with LPS. Plasma analysis by CAT is sensitive to changes in coagulation factor levels[46] and able to detect differences in thrombin generation parameters following a thrombotic event in human patients[47]. Our results show that $p16^{INK4a}$ transgenic mice are able to initiate thrombin generation faster, achieve a higher peak amount of thrombin, and peak at a faster rate than wild-type controls. Therefore, $p16^{INK4a}$ transgenic mice exhibit greater thrombin generation after LPS challenge compared to wild-type controls. To complement these data, $p16^{INK4a}$ transgenic mice also showed elevated plasma levels of TAT and PAI-1 following LPS challenge. These markers are commonly used to measure activation of coagulation (TAT)[48,49] and endothelial activation (PAI-1)[50,51]. Yamamoto et al showed that aged mice had elevated induction of PAI-1 compared to young mice after LPS treatment, suggesting PAI-1 is important in endotoxin-induced thrombosis[32]. Since PAI-1 is both a marker of endothelial cell senescence and a potent fibrinolysis inhibitor,[52] it could also participate in the delayed thrombus resolution seen in $p16^{INK4a}$ transgenic mice.

To begin establishing a mechanism for the observed differences between wild-type and $p16^{INK4a}$ transgenic mice, bone marrow transplants were performed to determine the contribution of hematopoietic cells to the prothrombotic phenotype. We found that wild-type mice given $p16^{INK4a}$ transgenic bone marrow had occlusion times very similar to that of transgenic controls. Similarly, $p16^{INK4a}$ transgenic mice given wild-type bone marrow had occlusion times very similar to wild-type controls. These data show that the prothrombotic

phenotype observed in mice overexpressing this gene is attributed to $p16^{INK4a}$ expression in hematopoietic cells.

A growing body of *in vitro* evidence suggests senescence in the vascular endothelium may also participate in the transition to a procoagulant state during aging. Senescence in the vascular endothelium is associated with an array of phenotypic changes with pathological consequences[7,8]. These changes include upregulation of PAI-1, inflammatory cytokines (including interleukin-1α and interleukin-6), matrix metalloproteinases, and the down-regulation of endothelial nitric oxide synthase[36,37,53]. Thus, a role for the endothelium cannot be discounted and may warrant further investigation in this model.

In contradistinction to the present data supporting a role for $p16^{INK4a}$ in venous thrombosis, a differing role for the expression of $p16^{INK4a}$ in arterial vascular diseases has been suggested. Through genome-wide association studies, several groups have found a link between single nucleotide polymorphisms (SNPs) on chromosome 9p21.3 close to the $p16^{INK4a}$ open-reading frame and several atherosclerotic diseases (coronary artery disease, ischemic stroke, abdominal aortic aneurysm)[54]. Liu *et al* have recently shown that individuals harboring the SNP genotypes associated with increased atherosclerotic risk exhibit decreased expression of $p16^{INK4a}$ and other *INK4/ARF* transcripts[55]. Individuals at increased risk appear to differ in the expression and splicing of linear and circular forms of *ANRIL*, a long, non-coding RNA emanating from the *INK4a/ARF* locus thought to participate in *INK4a/ARF* expression[56]. This observation suggests that decreased production of $p16^{INK4a}$ is associated with an increased risk of atherosclerosis, likely through limiting aberrant or excess proliferation of cellular components of atheromatous plaques. This suggests expression of anti-proliferative molecules at the *INK4a/ARF* locus protects individuals from

atherosclerosis[54,57]. In accord with this view, mice lacking $p16^{INK4a}$ have been shown to be more prone to vessel occlusion in a carotid artery injury model[58]. Our current data, combined with prior work in the venous system[36,37], suggest the intriguing possibility that age-induced $p16^{INK4a}$ expression and cellular senescence might play opposing roles with regard to thrombosis and atherosclerosis in the venous and arterial systems, respectively.

Characterizing the link between age-related genetic changes and age-related cardiovascular diseases such as venous thrombosis is of paramount importance. Overexpression of proteins such as $p16^{INK4a}$, which promote senescence and vascular dysfunction, could be the key age-related genetic change explaining cardiovascular maladies. Together, our results demonstrate that $p16^{INK4a}$ overexpression and cellular senescence contribute to a prothrombotic phenotype and defective thrombus resolution. The results of this study provide the foundation for research on the effects of vascular senescence on venous thrombosis.

3.5 References

1. Lowe GDO. Venous and arterial thrombosis: epidemiology and risk factors at various ages. *Maturitas*. 2004;47(4):259-263.

2. Esmon CT. Basic mechanisms and pathogenesis of venous thrombosis. *Blood Rev*. 2009;23(5):225-229.

3. Coon WW. Epidemiology of venous thromboembolism. *Ann. Surg*. 1977;186(2):149-164.

4. Merli GJ. Pathophysiology of venous thrombosis, thrombophilia, and the diagnosis of deep vein thrombosis-pulmonary embolism in the elderly. *Clin. Geriatr. Med*. 2006;22(1):75-92, viii-ix.

5. Silverstein RL, Bauer KA, Cushman M, et al. Venous thrombosis in the elderly: more questions than answers. *Blood*. 2007;110(9):3097-3101.

6. Jeyapalan JC, Sedivy JM. Cellular senescence and organismal aging. *Mech. Ageing Dev*. 2008;129(7-8):467-474.

7. Erusalimsky JD, Skene C. Mechanisms of endothelial senescence. *Exp. Physiol*. 2009;94(3):299-304.

8. Hayashi T, Yano K, Matsui-Hirai H, et al. Nitric oxide and endothelial cellular senescence. *Pharmacol. Ther*. 2008;120(3):333-339.

9. Adams PD. Healing and hurting: molecular mechanisms, functions, and pathologies of cellular senescence. *Mol. Cell*. 2009;36(1):2-14.

10. Stein GH, Dulić V. Molecular mechanisms for the senescent cell cycle arrest. *J. Investig. Dermatol. Symp. Proc*. 1998;3(1):14-18.

11. Krishnamurthy J, Torrice C, Ramsey MR, et al. Ink4a/Arf expression is a biomarker of aging. *J. Clin. Invest*. 2004;114(9):1299-1307.

12. Sharpless NE. Ink4a/Arf links senescence and aging. *Exp. Gerontol*. 2004;39(11-12):1751-1759.

13. Dimri GP. The search for biomarkers of aging: next stop INK4a/ARF locus. *Sci Aging Knowledge Environ*. 2004;2004(44):pe40.

14. Liu Y, Sanoff HK, Cho H, et al. Expression of p16(INK4a) in peripheral blood T-cells is a biomarker of human aging. *Aging Cell*. 2009;8(4):439-448.

15. Krishnamurthy J, Ramsey MR, Ligon KL, et al. p16INK4a induces an age-dependent decline in islet regenerative potential. *Nature*. 2006;443(7110):453-457.

16. Molofsky AV, Slutsky SG, Joseph NM, et al. Increasing p16INK4a expression decreases forebrain progenitors and neurogenesis during ageing. *Nature*. 2006;443(7110):448-452.

17. Janzen V, Forkert R, Fleming HE, et al. Stem-cell ageing modified by the cyclin-dependent kinase inhibitor p16INK4a. *Nature*. 2006;443(7110):421-426.

18. Campisi J, d'Adda di Fagagna F. Cellular senescence: when bad things happen to good cells. *Nat. Rev. Mol. Cell Biol*. 2007;8(9):729-740.

19. Buyue Y, Whinna HC, Sheehan JP. The heparin-binding exosite of factor IXa is a critical regulator of plasma thrombin generation and venous thrombosis. *Blood*. 2008;112(8):3234-3241.

20. Eitzman DT, Westrick RJ, Nabel EG, Ginsburg D. Plasminogen activator inhibitor-1 and vitronectin promote vascular thrombosis in mice. *Blood*. 2000;95(2):577-580.

21. Tchaikovski SN, VAN Vlijmen BJM, Rosing J, Tans G. Development of a calibrated automated thrombography based thrombin generation test in mouse plasma. *J. Thromb. Haemost*. 2007;5(10):2079-2086.

22. Pawlinski R, Wang J, Owens AP, et al. Hematopoietic and nonhematopoietic cell tissue factor activates the coagulation cascade in endotoxemic mice. *Blood*. 2010;116(5):806-814.

23. Wang X, Xu L. An optimized murine model of ferric chloride-induced arterial thrombosis for thrombosis research. *Thromb. Res*. 2005;115(1-2):95-100.

24. Westrick RJ, Winn ME, Eitzman DT. Murine models of vascular thrombosis (Eitzman series). *Arterioscler. Thromb. Vasc. Biol*. 2007;27(10):2079-2093.

25. Whinna HC. Overview of murine thrombosis models. *Thromb. Res*. 2008;122 Suppl 1:S64-69.

26. Jeske WP, Iqbal O, Fareed J, Kaiser B. A survey of venous thrombosis models. *Methods Mol. Med*. 2004;93:221-237.

27. Sachs UJH, Nieswandt B. In vivo thrombus formation in murine models. *Circ. Res*. 2007;100(7):979-991.

28. Rumbaut RE, Slaff DW, Burns AR. Microvascular thrombosis models in venules and arterioles in vivo. *Microcirculation*. 2005;12(3):259-274.

29. Wakefield TW, Myers DD, Henke PK. Mechanisms of venous thrombosis and resolution. *Arterioscler. Thromb. Vasc. Biol*. 2008;28(3):387-391.

30. Sattar N. Inflammation and endothelial dysfunction: intimate companions in the

pathogenesis of vascular disease? *Clin. Sci*. 2004;106(5):443-445.

31. Schouten M, Wiersinga WJ, Levi M, van der Poll T. Inflammation, endothelium, and coagulation in sepsis. *J. Leukoc. Biol*. 2008;83(3):536-545.

32. Yamamoto K, Shimokawa T, Yi H, et al. Aging accelerates endotoxin-induced thrombosis : increased responses of plasminogen activator inhibitor-1 and lipopolysaccharide signaling with aging. *Am. J. Pathol*. 2002;161(5):1805-1814.

33. Wang X. Lipopolysaccharide augments venous and arterial thrombosis in the mouse. *Thromb. Res*. 2008;123(2):355-360.

34. Wang J, Manly D, Kirchhofer D, Pawlinski R, Mackman N. Levels of microparticle tissue factor activity correlate with coagulation activation in endotoxemic mice. *J. Thromb. Haemost*. 2009;7(7):1092-1098.

35. Yanada M, Kojima T, Ishiguro K, et al. Impact of antithrombin deficiency in thrombogenesis: lipopolysaccharide and stress-induced thrombus formation in heterozygous antithrombin-deficient mice. *Blood*. 2002;99(7):2455-2458.

36. Erusalimsky JD, Kurz DJ. Cellular senescence in vivo: its relevance in ageing and cardiovascular disease. *Exp. Gerontol*. 2005;40(8-9):634-642.

37. Erusalimsky JD. Vascular endothelial senescence: from mechanisms to pathophysiology. *J. Appl. Physiol*. 2009;106(1):326-332.

38. Tseng MT, Dozier A, Haribabu B, Graham UM. Transendothelial migration of ferric ion in FeCl3 injured murine common carotid artery. *Thromb. Res*. 2006;118(2):275-280.

39. Mousa SA. In vivo models for the evaluation of antithrombotics and thrombolytics. *Methods Mol. Biol*. 2010;663:29-107.

40. Dubois C, Panicot-Dubois L, Merrill-Skoloff G, Furie B, Furie BC. Glycoprotein VI-dependent and -independent pathways of thrombus formation in vivo. *Blood*. 2006;107(10):3902-3906.

41. Woollard KJ, Sturgeon S, Chin-Dusting JPF, Salem HH, Jackson SP. Erythrocyte hemolysis and hemoglobin oxidation promote ferric chloride-induced vascular injury. *J. Biol. Chem*. 2009;284(19):13110-13118.

42. Farrehi PM, Ozaki CK, Carmeliet P, Fay WP. Regulation of arterial thrombolysis by plasminogen activator inhibitor-1 in mice. *Circulation*. 1998;97(10):1002-1008.

43. Eitzman DT, McCoy RD, Zheng X, et al. Bleomycin-induced pulmonary fibrosis in transgenic mice that either lack or overexpress the murine plasminogen activator inhibitor-1 gene. *J. Clin. Invest*. 1996;97(1):232-237.

44. Zaman AKMT, French CJ, Schneider DJ, Sobel BE. A profibrotic effect of plasminogen activator inhibitor type-1 (PAI-1) in the heart. *Exp. Biol. Med. (Maywood)*. 2009;234(3):246-254.

45. McDonald AP, Meier TR, Hawley AE, et al. Aging is associated with impaired thrombus resolution in a mouse model of stasis induced thrombosis. *Thromb. Res*. 2010;125(1):72-78.

46. Machlus KR, Colby EA, Wu JR, et al. Effects of tissue factor, thrombomodulin and elevated clotting factor levels on thrombin generation in the calibrated automated thrombogram. *Thromb. Haemost*. 2009;102(5):936-944.

47. ten Cate-Hoek AJ, Dielis AWJH, Spronk HMH, et al. Thrombin generation in patients after acute deep-vein thrombosis. *Thromb. Haemost*. 2008;100(2):240-245.

48. Wang J, Manly D, Kirchhofer D, Pawlinski R, Mackman N. Levels of microparticle tissue factor activity correlate with coagulation activation in endotoxemic mice. *J. Thromb. Haemost*. 2009;7(7):1092-1098.

49. Hron G, Kollars M, Weber H, et al. Tissue factor-positive microparticles: cellular origin and association with coagulation activation in patients with colorectal cancer. *Thromb. Haemost*. 2007;97(1):119-123.

50. Ruan QR, Zhang WJ, Hufnagl P, et al. Anisodamine counteracts lipopolysaccharide-induced tissue factor and plasminogen activator inhibitor-1 expression in human endothelial cells: contribution of the NF-kappa b pathway. *J. Vasc. Res*. 2001;38(1):13-19.

51. Zhang WJ, Wojta J, Binder BR. Notoginsenoside R1 counteracts endotoxin-induced activation of endothelial cells in vitro and endotoxin-induced lethality in mice in vivo. *Arterioscler. Thromb. Vasc. Biol*. 1997;17(3):465-474.

52. Gramling MW, Church FC. Plasminogen activator inhibitor-1 is an aggregate response factor with pleiotropic effects on cell signaling in vascular disease and the tumor microenvironment. *Thromb Res*. 2010. Available at: http://www.ncbi.nlm.nih.gov/pubmed/20079523 [Accessed March 12, 2010].

53. Rauscher FM, Goldschmidt-Clermont PJ, Davis BH, et al. Aging, progenitor cell exhaustion, and atherosclerosis. *Circulation*. 2003;108(4):457-463.

54. Jarinova O, Stewart AFR, Roberts R, et al. Functional analysis of the chromosome 9p21.3 coronary artery disease risk locus. *Arterioscler. Thromb. Vasc. Biol*. 2009;29(10):1671-1677.

55. Liu Y, Sanoff HK, Cho H, et al. INK4/ARF transcript expression is associated with chromosome 9p21 variants linked to atherosclerosis. *PLoS ONE*. 2009;4(4):e5027.

56. Burd CE, Jeck WR, Liu Y, et al. Expression of Linear and Novel Circular Forms of an INK4/ARF-Associated Non-Coding RNA Correlates with Atherosclerosis Risk. *PLoS Genet*. 2010;6(12):e1001233.

57. Visel A, Zhu Y, May D, et al. Targeted deletion of the 9p21 non-coding coronary artery disease risk interval in mice. *Nature*. 2010;464(7287):409-412.

58. Gizard F, Amant C, Barbier O, et al. PPAR alpha inhibits vascular smooth muscle cell proliferation underlying intimal hyperplasia by inducing the tumor suppressor p16INK4a. *J. Clin. Invest*. 2005;115(11):3228-3238.

Chapter 4.

Contribution of $p16^{INK4a}$ Expression in Monocytes and Macrophages to Thrombus Formation

4.1 Introduction

Age-related changes in hemostasis at the plasma and cellular levels contribute to the increased risk of cardiovascular disease in the elderly[1,2]. Senescence is a process that occurs with aging, limiting cellular proliferation and likely evolved to protect against malignant transformation. Cellular senescence is controlled at the molecular level by cell cycle inhibitors whose expression is stress-induced[3-6]. Among the cell cycle inhibitors, $p16^{INK4a}$ is most commonly associated with aging, as expression of this gene is positive correlated with age[7-10]. Age-dependent expression of $p16^{INK4a}$ has been studied in the context of vascular disorders and has been paradoxically implicated in both protection from and promotion of cardiovascular disease. More specifically, $p16^{INK4a}$ is thought to play a protective role in arterial disease by exhibiting its antiproliferative effects. In human studies, individuals harboring a single nucleotide polymorphism (SNP) on chromosome 9p21.3 that leads to decreased expression of $p16^{INK4a}$ have an increased risk of atherosclerosis[10]. This suggests $p16^{INK4a}$ protects against atherogenesis by inhibiting the aberrant proliferation of smooth muscle cells and foam cells during atherosclerotic plaque formation.

Conversely, a recent publication from our laboratory has shown that $p16^{INK4a}$ expression in mice promotes the development of age-related cardiovascular disease in the venous

circulation[11]. Mice transgenically overexpressing $p16^{INK4a}$ displayed accelerated thrombus formation, delayed thrombus resolution and plasma hypercoagulability. Adoptive transfer of this phenotype was observed in wild-type mice upon bone marrow transplantation from a $p16^{INK4a}$ transgenic donor. Likewise, the prothrombotic phenotype was obliterated in transgenic mice receiving wild-type bone marrow. These data suggest that $p16^{INK4a}$ expression in hematopoietic cells plays a critical role in venous thrombogenesis.

The goal of this study was to further characterize the effect of $p16^{INK4a}$ expression on venous thrombosis in a model of venous stasis. This thrombosis model is thought to be highly dependent on inflammatory cells originating in the hematopoietic compartment, thus an effect from $p16^{INK4a}$ in this cellular compartment should be observed.

4.2 Materials and Methods

Mice

All animal procedures were performed in accordance with protocols approved by the Institutional Animal Care and Use Committee, UNC-Chapel Hill. $p16^{INK4a}$ transgenic mice harbor a single copy integration of 60 kb of the murine $p16^{INK4a}$ locus, and exhibit a 3-8 fold increase in $p16^{INK4a}$ expression in all tissues examined to date. These mice do not overexpress other transcripts from the INK4/Arf locus (i.e., $p15^{INK4b}$ and Arf). Animals were bred on a C57BL/6J genetic background and backcrossed as detailed previously[12]. All mice included in this study were males at 8 weeks of age.

IVC Ligation

Stasis-induced venous thrombosis by inferior vena cava (IVC) ligation is a well-described model to study DVT in mice[13-15]. In this model, the IVC of anesthetized mice was exposed by laparotomy and dissected away from the aorta. A single ligature was placed around the IVC just below the renal vein branching using a 8-0 prolene suture. To achieve complete stasis, associated side and back branches were ligated or cauterized, respectively. The laparotomy was closed by first suturing the peritoneum with an absorbable, 5-0 vicryl suture followed by suturing the skin with an 8-0 prolene suture. Mice were euthanized 3 days post surgery and the IVC removed for analysis. Thrombi were normalized to length of the effected vessel and data are expressed as weight/length.

Immunohistochemistry

Tissues were extracted and fixed overnight in 4% paraformadehyde. Tissue embedding and cutting was performed in the UNC Linberger Comprehensive Cancer Center Animal Histopathology Core Facility. Briefly, 5 micron sections were cut from paraffin blocks and antigen retrieval was performed in Target Retrieval Solution (Dako – Capinteria, CA, S1699) in a 95°C water bath. Slides were blocked for 1 hour in 5% serum derived from the species in which the secondary antibody was made and subsequently stained with antibodies against fibrin (Gift of Dr. Marshall Runge and Dr. Alisa Wolberg, 59D8, 1:1000), PAI-1 (sc-8979, Santa Cruz Biotech, Santa Cruz, CA, USA, 1:250), F4/80 (Serotec MCA497GA, Serotec, Oxford, UK, 1:250), Ly6G (14-5931-82, eBioscience, San Diego, CA, USA 1:500), thrombomodulin (MAB3894, R&D Systems, Minneapolis, MN, USA, 1:500) or TF (Gift of Novo Nordisk, Bagsvaerd, Denmark and Dr. Maureane Hoffman,1:1000) for 1 hour at room temperature in a humidity-controlled chamber. Biotinylated secondary antibodies were obtained from Vector Laboratories. Tissue slides were developed using the avidin-biotin complex (ABC) method using reagents and protocols obtained from Dako. Negative control tissue sections were stained simultaneously in the absence of primary antibody. To analyze immunostained tissues, images were collected at 10x magnification (three images per tissue section) and the average number of positive pixels per image was quantified using Photoshop.

Monocyte/macrophage depletion

Liposomes packaged with clodronate or PBS were purchased from ClodronateLiposomes.org (Vrije Universiteit, Netherlands). Monocyte and macrophage depletion using clodronate

liposomes was performed as previously described[16,17]. Briefly, liposomes (1mg/mL) were injected twice intravenously via the retro-orbital plexus in a 0.2 mL volume. The first injection was 48 hours prior to IVC ligation surgery and the second injection was on the day of surgery. Depletion was confirmed by complete blood count (CBC) and by immunoblotting for the monocyte/macrophage marker F4/80 in the spleen.

Western Blotting Analysis

Tissues were homogenized using a PowerGen125 homogenizer (Fisher Scientific, Waltham, MA) in cold lysis buffer composed of 50 mM Tris, 150 mM NaCl, 1% Triton X-100, 1% deoxycholate, 1 mM EDTA, 0.1% sodium dodecylsulfate (SDS), 1 mM phenylmethanesulfonyl fluoride (PMSF), 5 mg/mL aprotinin, and 5 mg/mL leupeptin. Homogenized tissues were kept on ice for 30 minutes and centrifuged at 10,000 x g for 20 minutes at 4°C to separate insoluble material. Protein concentrations were measured using the BioRad Protein DC assay (BioRad, Hercules, CA, USA). Protein samples were separated on a 7.5% SDS polyacrylamide gel and electrophoretically transferred to a nitrocellulose membrane. Membranes were rinse in de-ionized water and non-specific binding was blocked using 5% non-fat dry milk in PBS containing 0.1% Tween 20 (PBST) for 1 hour at room temerature. Following blocking, the membranes were washed 3 times for 5 minutes in PBST. Membranes were incubated overnight at 4°C in primary antibody prepared in 2.5% non-fat dry milk on a rocker. Membranes were washed in PBST and incubated in secondary antibody prepared in 2.5% non-fat dry milk for 1 hour at room temperature. Membranes were washed in PBST and developed by chemiluminescence and exposure to X-ray film. The primary antibodies were rat anti-mouse F4/80 (1:2000) (Serotec, MCA497GA, Serotec,

Oxford, UK) with a peroxidase-conjugated secondary antibody used at a 1:4000 dilution and goat anti-human GAPDH (1:1000) (Santa Cruz Biotechnology, sc-48167, Santa Cruz, CA, USA) with a peroxidase conjugated secondary antibody used at a 1:3000 dilution.

Statistical Methods

All statistical analyses were performed with Graphpad Prism. All measurements are respresented as the mean ± standard error of the mean (SEM). Student's T-tests were performed to determine statistical relevance where indicated. Values of $p<0.05$ were considered statistically significant.

4.3 Results

Effect of $p16^{INK4a}$ expression on stasis-induced thrombus formation.

Mice overexpressing $p16^{INK4a}$ and wild-type littermate controls were compared in a model of stasis-induced thrombosis (n=4 per group). We found significantly larger thrombi in $p16^{INK4a}$ transgenic mice after a 3 day ligation compared to wild-type controls (Figure 4.1).

Histologic analysis of stasis-induced thrombi in wild-type and $p16^{INK4a}$ transgenic mice.

Fixed and paraffin embedded thrombi and associated vessel wall were analyzed histologically to determine any protein or cellular composition changes that may contribute to the increase in thrombus formation. No statistical differences were detected in fibrin content, tissue factor (TF), thrombomodulin (TM), plasminogen activator inhibitor (PAI-1), or neutrophil-associated LY6G levels (Figure 4.2A). However, a significant increase in the monocyte/macrophage marker F4/80 was observed in mice overexpressing $p16^{INK4a}$ (Figure 4.2B).

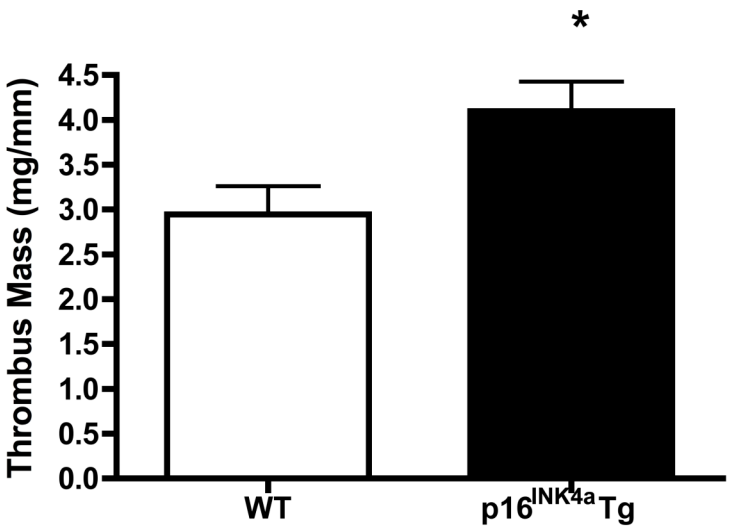

Figure 4.1. Mice overexpressing p16^{INK4a} have larger thrombi in a model of stasis-induced thrombosis. Wild-type and p16^{INK4a} transgenic mice (n=4 mice per group) underwent inferior vena cava (IVC) ligation to promote stasis-induced thrombosis. After a 3 day ligation, thrombi were extracted and analyzed for length and weight. Thrombus mass was determined by dividing thrombus weight by length. Data are represented as weight (mg) over length (mm). * denotes $p<0.05$

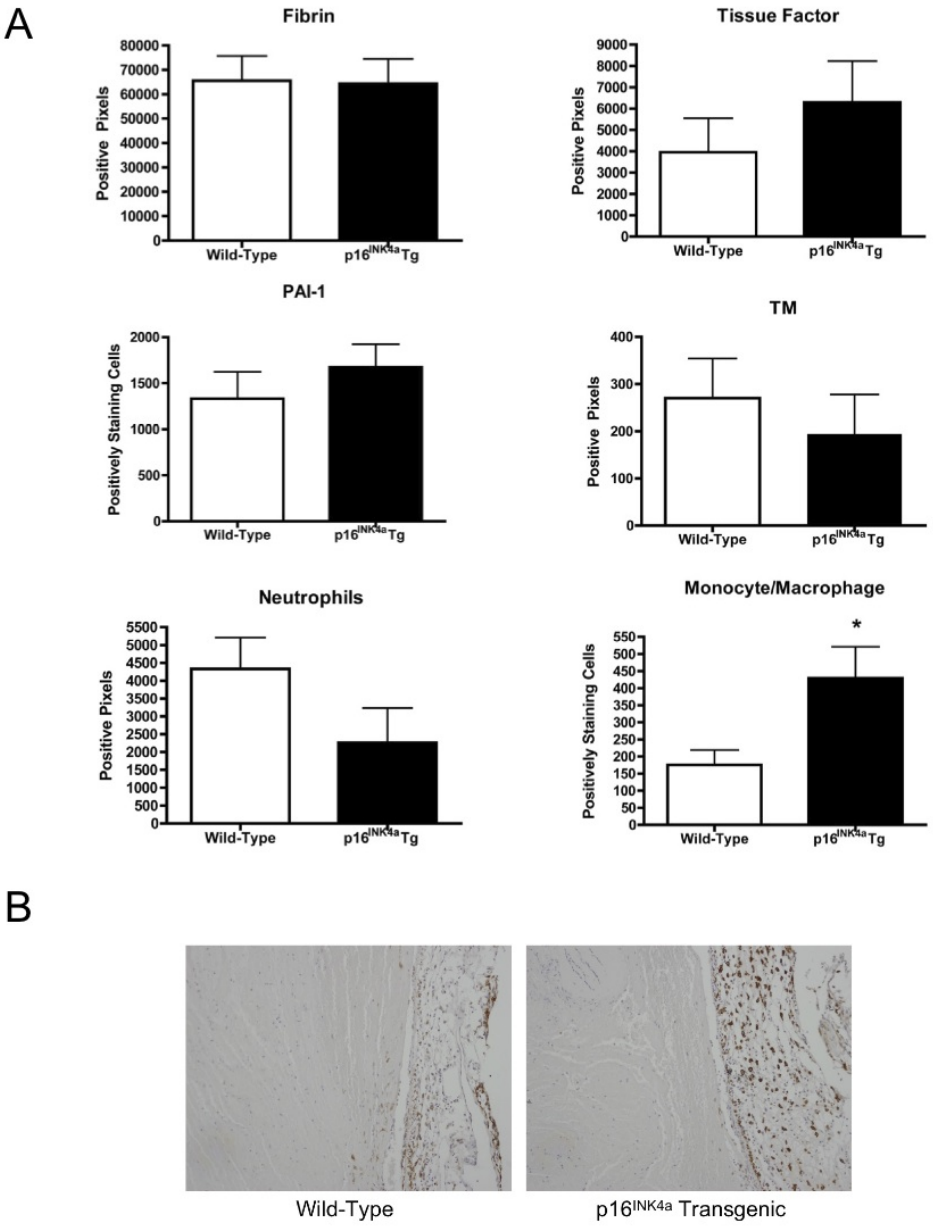

Figure 4.2. Immunostaining analysis of IVC containing thrombus. (A) Thrombosed IVCs were analyzed by immunohistochemistry to determine relative expression levels of several vessel wall and thrombus-associated proteins and inflammatory cells. Quantification was performed either in Photoshop or manually by counting positive cells and are expressed in number of positive pixels or number positively staining cells. * denotes $p<0.05$ (B) Representative images from F4/80 staining of thrombosed vessels.

Clodronate liposomes successfully deplete monocytes and macrophages.

Depletion of circulating monocytes by clodronate liposomes was confirmed by CBC of whole blood at the time of IVC collection. We detected approximately 50% depletion of monocytes in whole blood (Figure 4.3A). Depletion of tissue macrophages by clodronate liposomes was confirmed by immunoblot of the spleen at the time of IVC collection. The representative blot is shown with quantification by densitometry detecting approximately 45-50% depletion of tissue macrophages (Figure 4.3B).

Enhanced stasis-induced thrombosis is normalized to wild-type upon depletion of monocytes and macrophages.

To determine the contribution of $p16^{INK4a}$ expression in monocytes and macrophages in this model, both wild-type and $p16^{INK4a}$ transgenic mice were treated with clodronate liposomes 48 hours prior to, and on the day of IVC ligation surgery to deplete these cell types. We observed that while all mice receiving clodronate had larger thrombi when compared to those receiving PBS, thrombi from mice overexpressing $p16^{INK4a}$ were then the same size as wild-type controls (Figure 4.4).

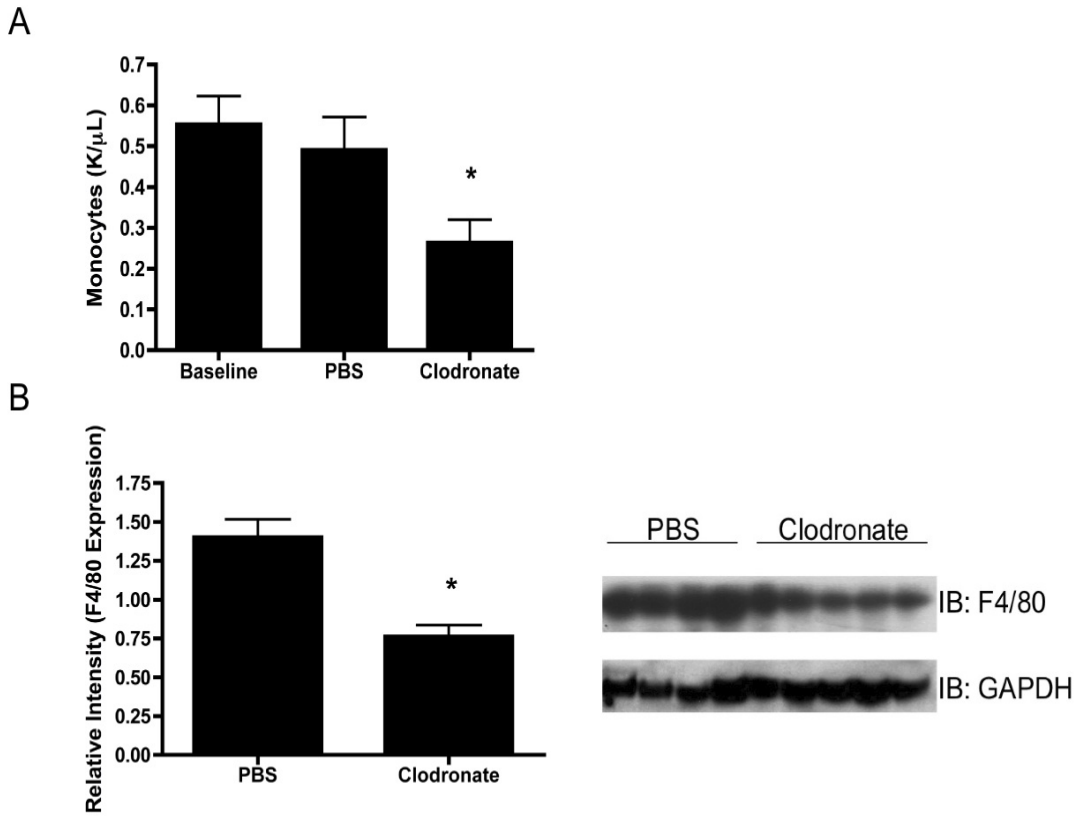

Figure 4.3. Clodronate liposomes deplete circulating monocytes and tissue macrophages. (A) Depletion of circulating monocytes was confirmed by blood count analysis using a Hemavet HV950FS. * denotes $p<0.05$ (B) Depletion of tissue macrophages was confirmed by homogenization and western blot analysis from spleens of liposome treated mice. Top panel shows a representative immunoblot of F4/80 macrophage marker expression in the spleens. Bottom panel shows quantification of immunoblot by densitometry. * denotes $p<0.01$

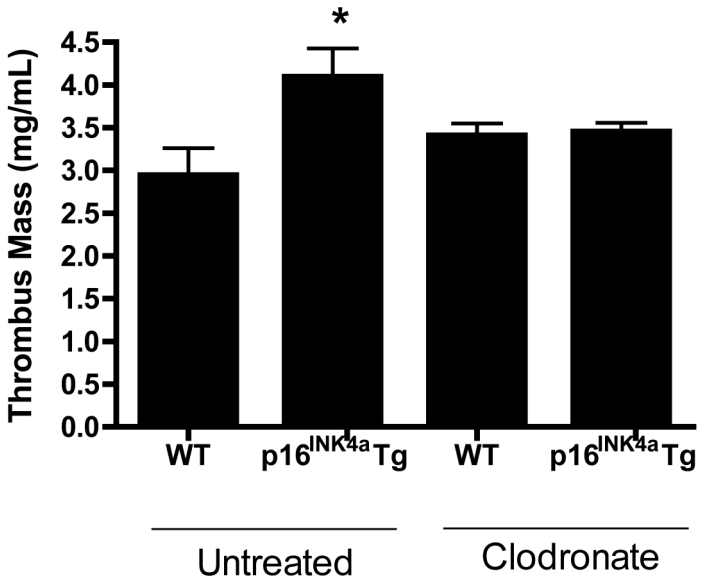

Figure 4.4. Monocyte and macrophage depletion normalizes p16^{INK4a} transgenic and wild-type stasis-induced thrombus size. IVC ligation thrombosis model was repeated in the presence of clodronate or control liposomes. Thrombus sizes show no difference between wild-type and transgenic mice. Data represented as thrombus weight (mg) over length (mm).

4.4 Discussion

Data on the contribution of $p16^{INK4a}$ expression to venous thrombosis in the elderly is largely non-existent. Previously, we have shown that expression of $p16^{INK4a}$ in hematopoietic cells is involved in promoting venous thrombosis in mouse models[11]. In this study, we use a stasis-induced thrombosis model to further characterize the effect of $p16^{INK4a}$ expression in inflammatory cells on promoting this process.

We found that mice overexpressing $p16^{INK4a}$ have significantly larger thrombi than wild-type after 3 days of IVC ligation (Figure 4.1). This finding confirmed our previous data showing $p16^{INK4a}$ transgenic mice display a prothrombotic phenotype. Qualitative histologic analysis by H&E staining showed no apparent differences in general composition or proteinaceous content between transgenic and control mice (data not shown). Upon further analysis by immunohistochemistry, we found no significant differences in endothelial-derived proteins such as PAI-1, TF, or TM. There are currently no data to suggest that elevated TF is a phenomenon associated with aging or senescence so these findings were not surprising. We previously found increases in circulating and liver-derived PAI-1 following endotoxemia. Elevated PAI-1 is a marker of both aging and endothelial cell senescence, however it does not appear to be playing a role in early stasis-induced thrombogenesis. Reduced TM has recently been found to exacerbate the response to endotoxin treatment in aged mice[18]. While we found a slight trend in TM reduction in $p16^{INK4a}$ overexpressing mice after IVC ligation, staining for TM in lungs for both untreated and LPS treated mice from an unrelated experiment showed no difference in TM expression between $p16^{INK4a}$ transgenic and control mice (data not included). This further confirmed our previous bone marrow transplantation data showing hematopoietic expression and not endothelial expression of

$p16^{INK4a}$ was responsible for driving this phenotype. Additionally, no difference in fibrin content by immunostaining was observed between $p16^{INK4a}$ transgenic and wild-type control mice (Figure 4.2A).

When staining for the presence of inflammatory leukocytes, no quantifiable difference was detected in neutrophil levels as measured by expression of the neutrophil surface marker Ly6G (Figure 4.2A). In the natural history of venous thrombosis, neutrophils are the first leukocytes detected in the thrombus, present as early as 2 hours following IVC ligation[19]. Neutrophils are thought to play a role in the clearance of early forming thrombi rather than promoting thrombogenesis, as data from Varma *et al* showed that neutrophil depletion led to increased thrombus size[20]. As no difference in neutrophil infiltration was apparent in our model, we conclude that the absence of neutrophils to promote early thrombus clearance was not the cause of greater thrombus size with $p16^{INK4a}$ overexpression.

Conversely, immunostaining for F4/80 monocyte/macrophage antigen showed significant increases in monocyte and macrophage infiltration in thrombi from $p16^{INK4a}$ overexpressing mice compared to wild-type (Figure 4.2). Macrophage responses during thrombosis occur following neutrophil infiltration, with 3 days post thrombogenesis likely representing one of the earliest points during infiltration, followed by linear increases in macrophage presence over time during thrombus resolution[21]. Macrophages are recruited to the thrombus in response to fibrinogen as well as toll-like receptors and selectin expressed on neutrophils and damaged endothelial cells. Macrophages play an important role in scavenging dead cells and promoting proteolysis and wound healing by releasing proteases, growth factors and cytokines[21]. However, macrophages also express procoagulant TF and antifibrinolytic PAI-1, therefore an overabundance of these cells, especially early on in thrombus formation might

exacerbate thrombosis by propagating thrombin generation and inhibiting plasminogen activation. The increase in monocytes/macrophages seen in our model align with our previous findings that thrombus formation was enhanced by $p16^{INK4a}$ expression in the hematopoietic compartment.

To determine the role of monocytes and macrophages in thrombus formation, we repeated the 3 day IVC ligation studies in $p16^{INK4a}$ transgenic and wild-type littermate control mice after reduction of monocytes and macrophages with clodronate liposomes. Cell reduction was confirmed by measuring circulating monocytes in whole blood by Hemavet analysis and also by measuring F4/80 surface marker expression in spleens, an organ known to be abundant in macrophages (Figure 4.3). We found that the thrombi extracted from monocyte/macrophage-depleted mice were indistinguishable in size between $p16^{INK4a}$ overexpressing and wild-type control mice (Figure 4.4). Mice treated with PBS control liposomes showed a similar increase in thrombus size in $p16^{INK4a}$ transgenic mice to those data reported in the absence of liposome treatment (n=2 per group, data not shown). These data suggest that $p16^{INK4a}$ expression in monocytes and macrophages is likely to be the driving force behind increased venous thrombosis in $p16^{INK4a}$ overexpressing mice. Had the effect been mediated by neutrophils or any other cell type or even circulating protein factor level, we would not have succeeded in normalizing the thrombus sizes.

One limitation of this study is that we collected data at only one time point during venous thrombosis. Our previous data showed delayed venous thrombus resolution over time in $p16^{INK4a}$ transgenic mice after $FeCl_3$ injury. Thus, it would be very important and interesting to see what is occurring at the earlier and later time points in this model, to determine if there is sustained elevation of macrophages and how this affects thrombus resolution.

Another limitation is that we found similar results upon depletion of monocytes and macrophages as Valmar *et al* found when depleting neutrophils. Mice treated with clodronate liposomes have much larger thrombus mass than those untreated or treated with control liposomes. While there was no difference in neutrophil counts that would suggest unintended phagocytosis of liposomes by these cells, this could be explained by the lack of early thrombus clearance by monocytes trapped within the growing thrombus. Additionally, the effects of free clonodronate to the circulation are unknown. It is thought that upon phagocytosis of liposomes, any free clondronate released upon cellular apoptosis is rapidly cleared by the kidneys[22]. However, any effects exhibited prior to clearance are unexplored.

These data remain preliminary as a prior attempt at performing this experiment using a three-dose treatment strategy resulted in post-surgical death of all animals, leaving a cohort of only 3 animals per group receiving 2 doses of clodronate liposomes. More mice are required to repeat this experiment with treatment of both clodronate and PBS control liposomes. Additionally, repeating the IVC ligation studies in monocyte/macrophage specific $p16^{INK4a}$ knock-out or $p16^{INK4a}$ overexppressing mice would more directly test our hypothesis that expression of this protein in monocytes and macrophges is responsible for the prothrombotic phenotype.

In conclusion, we have found that $p16^{INK4a}$ expression in monocytes and macrophages does contribute to venous thrombosis. It remains unclear whether this is simply due to enhanced recruitment of these cells to the thrombus or if perhaps these cells also have an altered phenotype making them more procoagulant, proinflammatory, and antifibrinolytic than wild-type counterparts. Interestingly, recent literature describes phenotypic changes in senescent monocytes that could have important pathophysiologic consequences. In healthy

individuals, the vast majority of circulating monocytes express $CD14^{++}CD16^{-}$ surface antigens, however elderly individuals and those with chronic illnesses show expansion of a $CD14^{+}CD16^{+}$ monocyte population. These cells exhibit similar characteristics to senescent cells and have increased antigenic sensitivity, more proinflammatory secretions, increased expression of vascular adhesion molecules, and increased endothelial cell adhesion[23]. This suggests the interesting possibility that monocytes and macrophages from $p16^{INK4a}$ overexpressing mice could be phenotypically distinct from wild-type control cells, and that $p16^{INK4a}$ upregulation in aging humans could be promoting this cellular population shift. This data strongly suggests that $p16^{INK4a}$ expression in monocytes and macrophages is important for venous thrombosis.

4.5 References

1. Mari D, Coppola R, Provenzano R. Hemostasis factors and aging. *Exp. Gerontol*. 2008;43(2):66-73.

2. Tofler GH, Massaro J, Levy D, et al. Relation of the prothrombotic state to increasing age (from the Framingham Offspring Study). *Am. J. Cardiol*. 2005;96(9):1280-1283.

3. Jeyapalan JC, Sedivy JM. Cellular senescence and organismal aging. *Mech. Ageing Dev*. 2008;129(7-8):467-474.

4. Adams PD. Healing and hurting: molecular mechanisms, functions, and pathologies of cellular senescence. *Mol. Cell*. 2009;36(1):2-14.

5. Erusalimsky JD, Skene C. Mechanisms of endothelial senescence. *Exp. Physiol*. 2009;94(3):299-304.

6. Hayashi T, Yano K, Matsui-Hirai H, et al. Nitric oxide and endothelial cellular senescence. *Pharmacol. Ther*. 2008;120(3):333-339.

7. Krishnamurthy J, Torrice C, Ramsey MR, et al. Ink4a/Arf expression is a biomarker of aging. *J. Clin. Invest*. 2004;114(9):1299-1307.

8. Sharpless NE. Ink4a/Arf links senescence and aging. *Exp. Gerontol*. 2004;39(11-12):1751-1759.

9. Dimri GP. The search for biomarkers of aging: next stop INK4a/ARF locus. *Sci Aging Knowledge Environ*. 2004;2004(44):pe40.

10. Liu Y, Sanoff HK, Cho H, et al. INK4/ARF transcript expression is associated with chromosome 9p21 variants linked to atherosclerosis. *PLoS ONE*. 2009;4(4):e5027.

11. Cardenas JC, Owens AP, Krishnamurthy J, et al. Overexpression of the cell cycle inhibitor p16INK4a promotes a prothrombotic phenotype following vascular injury in mice. *Arterioscler. Thromb. Vasc. Biol*. 2011;31(4):827-833.

12. Krishnamurthy J, Ramsey MR, Ligon KL, et al. p16INK4a induces an age-dependent decline in islet regenerative potential. *Nature*. 2006;443(7110):453-457.

13. Wrobleski SK, Farris DM, Diaz JA, Myers DD, Wakefield TW. Mouse complete stasis model of inferior vena cava thrombosis. *J Vis Exp*. 2011;(52). Available at: http://www.ncbi.nlm.nih.gov/pubmed/21712794 [Accessed April 20, 2012].

14. Nosaka M, Ishida Y, Kimura A, Kondo T. Time-dependent appearance of intrathrombus neutrophils and macrophages in a stasis-induced deep vein thrombosis model and its application to thrombus age determination. *Int. J. Legal Med*. 2009;123(3):235-240.

15. Zhou J, May L, Liao P, Gross PL, Weitz JI. Inferior vena cava ligation rapidly induces tissue factor expression and venous thrombosis in rats. *Arterioscler. Thromb. Vasc. Biol*. 2009;29(6):863-869.

16. Danenberg HD, Fishbein I, Gao J, et al. Macrophage depletion by clodronate-containing liposomes reduces neointimal formation after balloon injury in rats and rabbits. *Circulation*. 2002;106(5):599-605.

17. Zandbergen HR, Sharma UC, Gupta S, et al. Macrophage depletion in hypertensive rats accelerates development of cardiomyopathy. *J. Cardiovasc. Pharmacol. Ther*. 2009;14(1):68-75.

18. Starr ME, Ueda J, Takahashi H, et al. Age-dependent vulnerability to endotoxemia is associated with reduction of anticoagulant factors activated protein C and thrombomodulin. *Blood*. 2010;115(23):4886-4893.

19. von Brühl M, Stark K, Steinhart A, et al. Monocytes, neutrophils, and platelets cooperate to initiate and propagate venous thrombosis in mice in vivo. *J. Exp. Med*. 2012;209(4):819-835.

20. Varma MR, Varga AJ, Knipp BS, et al. Neutropenia impairs venous thrombosis resolution in the rat. *J. Vasc. Surg*. 2003;38(5):1090-1098.

21. Saha P, Humphries J, Modarai B, et al. Leukocytes and the natural history of deep vein thrombosis: current concepts and future directions. *Arterioscler. Thromb. Vasc. Biol*. 2011;31(3):506-512.

22. Claassen I, Van Rooijen N, Claassen E. A new method for removal of mononuclear phagocytes from heterogeneous cell populations in vitro, using the liposome-mediated macrophage 'suicide' technique. *J. Immunol. Methods*. 1990;134(2):153-161.

23. Merino A, Buendia P, Martin-Malo A, et al. Senescent CD14+CD16+ monocytes exhibit proinflammatory and proatherosclerotic activity. *J. Immunol*. 2011;186(3):1809-1815.

Chapter 5.

Vascular Endothelial Cell Senescence is Associated with a Prothrombotic Phenotype

5.1 Introduction

Venous thrombosis is a dynamic process involving dysregulation of pro and anticoagulant processes in the blood and vessel wall. The vascular endothelium is an important tissue in both the venous and arterial circulation, providing the barrier between the luminal blood and intima of the vessel wall. As the only non-circulating cell type in direct contact with the flowing blood, endothelial cells are pivotal in preventing thrombosis while still maintaining hemostasis[1,2]. Anticoagulant in nature, endothelial cells produce an array of proteins designed to inhibit the generation of thrombin such as heparin and dermatan sulfates, which enhance the activity of circulating antithrombin[3,4], and also thrombomodulin and its cofactor endothelial protein C receptor (EPCR), which activate anticoagulant protein C upon binding of thrombin[5,6]. In addition to inhibiting thrombin generation, endothelial cells express tissue factor pathway inhibitor (TFPI), a key inhibitor of tissue factor (TF)[7], which is the most potent initiator of extrinsic blood coagulation. Endothelial cells are also key mediators of fibrinolysis through production of both tissue and urokinase plasminogen activators (tPA and uPA) and the physiologic inhibitor of these molecules, plasminogen activator inhibitor (PAI-1)[8-10]. Additionally, expression of adhesion molecules, nitric oxide, and prostacyclin make endothelial cells key mediators of leukocyte binding, platelet activation/inactivation, and vasoconstriction/dilation[11-14]. Thus, the vascular endothelium is a

very important regulator of events involving the initiation, propogation and dissolution of blood clots.

Endothelial dysfunction can cause the endothelium to go from a quiescent, anticoagulant surface to one that is procoagulant and is thought to be a consequence of human aging[15]. Endothelial dysfunction is associated with increased expression of procoagulant TF[16], antifibrinolytic PAI-1[17], proinflammatory cytokines[18] with a concomitant decrease in anticoagulant thrombomodulin[19] and the vasodialtor nitric oxide[20,21]. All are changes that can contribute to venous thrombogenesis. Endothelial dysfunction during aging is not well understood, however one potential cause is cellular senescence.

Senescence is a process through which mitotic division is irreversibly halted either by cellular sensing of telomere shortening or through stress-induced expression of cell cycle inhibitors. Vascular endothelial cells will undergo senescence in response to a variety of stressors including inflammation or oxidative damage through upregulation of the cell cycle inhibitor, $p16^{INK4a}$[22,23]. $p16^{INK4a}$ functions by binding to cyclin-dependent kindases (CDK) 4 and 6, disrupting phosphorylation of the retinoblastoma protein (Rb) by these kinases, causing a G1 cell cycle arrest[24]. Senescence in the vascular endothelium is associated with an array of phenotypic changes with possible cardiovascular consequences[25,26]. These include upregulation of PAI-1, multiple inflammatory cytokines, and matrixmetalloproteases (MMPs)[25]. These changes, combined with other effects of aging in endothelial cells mentioned previously, can contribute to venous thrombotic complications in the elderly. The aim of this study was to examine the phenotypic changes that occur when vascular endothelial cells undergo senescence and how this affects blood coagulation on the endothelial cell surface.

5.2 Materials and Methods

Cell Culture

Human umbilical vein endothelial cells (HUVEC) pooled from multiple donors were obtained from Lonza. HUVEC were maintained in endothelial basal medium (EBM-2) supplemented with 0.2% FBS, 0.4% hFGF-B, 0.1% VEGF, 0.1% IGF-1, 0.1% Ascorbic Acid, 0.1% hEGF, 0.1% GA-1000, 0.1% heparin, 1% L-glutamine, and 1% penicillin/streptomycin solution. HUVEC were grown in a humidified chamber at 37°C with 5% CO_2.

Senescence-associated (SA) β-Galactosidase Activity Assay

SA β-galactosidase activity staining was performed using a kit (Cell Signaling, 9860S, Beverly, MA, USA). Briefly, HUVEC were grown to 80% confluency in a 6 well plate, washed with PBS and fixed with 2% formaldehyde and 0.2% glutaraldehyde. Cells were washed and stained with β-galactosidase solution containing 5-bromo-4-chloro-3-indolyk-βD-galactopyranoside (X-gal), potassium ferrocyanide, and potassium ferricyanide in citric acid/sodium phosphate.

Quantitative Polymerase Chain Reaction (PCR)

RNA isolation from HUVEC was performed using Trizol reagent (Invitrogen) according to the manufacturer's specifications. RNA was reverse transcribed (2 μg) with Moloney murine leukemia virus reverse transcriptase (Biorad, iScript™) according to the manufacturer's instructions. Initial denaturation was performed at 95°C for 5 min followed by cDNA amplification over 40 cycles (denaturation at 95°C for 20 sec, annealing at 55°C for 1 min,

elongation at 68°C for 30 sec) using an Eppendorf thermocycler. SYBR Green probe was used for quantitative reactions (Applied Biosystems, Foster City, CA, USA). Sequences for the primers used were: HPRT forward, TGG AGT CCT ATT GAC ATC GCC AGT; HPRT reverse, AAC AAC AAT CCG CCC AAA GGG AAC; GAPDH forward, ACC ACA GTC CAT GCC ATC AC; GAPDH reverse, TCC ACC ACC CTG TTG CTG TA; PAI-1 forward, 5'-AAT CAG ACG GCA GCA CTG TC-3'; PAI-1 reverse, 5'CTG AAC ATG TCG GTC ATT CC-3'. Primers for $p16^{INK4a}$ were purchased from Santa Cruz (Santa Cruz Biotechnology, sc-36143-PR, Santa Cruz, CA, USA). Ct vales were averaged for each reaction and expression was normalized to HPRT or GAPDH loading control. Relative expression was determined with the $2^{-\Delta\Delta Ct}$ method, normalizing expression of passage 3 HUVEC to 1.

Western Blotting Analysis

Confluent cells were lysed in cold lysis buffer composed of 50 mM Tris, 150 mM NaCl, 1% Triton X-100, 1% deoxycholate, 1 mM EDTA, 0.1% sodium dodecylsulfate (SDS), 1 mM phenylmethanesulfonyl fluoride (PMSF), 5 mg/mL aprotinin, and 5 mg/mL leupeptin. Cell lysates were kept on ice and centrifuged at 10,000 x g for 20 minutes at 4°C to separate insoluble material. Protein concentrations were measured using the BioRad Protein DC assay (BioRad, Hercules, CA, USA). Protein samples were separated on a 7.5% SDS polyacrylamide gel and electrophoretically transferred to a nitrocellulose membrane. Membranes were rinse in de-ionized water and non-specific binding was blocked using 5% non-fat dry milk in PBS containing 0.1% Tween 20 (PBST) for 1 hour at room temerature. Following blocking, the membranes were washed 3 x 5 minutes in PBST. Membranes were

incubated overnight at 4°C in primary antibody prepared in 2.5% non-fat dry milk on a rocker. Membranes were washed 3 x 5 minutes in PBST and incubated in secondary antibody prepared in 2.5% non-fat dry milk for 1 hour at room temperature. Membranes were washed 3 x 5 minutes in PBST and developed by chemiluminescence and exposure to X-ray film. The primary antibodies were used at a 1:1000 dilution and secondary antibodies at a 1:3000 dilution unless otherwise noted. Primary antibodies used for these experiments were $p16^{INK4a}$ (Santa Cruz Biotechnology, sc- 468, Santa Cruz, CA, USA), TM (Abcam, ab6980, Cambridge, MA, USA), EPCR (JNK1494, Gift of Dr. Chuck Esmon, primary 1:2000, secondary 1:6000), PAI-1 (Molecular Innovations, ASHPAI, Novi, MI), and GAPDH (Santa Cruz Biotechnology, sc-48167, Santa Cruz, CA, USA).

Clot formation assay

Clot formation was initiated on the surface of HUVEC in a 96-well plate by adding calcium (10 mM, final) and normal pooled plasma (87%, final). Clot formation was monitored by turbidity at 405 nM for 1 hour at 37°C using a SpectraMax Plus 384 (Molecular Devices, Sunnyvale, CA, USA) plate reader.

Thrombin Generation

Thrombin generation was measured by calibrated automated thrombography (CAT) using Z-Gly-Gly-Arg-AMC fluorogenic substrate for thrombin (Diagnostica Stago, Parsippany, NJ) on a Fluoroskan Ascent fluorometer (ThermoLabsystem, Helsinki, Finland). Normal pooled human plasma (80 μL) was added to the washed HUVEC monolayer to initiate the reaction. Variations in plasma color were accounted for using a α2-macroglobulin/thrombin calibrator

reagent (Diagnostica Stago, Parsippany, NJ). Parameters were calculated by Thrombinoscope software version 3.0.0.29 (Thrombinoscope BV, Maastricht, Netherlands).

Clot structure analysis by laser scanning confocal microscopy

Clot structure was analyzed as described previously[27]. HUVEC were plated in Lab-Tek II chamber slides (Nalge Nunc International) at a density of 33,000 cells/well). Once cells reached 80% confluency, clots were formed on the washed cell surface using normal pooled plasma (87%, final) and calcium (10 nM, final) in the presence of AlexaFluor-488-labeled fibrinogen (10ug/150uL volume, 3.2% of total fibrinogen, Gift of Dr. Alisa Wolberg). A clotting assay was performed in parallel on cells plated at the same time in a 96 well plate to ensure a constant final turbidity was achieved prior to microscopy analysis. Clots were imaged using a Zeiss LSM5 Pascal laser scanning confocal microscope under the conditions previously described[27].

Density of the fibrin network was analyzed in ImageJ. A random grid of 2 pixel crosses was placed over deconvolved z-stack images and the fibers that crossed through the intersection of those crosses was counted manually and divided by the number of crosses on the image.

TF activity

TF activity on HUVEC surface was measured by incubating washed cells with calcium (5 mM), FVIIa (100 pM) and FX (135 nM) for 5 minutes. Generation of FXa was then measured by cleavage of a chromogenic substrate (0.5 mM) detected at 405 nm for 30 minutes. Cells were stimulated with 3 ng/mL TNF-α 4 hours prior to TF activity assay. This

is assay was done in the presence of anti-TF antibody (10 μg/mL, gift Dr. Nigel Mackman) or control IgG (10 μg/mL) which was added 5 minutes prior to assay reagents.

Activated Protein C Generation

The ability to generate APC on HUVEC surface was measured by incubating washed cells with thrombin (10 nM), and protein C (0.5 μM) in buffer containing 1% bovine serum albumin, 3 mM $CaCl_2$ and 0.6 mM $MgCl_2$ for 30 minutes. The reaction was then quenched by the addition of heparin (2 U/mL) and antithrombin (0.5 μM). The generation of APC was then monitored by cleavage of a chromogenic substrate (0.15 mM) detected at 405 nM for 30 minutes. This is assay was done in the presence of anti-TM antibody (20 μg/mL, gift Dr. Chuck Esmon) or control IgG (20 μg/mL) which was added 5 minutes prior to assay reagents.

Immunohistochemistry

Tissues were extracted and fixed overnight in 4% paraformadehyde. Tissue embedding and cutting was performed in the UNC Linberger Comprehensive Cancer Center Animal Histopathology Core Facility. Briefly, 5 micron sections were cut from paraffin blocks and antigen retrieval was performed in Target Retrieval Solution (Dako – Capinteria, CA, S1699) in a 95°C water bath. Slides were blocked for 1 hour in 5% serum derived from the species in which the secondary antibody was made and subsequently stained with an antibody against thrombomodulin (MAB3894, R&D Systems, Minneapolis, MN, USA, 1:500) for 1 hour at room temperature in a humidity-controlled chamber. Biotinylated secondary antibodies were obtained from Vector Laboratories. Tissue slides were developed using the avidin-biotin

complex (ABC) method using reagents and protocols obtained from Dako. Negative control tissue sections were stained simultaneously in the absence of primary antibody. To analyze immunostained tissues, images were collected at 10x magnification (three images per tissue section) and the average number of positive pixels per image was quantified using Photoshop.

Statistical Methods

All statistical analyses were performed with Graphpad Prism. All measurements are respresented as the mean ± standard error of the mean (SEM). Student's T-tests were performed to determine statistical relevance where indicated. Values of $p<0.05$ were considered statistically significant.

5.3 Results

Serial passaging induces $p16^{INK4a}$ upregulation and cellular senescence in endothelial cells.

Human umbilical vein endothelial cells (HUVEC) were serial passaged to induce replicative senescence in vitro. HUVEC were compared at early passage (3), middle passage (6) and late passage (9) for markers of endothelial senescence. We observed significant increases in SA β-galactosidase expression in late passage HUVEC when compared to early and middle passages (Figure 5.1A). This was accompanied by elevated $p16^{INK4a}$ mRNA and protein levels (Figure 5.1B). Plasminogen activator inhibitor (PAI-1) is a known marker of senescence specific to endothelial cells[17,28]. We observe increases in PAI-1 expression at both the mRNA and protein levels (Figure 5.1C).

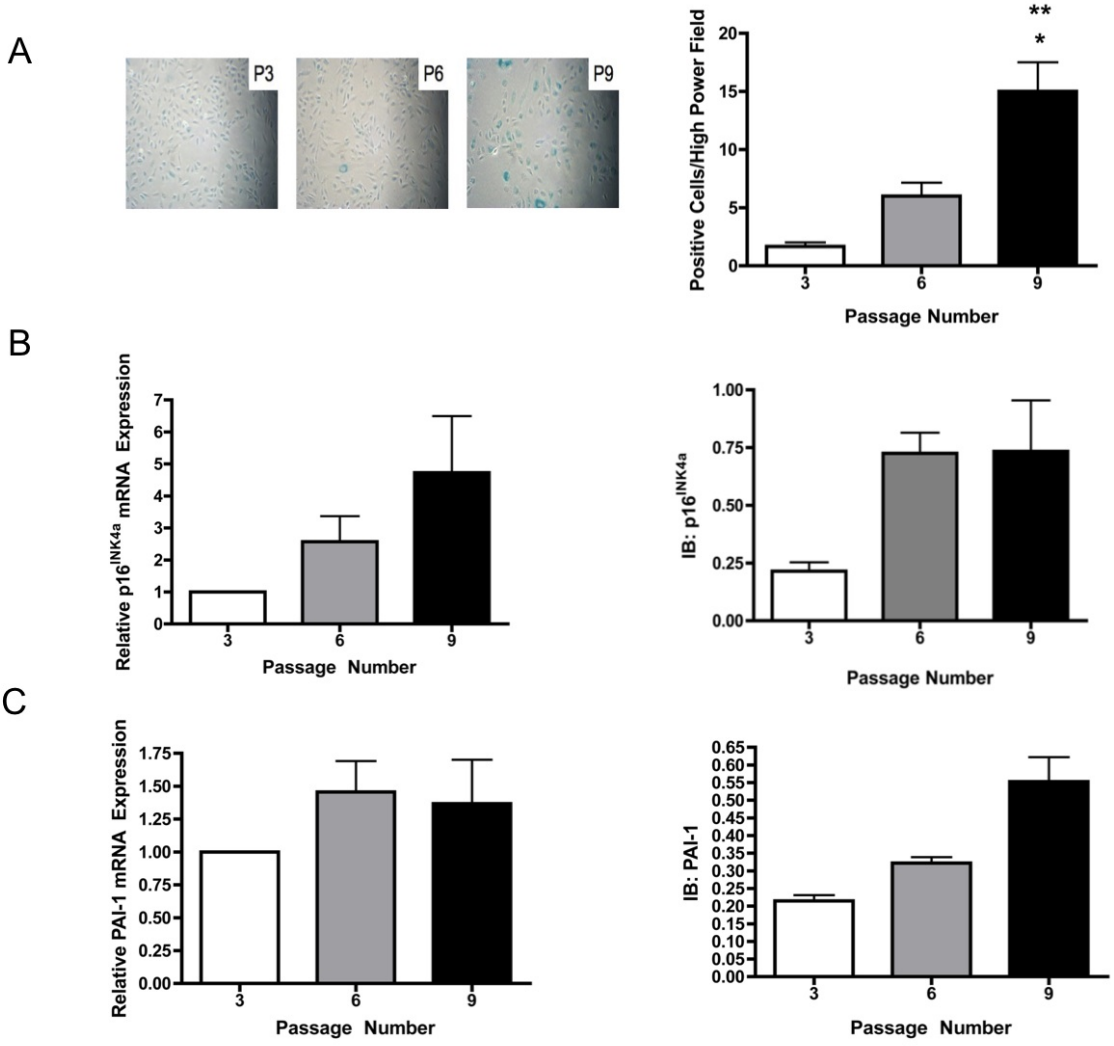

Figure 5.1. Endothelial cell senescence is induced through serial passaging. (A) Senescence-associated beta galactosidase stain comparing passages 3, 6, and 9. Expression levels of $p16^{INK4a}$ (B) and PAI-1 (C) in serial passaged HUVEC at the mRNA and protein level. mRNA expression analysis was performed by real time PCR and is relative to GAPDH. Protein levels were measured by immunoblot (IB) and expression levels were quantied relative to GAPDH using ImageJ. * denotes $p<0.05$ and ** denotes $p<0.01$ vs passage 3.

Serial passaging is associated with faster rates of clot formation and increased thrombin generation.

In order to determine procoagulant potential of senescent endothelial cells, HUVEC were stimulated with TNF-α and examined by plasma clotting assays. We observed that the rate of fibrin assembly increases with passage number (Figure 5.2A), indicative of faster clot formation. We also observed increases in the peak amount of thrombin generation by CAT (Figure 5.2B), suggesting that senescent HUVEC support greater thrombin generation on the cell surface.

Effect of serial passaging on the fibrin network density of clots formed on the cell surface.

Thrombin concentration is known to determine clot fibrin network density[29,30]. Clots with denser, more tightly woven fibrin networks are more stable and less prone to lysis than those clots with loosely woven fibrin networks. We used confocal microscopy to measure this parameter in senescent HUVEC. We observed that fibrin network density increases with serial passaging (Figure 5.3). This suggests that as HUVEC undergo senescence, they support the formation of more dense, stable clots on the cell surface.

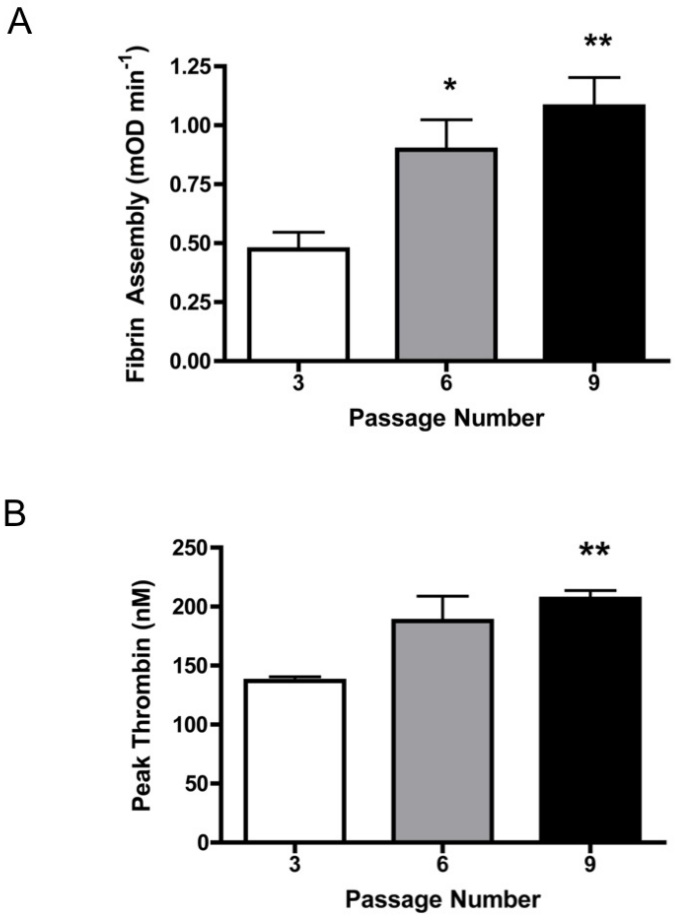

Figure 5.2. Senescent endothelial cells display faster clot formation and increased thrombin generation. (A) Rate of clot formation over cells as measured by plasma clotting assay. (B) Peak thrombin generation in plasma over cells measured by calibrated automated thrombography (CAT). * denotes $p<0.05$ and ** denotes $p<0.01$ vs passage 3.

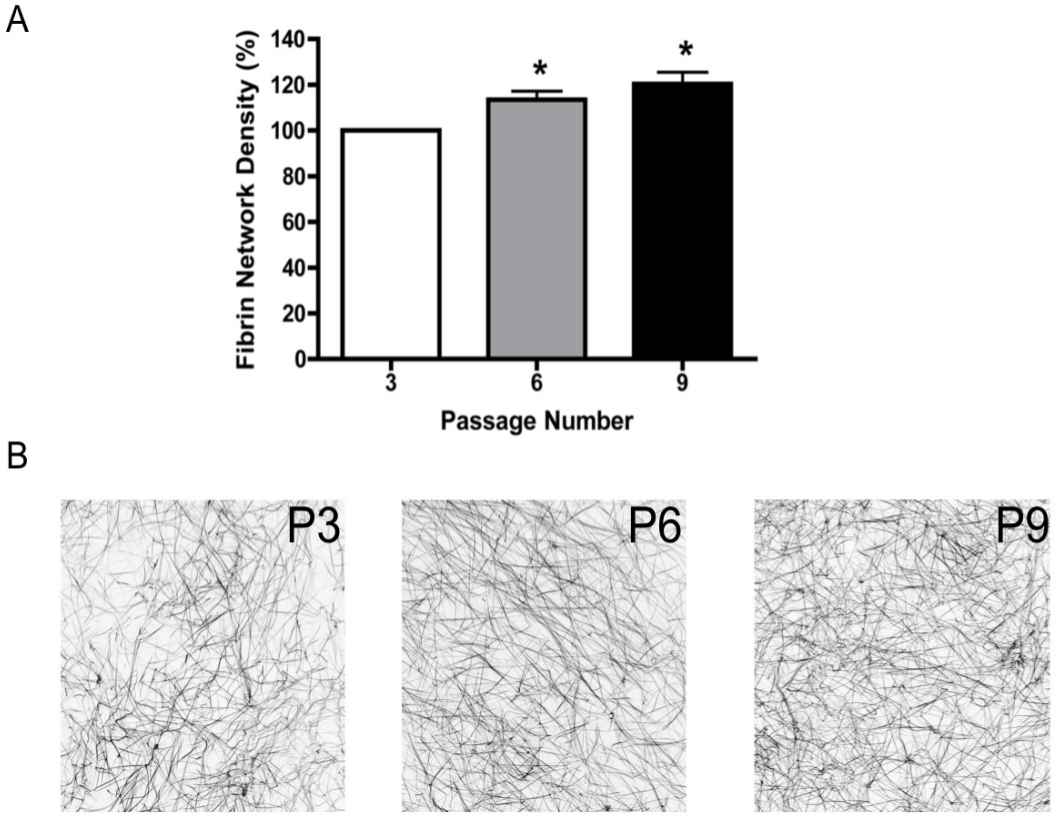

Figure 5.3. Clots formed over senescent endothelial cells show increased fibrin network density. (A) Plasma clots formed over cells using FITC-labeled fibrinogen were analyzed by confocal microscopy**.** Images were quantified using ImageJ. * denotes $p<0.01$ vs passage 3. Data are expressed as percent density compared to passage 3. (B) Representative images from passage 3 (left), 6 (middle), and 9 (right) are shown. N = 3 separate experiments with samples in triplicate.

Increases in the rate of clot formation and fibrin network density are independent of increased tissue factor activity.

Endothelial-derived tissue factor (TF) is a potent modulator of clot formation in vitro. We analyzed TF activity on serial passaged HUVEC by measuring generation of FXa. We observed no difference in FXa generation (Figure 5.4), suggesting the changes in clotting parameters were not due to elevated TF activity on the endothelial cell surface.

Serial passaged HUVEC generate less activated protein C and express less thrombomodulin.

The protein C system is an important negative regulatory pathway that limits the propagation of thrombin when activated protein C (APC) is generated on the endothelial cell surface[6,31]. The cleavage of protein C to APC was measured in senescent HUVEC by chromogenic assay. We observed significant reductions in APC generation as HUVEC were serial passaged (Figure 5.5A). This could be due to either reduced expression of thrombomodulin (TM) or endothelial protein C receptor (EPCR). Immunoblot analysis showed reduced expression of TM in late passage HUVEC with no change in EPCR expression (Figure 5.5B).

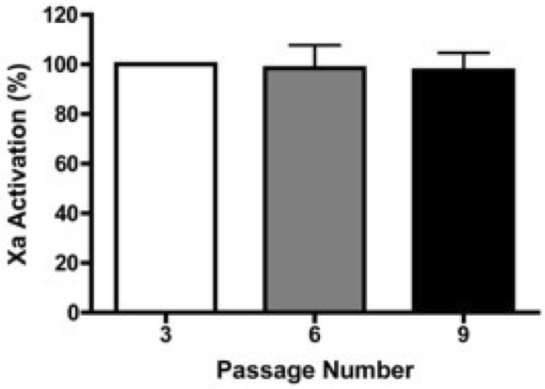

Figure 5.4. Endothelial cell senescence is not associated with increased tissue factor activity. Tissue factor (TF) activity assay performed using a chromogenic substrate for FXa after incubating cells with FVIIa and FX. Data are expressed as percent FXa generation compared to passage 3.

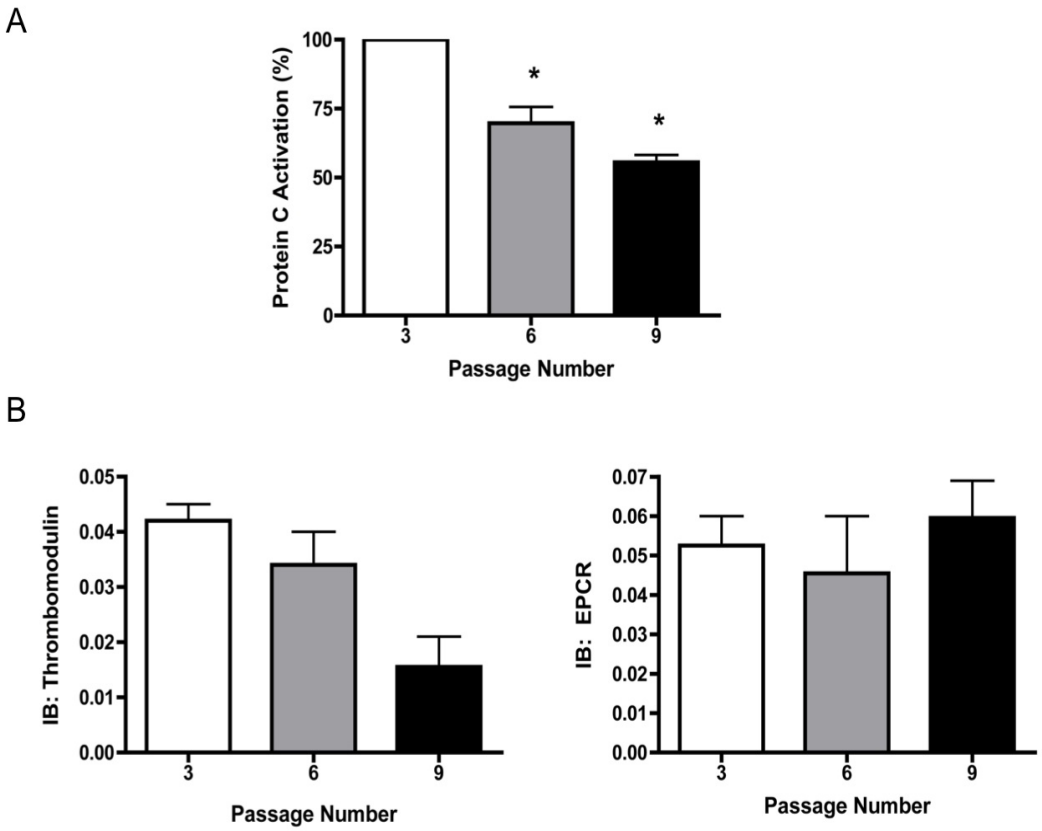

Figure 5.5. Senescent endothelial cells show reduced protein C activation. (A) The cellular potential to activate protein C was assessed using a chromogenic substrate activated protein C after incubating cells with thrombin and protein C and quenching the reaction with antithrombin and heparin. * denotes $p<0.01$ vs passage 3. Data are expressed as percent protein C activation compared to passage 3. (B) Western blot analysis quantifed in ImageJ showing protein throbomodulin (left) and endothelial protein C receptor (EPCR) (right) levels relative to GAPDH.

Aged mice display decreased endothelial thrombomodulin expression.

Our results showing reduced TM expression in serial passaged HUVEC was confirmed *in vivo* using lungs from aged mice. Lungs were subjected to IHC analysis and representative images are shown from 2 month (top) and 24 month (bottom) old mice (Figure 5.6). Aged mice display reduced TM staining, consistent with our *in vitro* findings and *in vivo* findings from other groups[19].

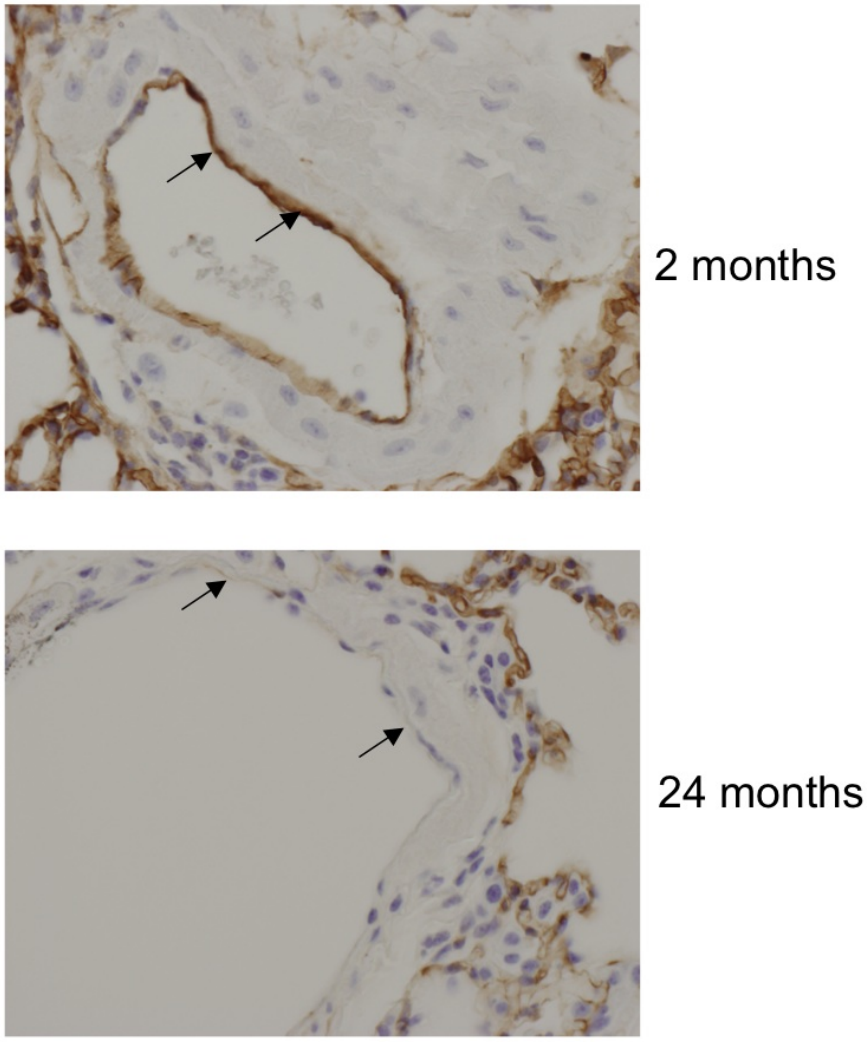

Figure 5.6. Decreased thrombomodulin expression is observed in aged mice. Mouse lungs were analyzed by immunohistochemistry to determine thrombomodulin protein levels between 2month (top) and 24 month (bottom) old mice. Representative images are shown. Arrows demonstrate vascular endothelium.

5.4 Discussion

The vascular endothelium is an important regulator of blood homeostasis. Maintaining vascular endothelial cell integrity and function is critically important for conserving the anticoagulant nature of the vessel wall and preventing the inappropriate formation of thrombi. Endothelial cell dysfunction is a major risk factor for venous thrombosis and also a known consequence of aging in humans[15,32,33]. Cellular senescence can promote vascular dysfunction with aging by causing phenotypic changes in endothelial cells that may predispose the elderly to venous thrombosis[25,26]. There is little current literature demonstrating these phenotypic changes in senescent endothelial cells in vitro and no reports on how these changes alter clotting parameters on the cell surface. Here we observe that serial passaging HUVEC induces cellular senescence in vitro and is associated with several phenotypic changes consistent with previous reports, in addition to novel changes and how they affect plasma clotting.

In order to induce cellular senescence in vitro, HUVEC were serial passaged and cells at early (3), middle (6) and late (9) passage were compared for markers of senescence. We observed increased expression of SA β-galactosidase, $p16^{INK4a}$, PAI-1 which are known markers of endothelial cell senescence (Figure 5.1). These data suggest that cellular senescence can be induced in vitro in HUVEC by serial passaging.

Vascular endothelial cells are important mediators of coagulation by providing both pro and anticoagulant factors. Differences in cellular contributions to clotting can be measured by standardizing plasma factor contributions by using normal, pooled, platelet-free plasma. Thus, any observed differences in clotting parameters are not due to varying plasma or platelet factors, but are due to changes in procoagulant potential of the cellular conditions

tested[34]. Once a model of endothelial cell senescence had been established, the effect of senescence on procoagulant potential was analyzed in plasma-based assays. We observed increases in the rate of fibrin assembly (Figure 5.2A) and increases in thrombin generation (Figure 5.2B) on the cell surface of senescent HUVEC. This suggests that senescent endothelial cells generate clots more rapidly and support greater thrombin generation, and are therefore prothrombotic.

Fibrin clot structure is thought to be important in determining pathophysiologic features of bleeding and thrombosis[29,30]. The density and stability of a fibrin clot is determined by the concentration of thrombin in the reaction. Clots formed in the presence of low levels of thrombin have thick, loosely woven fibrin fibers that are easily dissolved by lytic proteins. These clots are considered to be less stable and could potentiate bleeding. On the contrary, clots formed in the presence of high concentrations of thrombin are composed of thin, tightly woven fibrin fibers. These clots are more stable, however less susceptible to fibrinoysis and may predispose individuals to thrombosis[29]. Thus, the ability of senescent endothelial cells to support greater thrombin generation could have a significant effect on clot stability. Fibrin clot structure was measured by confocal microscopy in clots formed on the cell surface of serial passaged HUVEC in the presence of fluorescently tagged fibrinogen. We observed increased density of fibrin networks in clots formed over late passage HUVEC compared to those formed over early passage HUVEC (Figure 5.3). These data suggest that clots formed over senescent HUVEC are more stable, would be less prone to lysis and could contribute to pathologic thrombus formation in an *in vivo* setting.

Tissue factor (TF) is a potent initiator of coagulation. The amount of TF produced by a cell directly affects clot formation and thrombin generation and is a major determinant of

cellular procoagulant activity[27]. In order to determine if increased TF activity in senescent HUVEC was the cause of increases in thrombin generation and rates of clot formation and stability, TF activity was measured by extrapolating the rate of FXa generation in a chromogenic assay. No difference in TF activity was detected between serial passaged HUVEC (Figure 5.4), suggesting that the prothrombotic phenotype observed in senescent cells was independent of TF.

Changes in anticoagulant proteins could also contribute to a prothrombotic phenotype secondary to senescence. The protein C pathway inhibits the propagation of thrombin. The key regulatory protease of the protein C pathway is activated protein C (APC), which is generated when thrombomodulin (TM) on the endothelial cell surface binds to thrombin and cleaves zymogen protein C. Protein C is brought to the thrombin/TM complex following binding to endothelial protein C receptor (EPCR). APC, with its cofactor protein S, downregulates thrombin generation by inactivating factors Va and VIIIa[6,31]. *In vivo* murine models demonstrated that loss of TM on the endothelial surface leads to a reduced capacity to generate APC and results in spontaneous thrombosis[35]. Importantly, a recent publication has shown that high mortality associated with induction of endotoxemia in aged mice was correlated with decreased expression of TM and reduced APC generation[19]. To determine if the increased thrombin generation and enhanced fibrin clotting parameters in senescent HUVEC were the result of dysregulation of the protein C pathway, the ability to support APC generation on the cell surface of serial passaged HUVEC was measured by chromogenic assay. We observed a significant reduction in APC generation as endothelial cells were passaged (Figure 5.5A). This reduction in APC generation can be due to either decreases in endothelial production of TM or EPCR. Expression levels of both proteins was

measured by immuoblot analysis. We found that serial passaging was associated with decreased production of TM, with no observed effect in EPCR levels (Figure 5.5B). We confirmed this finding and the reports from other groups of reduced TM in aging endothelial cells, by performing IHC analysis on lungs from mice aged 2 and 24 months. Here we see a reduction in endothelial TM staining in the lung (Figure 5.6), suggesting that decreased TM expression in endothelial cells leads to reduced APC generation both *in vitro* and *in vivo*.

In conclusion, these findings suggest that endothelial cell senescence could be an important mediator of vascular dysfunction in the elderly. Although it is not entirely clear whether these endothelial changes are $p16^{INK4a}$-dependent or are an artifact of cell culture, corroborative data in vivo suggests that these results are relevant and provide a novel report of changes in the aging vasculature could predispose elderly individuals to venous thrombosis.

5.5 References

1. Verhamme P, Hoylaerts MF. The pivotal role of the endothelium in haemostasis and thrombosis. *Acta Clin Belg*. 2006;61(5):213-219.

2. Sagripanti A, Carpi A. Antithrombotic and prothrombotic activities of the vascular endothelium. *Biomed. Pharmacother*. 2000;54(2):107-111.

3. Shworak NW, Kobayashi T, de Agostini A, Smits NC. Anticoagulant heparan sulfate to not clot--or not? *Prog Mol Biol Transl Sci*. 2010;93:153-178.

4. Tovar AMF, de Mattos DA, Stelling MP, et al. Dermatan sulfate is the predominant antithrombotic glycosaminoglycan in vessel walls: implications for a possible physiological function of heparin cofactor II. *Biochim. Biophys. Acta*. 2005;1740(1):45-53.

5. Van de Wouwer M, Collen D, Conway EM. Thrombomodulin-protein C-EPCR system: integrated to regulate coagulation and inflammation. *Arterioscler. Thromb. Vasc. Biol*. 2004;24(8):1374-1383.

6. Esmon CT. The protein C pathway. *Chest*. 2003;124(3 Suppl):26S-32S.

7. Maroney SA, Mast AE. Expression of tissue factor pathway inhibitor by endothelial cells and platelets. *Transfus. Apher. Sci*. 2008;38(1):9-14.

8. van Hinsbergh VW. The endothelium: vascular control of haemostasis. *Eur. J. Obstet. Gynecol. Reprod. Biol*. 2001;95(2):198-201.

9. Nishimura H, Tsuji H, Yoshizumi M, Nakagawa M. [The regulation of blood coagulation and fibrinolysis by vascular endothelial cells]. *Nippon Rinsho*. 1999;57(7):1492-1496.

10. Booyse FM, Aikens ML, Grenett HE. Endothelial cell fibrinolysis: transcriptional regulation of fibrinolytic protein gene expression (t-PA, u-PA, and PAI-1) by low alcohol. *Alcohol. Clin. Exp. Res*. 1999;23(6):1119-1124.

11. Pate M, Damarla V, Chi DS, Negi S, Krishnaswamy G. Endothelial cell biology: role in the inflammatory response. *Adv Clin Chem*. 2010;52:109-130.

12. Tedder TF, Steeber DA, Chen A, Engel P. The selectins: vascular adhesion molecules. *FASEB J*. 1995;9(10):866-873.

13. Gordon JL. Endothelium as a modulator of platelet reactivity. *Adv. Exp. Med. Biol*. 1985;192:419-425.

14. Arnal JF, Dinh-Xuan AT, Pueyo M, Darblade B, Rami J. Endothelium-derived nitric oxide and vascular physiology and pathology. *Cell. Mol. Life Sci*. 1999;55(8-9):1078-1087.

15. Herrera MD, Mingorance C, Rodríguez-Rodríguez R, Alvarez de Sotomayor M. Endothelial dysfunction and aging: an update. *Ageing Res. Rev*. 2010;9(2):142-152.

16. Levi M, van der Poll T, ten Cate H. Tissue factor in infection and severe inflammation. *Semin. Thromb. Hemost*. 2006;32(1):33-39.

17. Comi P, Chiaramonte R, Maier JA. Senescence-dependent regulation of type 1 plasminogen activator inhibitor in human vascular endothelial cells. *Exp. Cell Res*. 1995;219(1):304-308.

18. Csiszar A, Ungvari Z, Koller A, Edwards JG, Kaley G. Aging-induced proinflammatory shift in cytokine expression profile in coronary arteries. *FASEB J*. 2003;17(9):1183-1185.

19. Starr ME, Ueda J, Takahashi H, et al. Age-dependent vulnerability to endotoxemia is associated with reduction of anticoagulant factors activated protein C and thrombomodulin. *Blood*. 2010;115(23):4886-4893.

20. Matsushita H, Chang E, Glassford AJ, et al. eNOS activity is reduced in senescent human endothelial cells: Preservation by hTERT immortalization. *Circ. Res*. 2001;89(9):793-798.

21. Yoon HJ, Cho SW, Ahn BW, Yang SY. Alterations in the activity and expression of endothelial NO synthase in aged human endothelial cells. *Mech. Ageing Dev*. 2010;131(2):119-123.

22. Chen J, Huang X, Halicka D, et al. Contribution of p16INK4a and p21CIP1 pathways to induction of premature senescence of human endothelial cells: permissive role of p53. *Am. J. Physiol. Heart Circ. Physiol*. 2006;290(4):H1575-1586.

23. Chen J, Goligorsky MS. Premature senescence of endothelial cells: Methusaleh's dilemma. *Am. J. Physiol. Heart Circ. Physiol*. 2006;290(5):H1729-1739.

24. Stein GH, Dulić V. Molecular mechanisms for the senescent cell cycle arrest. *J. Investig. Dermatol. Symp. Proc*. 1998;3(1):14-18.

25. Erusalimsky JD, Kurz DJ. Cellular senescence in vivo: its relevance in ageing and cardiovascular disease. *Exp. Gerontol*. 2005;40(8-9):634-642.

26. Erusalimsky JD. Vascular endothelial senescence: from mechanisms to pathophysiology. *J. Appl. Physiol*. 2009;106(1):326-332.

27. Campbell RA, Overmyer KA, Selzman CH, Sheridan BC, Wolberg AS. Contributions of extravascular and intravascular cells to fibrin network formation, structure, and stability. *Blood*. 2009;114(23):4886-4896.

28. Coleman PR, Hahn CN, Grimshaw M, et al. Stress-induced premature senescence mediated by a novel gene, SENEX, results in an anti-inflammatory phenotype in endothelial

cells. *Blood*. 2010;116(19):4016-4024.

29. Wolberg AS. Plasma and cellular contributions to fibrin network formation, structure and stability. *Haemophilia*. 2010;16 Suppl 3:7-12.

30. Wolberg AS. Thrombin generation and fibrin clot structure. *Blood Rev*. 2007;21(3):131-142.

31. Esmon CT. Coagulation and inflammation. *J. Endotoxin Res*. 2003;9(3):192-198.

32. Mazzoccoli G, Fontana A, Grilli M, et al. Idiopathic deep venous thrombosis and arterial endothelial dysfunction in the elderly. *Age (Dordr)*. 2012;34(3):751-760.

33. Virdis A, Ghiadoni L, Giannarelli C, Taddei S. Endothelial dysfunction and vascular disease in later life. *Maturitas*. 2010;67(1):20-24.

34. Hoffman M, Monroe DM. A cell-based model of hemostasis. *Thromb. Haemost*. 2001;85(6):958-965.

35. Isermann B, Hendrickson SB, Zogg M, et al. Endothelium-specific loss of murine thrombomodulin disrupts the protein C anticoagulant pathway and causes juvenile-onset thrombosis. *J. Clin. Invest*. 2001;108(4):537-546.

Chapter 6.

Age-related Changes in Thrombus Formation, Thrombus Resolution, and Blood Coagulability in Mice

6.1 Introduction

Venous thromboembolism (VTE) is the term encompassing both deep vein thrombosis (DVT) and pulmonary embolism (PE), a very serious and lethal complication of DVT. The incidence of VTE is approximately 1 in 1000 individuals in the general population[1,2] and it is estimated that over 250,000 VTE patients are hospitalized each year, contributing to the significant healthcare burden associated with cardiovascular disease[3]. The strongest and yet most unchangeable risk factor for VTE is age[4]. After the age of 55, the risk of suffering from VTE goes up substantially and the incidence of those 75 years and older increases to 1 in 100 individuals; a ten-fold increase from the overall, non-stratified population incidence[2,5].

The relationship between aging and VTE is not well understood. The natural history of venous thrombosis and thrombus resolution includes a role for both plasma and endothelial derived proteins, platelet adhesion/activation/aggregation, static flow conditions, and leukocyte migration. Therefore, elevated plasma factor levels, decreased natural anticoagulant production, endothelial dysfunction, thickening of venous valves, blood cell composition and inflammation are all potential contributors to the risk of thrombosis with age.

Several groups have described phenotypic changes occurring in genetic mouse models of premature aging. However, there is limited literature on mouse models of true aging and the effects on venous thrombosis. Naturally-aged mice are more susceptible to endotoxemia, with augmented upregulation of PAI-1 transcription and renal fibrin deposition following treatment with lipopolysaccharide[6]. Endotoxemia also caused greater loss of activated protein C (APC) generation due to reduced thrombomodulin expression in lungs of aged mice[7], suggesting dysregulation of this important thrombin-regulating pathway may also contribute to thrombotic risk with age. Elevated levels of circulating tissue necrosis factor alpha (TNFα) observed in aged mice following restraint stress led to significant induction of tissue factor (TF) expression, a potent initiator of coagulation[8]. Additionally, stasis is a well-known risk factor for venous thrombosis and stasis promoted by immobility is common in the elderly. Aging in mice was found to enhance stasis-induced thrombosis with marked increases in several endothelial and circulating factors including endothelial P-selectin and PAI-1 expression, leukocyte microparticle (MP) formation and MP-TF activity[9]. Conversely, Stampfli *et al* found no increase in arterial thrombosis in old compared to young mice. However, they reported impaired arterial endothelium vaso-relaxation but with no changes in TF, TM, PAI-1 and inflammatory mediator expression in aged mice[10]. Taken together, these studies collectively suggest that the pathophysiology of thrombosis in the elderly is multifactorial and that aging may disproportionately affect venous over arterial thrombosis in mouse models.

Coagulation and aging are two complex biological processes and the relationship between them is not well understood. In this study, we characterize several hemostatic

parameters in aged, wild-type C57BL/6 mice and the effects on venous thrombosis to determine mechanistic insights behind the increased risk of VTE in the elderly.

6.2 Materials and Methods

Mice

All animal procedures were performed in accordance with protocols approved by the Institutional Animal Care and Use Committee, UNC-Chapel Hill. Mice aged 6 and 12 months were purchased from the Aged Rodent Colony through the National Institute on Aging. Young, 2 month old control mice were purchased through Charles River Laboratories International, Inc. All mice included in this study were male, C57BL/6 (wild-type).

Complete Blood Count

Whole blood collected from inferior vena cava venipuncture into citrated (1:9) tubes was analyzed for complete blood counts (CBC) in house using a Hemavet® HV950FS Multispecies Hematology Instrument (Drew Scientific, Inc.).

$FeCl_3$ Vascular Injury

The ferric chloride ($FeCl_3$) injury model to the saphenous vein was performed as previously described[11]. Briefly, the saphenous vein of anesthetized mice was exposed and dissected away from the saphenous artery. A 0.5 x 2 mm piece of filter paper was soaked in 7.5% $FeCl_3$ (Sigma Aldrich – F7134), and laid over the saphenous vein for 2 minutes. The filter paper was then removed and the tissue was washed 3 times with warm saline. Blood flow was monitored using a 20-MHz Doppler flow probe (Indus Instruments – Webster, TX). Occlusion was defined as the absence of blood flow for one minute.

Thrombin Generation

Thrombin generation was measured by calibrated automated thrombography (CAT) using Z-Gly-Gly-Arg-AMC fluorogenic substrate for thrombin (Diagnostica Stago, Parsippany, NJ) on a Fluoroskan Ascent fluorometer (ThermoLabsystem, Helsinki, Finland). Mouse plasma was analyzed as previously described[12]. Briefly, mouse plasma samples were diluted 1:4 in phosphate buffered saline and 80 μL of plasma was added to 20 μL low tissue factor (1 pM) reagent to initiate thrombin generation upon administration of substrate containing calcium. Variations in plasma color were accounted for using a α2-macroglobulin/thrombin calibrator reagent (Diagnostica Stago, Parsippany, NJ). Parameters were calculated by Thrombinoscope software version 3.0.0.29 (Thrombinoscope BV, Maastricht, Netherlands).

TAT ELISA

TAT complexes were detected in mouse plasma using an Enzygnost TAT complex ELISA (Siemens – New York, NY, USA). Plasma samples were diluted 1:10 in Enzygnost ELISA sample buffer. ELISA was performed according to the company protocols and standard curves were generated using proteins supplied by the company.

IVC Ligation

Stasis-induced venous thrombosis by inferior vena cava (IVC) ligation was performed in anesthetized mice by exposing the IVC by laparotomy and dissecting it away from the aorta. A single ligature was placed around the IVC just below the renal vein branching using a 8-0 prolene suture. To achieve complete stasis, associated side and back branches were ligated or cauterized, respectively. The laparotomy was closed by first suturing the peritoneum with

an absorbable, 5-0 vicryl suture followed by suturing the skin with an 8-0 prolene suture. Mice were euthanized 1, 3, 7, and 14 days post surgery for collection of thrombi. Thrombi were normalized to length of the effected vessel and data are expressed as weight/length.

Histology and Immunohistochemistry

Tissues were extracted and fixed overnight in 4% paraformadehyde. Tissue embedding and cutting was performed in the UNC Linberger Comprehensive Cancer Center Animal Histopathology Core Facility. Five micron sections were cut from paraffin blocks and deparaffinized and rehydrated for histologic staining and for immunohistochemistry (IHC). Tissues were hematoxylin and eosin (H&E) stained to visualize thrombi. Trichrome staining for collagen was performed using a kit purchased from Sigma (HT15-1KT) according to the supplier instructions. For IHC, antigen retrieval was performed in Target Retrieval Solution (Dako – Capinteria, CA, S1699) in a 95°C water bath for 10 minutes. Slides were blocked for 1 hour in 5% serum derived from the species in which the secondary antibody was made and subsequently stained with antibodies against fibrin (Gift of Dr. Marshall Runge and Dr. Alisa Wolberg, 59D8, 1:1000), PAI-1 (Molecular Innovations ASMPAI-GF-HT, 1:250 dilution), F4/80 (Serotec MCA497GA, 1:250), Ly6G (eBioscience 14-5931-82, 1:500) or Thrombomodulin (R&D Systems MAB3894, 1:500) for 1 hour at room temperature in a humidity-controlled chamber. Biotinylated secondary antibodies were obtained from Vector Laboratories. Tissue slides were developed using the avidin-biotin complex (ABC) method using reagents and protocols obtained from Dako. Negative control tissue sections were stained simultaneously in the absence of primary antibody. To analyze stained tissues, images were collected at 10x magnification with an Olympus BX51W1 light microscope

(three images per tissue section) and the average number of positive pixels per image was quantified using Adobe Photoshop™ (version 10.0.1).

Statistics

All statistics were performed using GraphPad Prism. One-way ANOVA or Students T-test were performed where indicated. Vertical bars represent either standard error of the mean (SEM), 95% confidence interval (CI), or range where indicated. Values of $p<0.05$ were considered statistically significant.

6.3 Results

Aging in mice accelerates occlusive thrombus formation in a $FeCl_3$ injury model.

The prothrombotic potential in aged mice was examined in an acute $FeCl_3$ injury model to the saphenous vein. Vascular occlusion times were measured in mice aged 2, 6, and 12 months after treatment with 7.5% $FeCl_3$ to the saphenous vein (n=4-7 mice per group). While a trend was apparent across all ages, a significantly shorter time to occlusion was observed in 12 month old mice (6.9 ± 1.2 min) compared to 2 month old mice (9.1 ± 1.5 min) (Figure 6.1). These results in mice are consistent with the notion that aging in humans is associated with an increased risk of venous thrombosis following vessel wall injury[13,14].

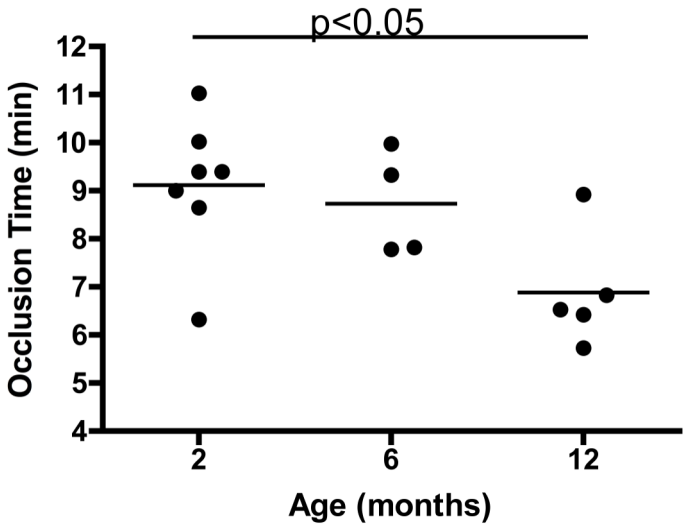

Figure 6.1. Aged mice display a decreased time to vascular occlusion in a $FeCl_3$ injury model. Vascular occlusion times were compared between mice aged 2, 6, and 12 months after 7.5% $FeCl_3$ injury to the saphenous vein. Occlusion was defined as the absence of blood flow for 1 minute as measured by doppler. Data is represented as time to form an occlusive thrombus in minutes. * denotes $p<0.05$ compared to 2 month old mice by student t-test.

Effect of aging in mice on Complete Blood Count (CBC).

In order to determine if differences in murine blood cell composition with age could contribute to differences in $FeCl_3$-mediated occlusion times, complete blood counts (CBC) were measured in mice aged 2, 6, and 12 months (n=5 mice per group). In general, levels of circulating platelets and leukocytes were increased with age in mice. More specifically, an age-dependent increase in platelet counts was observed between 2, 6, and 12 month old mice (596.2 ± 32.3, 719.2 ± 47.7, and 812.8 ± 64.8 $x10^3/\mu L$, respectively). Lymphocyte counts ranged from 5.6 ± 1.1 $x10^3/\mu L$ at 2 months to 5.5 ± 0.9 $x10^3/\mu L$ at 6 months and 7.4 ± 0.9 $x10^3/\mu L$ at 12 months. Neutrophil counts were increased in 12 month old mice (1.0 ± 0.3 $x10^3/\mu L$) compared to 2 month old mice (0.5 ± 0.1 $x10^3/\mu L$). Lastly, monocyte counts were only slightly elevated at 12 months of age (0.2 ± 0.04 $x10^3/\mu L$) compared to 2 months (0.3 ± 0.2 $x10^3/\mu L$). These results are consistent with previous findings showing similar relative changes in blood cell counts as mice age[15].

Figure 6.2 shows our aging mouse results compared with findings in aging humans. Interestingly, aging in humans is associated with a decrease in platelet count[16]. Additionally, aging humans also show decreases in lymphocytes[17], neutrophils and monocytes[18] with age. Collectively, these results show that CBC values in mice (C57BL/6) and humans follow very different trends during aging.

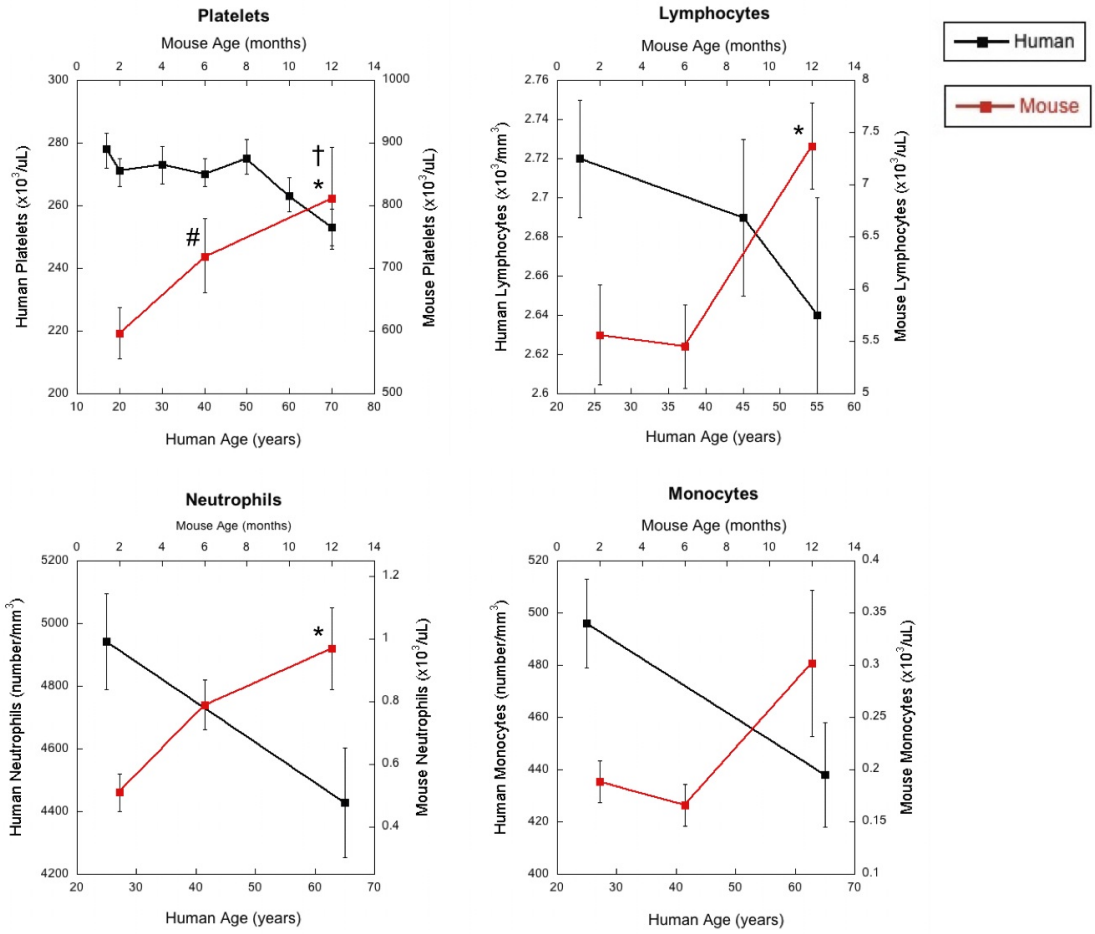

Figure 6.2. Aged mice have increased circulating platelet and leukocyte counts. Complete blood counts with differentials were performed on mice aged 2, 6, and 12 months. These data are plotted against historical data on human platelet and leukocytes counts for comparison[16-18]. Vertical bars on mouse data points were plotted to represent those published for human data: Platelet data – vertical bars represent 95% CI, # denotes $p<0.01$ vs 2 month, * denotes $p<0.05$ vs 6 month, † denotes $p<0.001$ vs 2 month. Lymphocyte data – vertical bars represent SEM, * denotes $p<0.05$ versus both 2 and 6 month. Neutrophil data – vertical bars represent SEM, * denotes $p<0.05$ vs 2 month. Monocyte data – vertical bars represent SEM.

Aging in mice is not associated with increased plasma hypercoagulability.

Circulating thrombin/antithrombin (TAT) complex formation and thrombin generation were used as markers of hypercoagulability in plasma from aged mice (n=4-5 per group). No difference in circulating TAT complex levels was observed in the plasma from mice aged 2, 6, and 12 months (10.3 ± 3.7, 7.3 ± 0.8, and 8.3 ± 2.8 ng/mL, respectively) (Figure 6.3A). Interestingly, this is contrary to historical findings in aged humans[19] (Figure 6.3A).

Next, plasma from untreated mice aged 2, 6, and 12 months was analyzed by calibrated automated thrombography (CAT) (n=5 per group). CAT parameters demonstrated reduced thrombin generation in plasma with age as evidenced by prolonged lagtime between 2, 6, and 12 month old mice (4.0 ± 0.3, 4.3 ± 0.2 and 5.3 ± 0.9 min, respectively), time to peak (TTP) between 2 and 12 month old mice (9.6 ± 0.6 and 17.83 ± 5.4 min, respectively) and diminished peak thrombin levels between 2 and 12 month old mice (26.2 ± 2.8 and 21.2 ± 2.5, respectively). No significant difference between young (737.4 ± 124.9 nM) and aged (672.5 ± 256.6 nM) mice was detected in endogenous thrombin potential (ETP). Figure 6.3B shows data generated in aged mice compared with representative data on human thrombin generation by CAT[20]. As humans age, they display shortened lagtime and TTP and elevated peak and ETP, which implies plasma hypercoagulability as humans age. In contrast, our results in mice show reduced thrombin generation with age, suggesting plasma hypocoagulability.

A

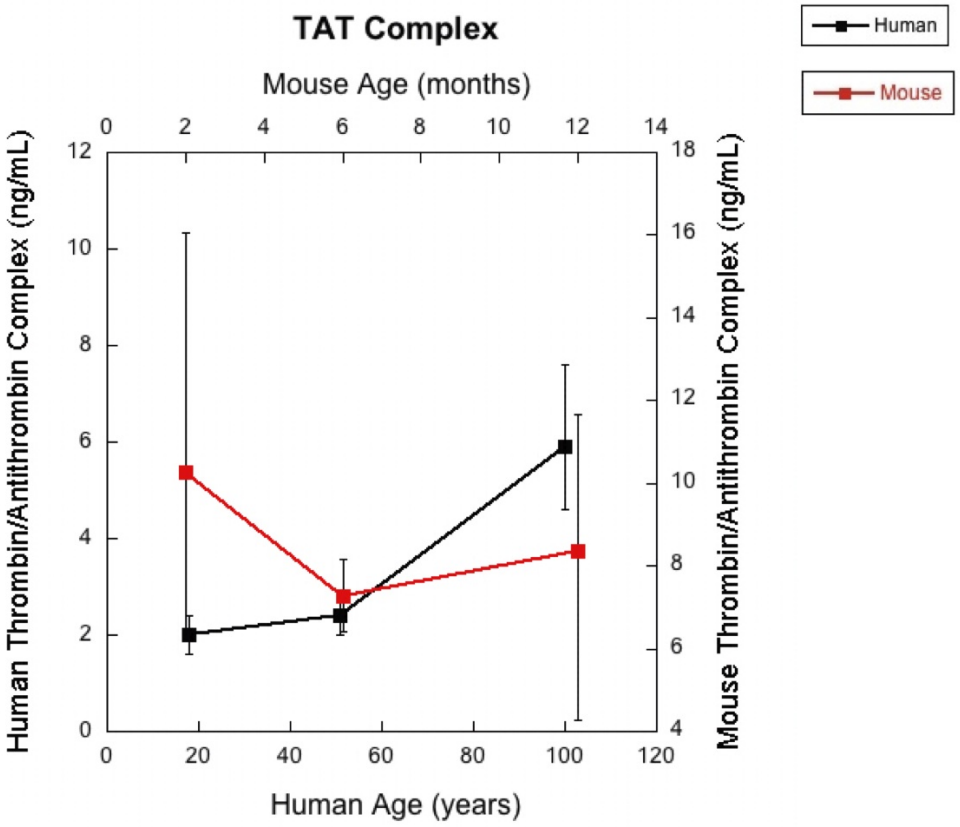
TAT Complex
Mouse Age (months)
0
2
4
6
8
10
12
14
Human
Mouse
Human Thrombin/Antithrombin Complex (ng/mL)
Mouse Thrombin/Antithrombin Complex (ng/mL)
0
2
4
6
8
10
12
0
2
4
6
8
10
12
14
16
18
0
20
40
60
80
100
120
Human Age (years)

B

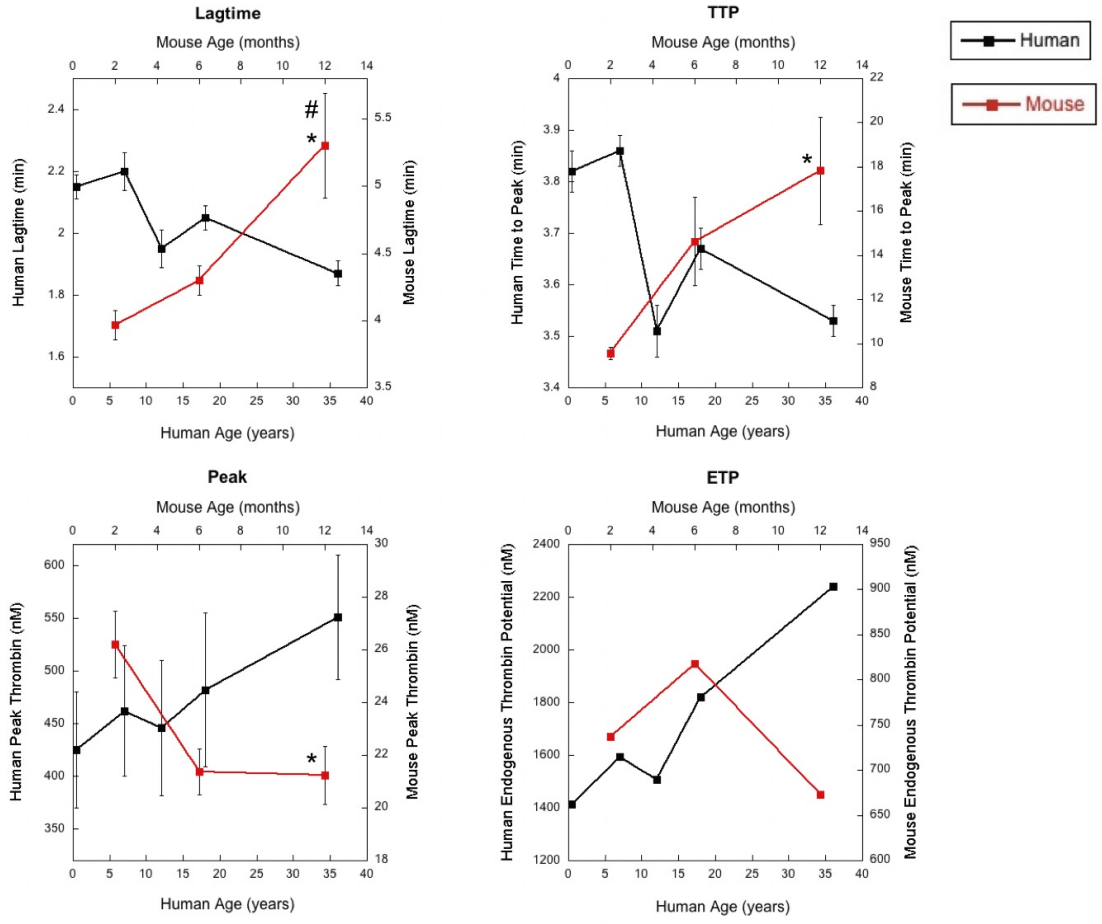

Figure 6.3. Aged mice generate less thrombin but have no difference in circulating TAT levels. (A) Levels of circulating TAT complex were measured by ELISA in plasma from mice aged 2, 6, and 12 months. These data are plotted against historical data on human TAT levels with age[19]. Vertical bars represent 95% CI. **(B)** Mouse plasma samples were diluted 1:4 and analyzed by CAT to measure thrombin generation parameters. These data are plotted against historical data on human thrombin generation parameters measure by CAT[20]. Vertical bars represent SEM. * denotes $p<0.05$ vs 2 month with the exception of data for lagtime for which * denotes $p<0.05$ vs 6 month and # denotes $p<.01$ vs 2 month.

Effect of aging in mice on stasis-induced thrombus formation and resolution.

To further explore the age-related changes in thrombus formation, especially given the differences seen between the $FeCl_3$ results with the accompanying CBC and plasma coagulability values, we performed stasis-induced thrombosis by inferior vena cava (IVC) ligation. Mice aged 2 and 12 months (n=4-8 per group) were analyzed in a model of IVC stasis-induced thrombosis to compare thrombus formation and resolution over time (up to 14 days). There was no significant differences between young and old mice either in thrombus formation or in resolution, as measured by thrombus size over time (Figure 6.4A).

Further histological analysis was performed on thrombi to determine if there were qualitative or quantitative differences between the young and old mice that could not be detected by gross measurements. Fixed and paraffin embedded thrombi with associated vessel wall were analyzed histologically to determine differences in thrombus composition between young (2 months) versus old (12 months) mice. Hematoxylin and Eosin (H&E) staining did not show relevant differences in morphology, with the exception of increased proteinaceous content in the thrombi from aged mice at the 1 day time point. Representative H&E images are shown in Figure 6.4B.

Immunostaining was performed on thrombi to determine any quantifiable differences in thrombus composition by examining relevant vessel wall and soluble proteins, as well as relevant inflammatory leukocytes. As seen in Figure 6.4C, heavy fibrin content is present early in thrombus formation with fibrin staining decreasing over time as inflammation and resolution occurs. We observed endothelial expression of thrombomodulin (TM) at early time points, followed by diminished expression over time. Trending decreases in TM staining at the 1-day time point was observed in aged mice, similar to that recently reported[7].

Neutrophil infiltration, evidenced by staining for the neutrophil marker Ly6G, occurred by 3 days post ligation, peaked at 7 days and decreased as macrophage infiltrates were subsequently recruited into the thrombus (F4/80 surface marker) in both aged and young. PAI-1 staining was seen only on the endothelium at early time points; however, increases in soluble PAI-1 staining was found within the thrombus at later days in both mice. Significant increases in PAI-1 expression were found in old mice, consistent with previous reports[6]. Collagen deposition occurred at later stages, with no differences between young and old mice observed. With the exception of changes to PAI-1 levels, these results suggest that there is no apparent differences in thrombus mass or composition between 2 and 12 month-old mice using a stasis-induced IVC thrombosis model.

A

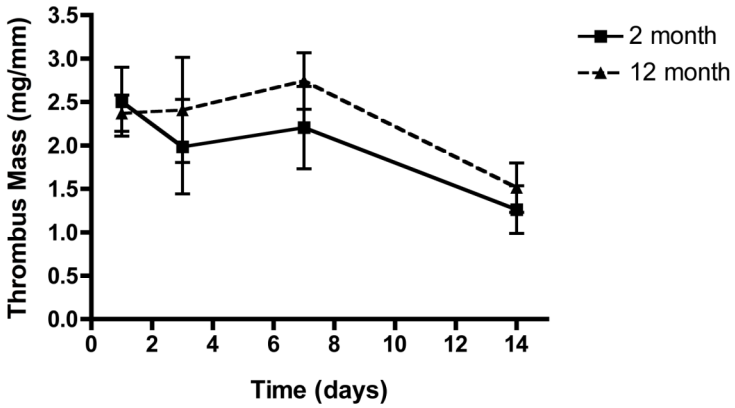
Thrombus Mass (mg/mm)
3.5
3.0
2.5
2.0
1.5
1.0
0.5
0.0
0
2
4
6
8
10
12
14
Time (days)
2 month
12 month

B

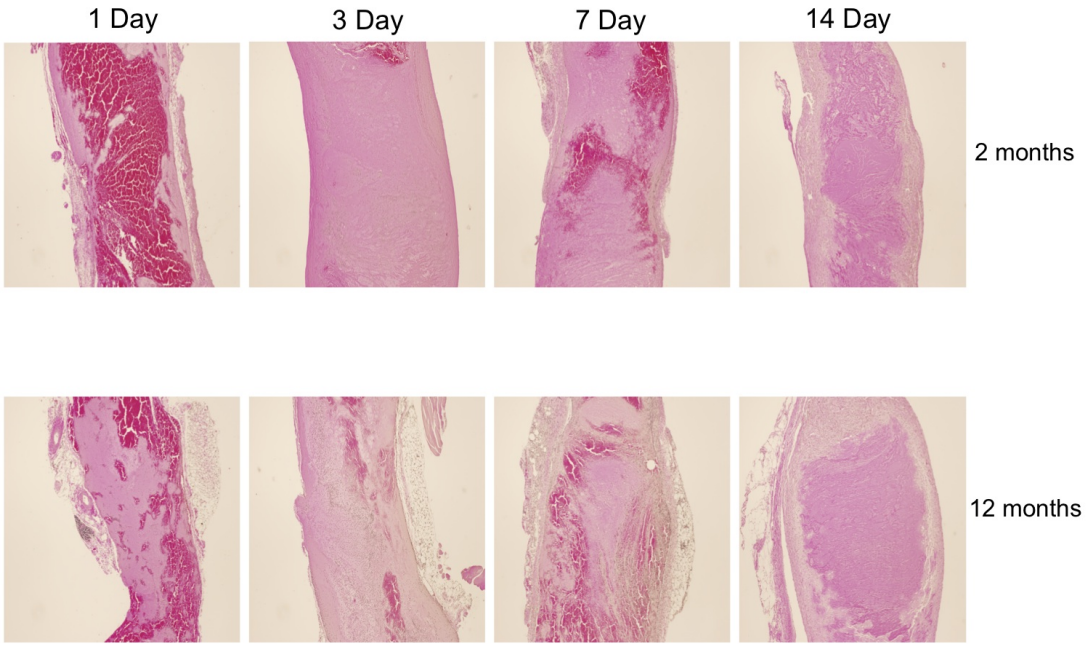
1 Day
3 Day
7 Day
14 Day
2 months
12 months

C

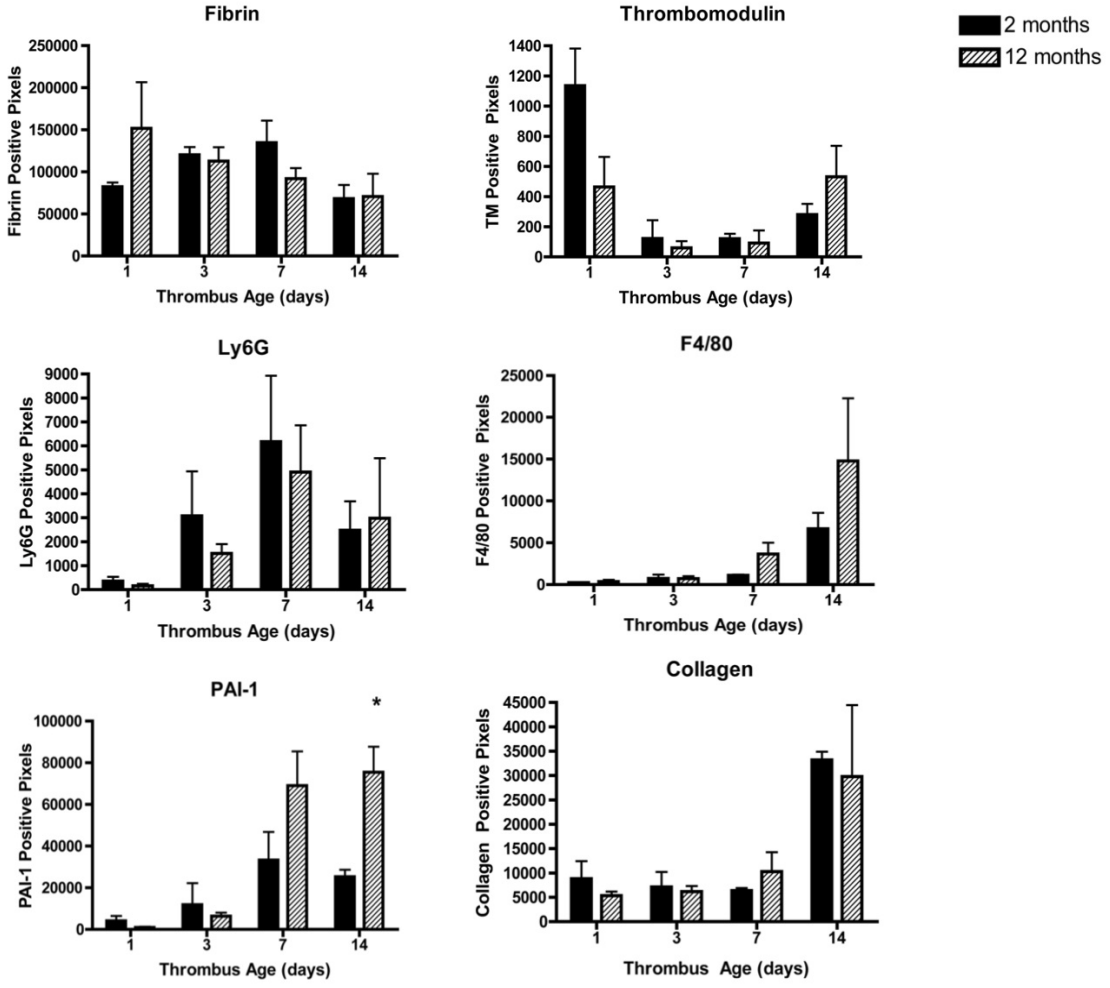

Figure 6.4. No difference in stasis-induced thrombus size or histologic properties are observed in young compared to old mice. (A) Mice aged 2 and 12 months were subjected to IVC ligation to promote stasis-induced thrombosis. Thrombus mass was measured over time and represented as thrombus weight over length. **(B)** Thrombi were H&E stained and representative images selected for comparison. **(C)** Thrombi were immunostained for proteins and cell markers involved in venous thrombus formation and resolution. Quantification was performed using Photoshop to count the number of positively stained pixels. Data are represented as positive pixels throughout thrombus age in days.

6.4 Discussion

The increased risk of VTE with age is poorly understood. Several groups have reported phenotypic changes or altered responses to injury in mouse models of aging that have offered mechanistic insight behind the relationship of age to thrombosis[6-10,21]. The goal of this study was to further define these age-dependent changes that may contribute to VTE using well-defined thrombosis models in aged mice.

Initially, we confirm the findings of other groups that aged mice display a prothrombotic phenotype[9]. We performed an acute chemical injury to the saphenous vein using $FeCl_3$ to initiate thrombosis and monitored the time to vascular occlusion by Doppler flow meter. Aged mice had a significantly shorter time to occlusion compared to young controls suggesting that aging is associated with a prothrombotic phenotype in mice in this model.

According to Virchow's Triad, venous thrombosis is caused by alterations to one or more of the three critical components in the venous circulation: blood cell and plasma composition, the vessel wall, and shear stress/flow[22-24]. In that light, we explored changes to these components in aged mice that may contribute to the observed prothrombotic phenotype. We analyzed whole blood by CBC to determine age-dependent differences that may be driving thrombus formation. We found that aged mice had significant increases in platelet counts and several leukocyte subsets that could contribute to increased thrombosis. Importantly, this is not a phenomenon seen in aging humans, who typically display age-dependent decreases in platelet and leukocyte counts[16-18].

Plasma hypercoagulability is another well-documented phenomenon in human VTE patients and elderly individuals and is thought to contribute to the increased risk of thrombosis. We also analyzed aged mouse plasma to determine if plasma hypercoagulability

was contributing to the prothrombotic phenotype. Interestingly, we found reduced overall thrombin generation and no difference in circulating TAT levels in aged mice. These data suggest that mice do not display age-related plasma hypercoagulability, which is in contrast to aging in humans[19,20].

In order to determine if the prothrombotic phenotype observed in aged mice upon acute chemical injury was apparent in another mouse model of thrombosis, we performed IVC ligation on 2 and 12 month old mice to promote stasis-induced thrombosis. This model is widely used to study venous thrombosis in a more physiologically relevant setting to augment studies using chemical, photoreactive or laser injuries[25-27]. We observed no difference in stasis-induced thrombosis and resolution over time between young and old mice, suggesting that aged mice are not prothrombotic in this model. Our data differ from those reported in McDonald *et al* where a significant difference in thrombus size between young and old mice was observed following IVC ligation for 2 days[9]. Indeed, we did see a slight increase in thrombus size at this early time point, however expanding this study out to longer time points revealed no significant difference.

As previously mentioned, Stampfli *et al* reported endothelial dysfunction with aging in mice in the absence of any prothrombotic phenotye in the arterial circulation. There was also no observed difference in several key hemostasis factors (including TF, TFPI, TM, and PAI-1), TAT complex levels, PT and aPTT, and platelet function. These data suggested that in the absence of other physiologic modifiers (e.g. atherosclerosis, hypertension or diabetes) during normal mouse aging on a standard chow diet, aging alone is not sufficient to promote arterial thrombosis[10].

We observe that the age-related susceptibility to venous thrombosis is dependent upon the thrombosis model used. Similar to data from Stampfli et al and in agreement with the notion that aging is associated with oxidative stress[28-31], we find that directly damaging the vessel wall with $FeCl_3$ and inducing oxidative damage results in an accelerated time to occlusion in aged mice. The observed prothrombotic phenotype in this model could be due to endothelial dysfunction in aged mice increasing the susceptibility to chemical damage, increasing the vessel wall permeability allowing $FeCl_3$ to come in contact with flowing blood, or enhanced endothelial denudation enabling exposure of subendothelial tissue factor and other matrix proteins. Increases in platelet and leukocyte numbers could also play a role in promoting vascular occlusion in this model through enhanced recruitment and binding of these cell types to the damaged vessel. Conversely, we did not see an effect of age in a model of stasis-induced thrombosis. While we did observe increased PAI-1 levels, trending increases in F4/80 positive leukocytes and trending decreases in TM in aged mice, this did not have an effect on thrombus weight. Therefore, while aged mice are prothrombotic following oxidative vascular injury, they are not increasingly susceptible to stasis-induced thrombosis compared to young mice.

In conclusion, our data suggest that increased venous thrombosis in aged mice is dependent on the coagulation stimulus. Importantly, C57BL/6 mice display age-related changes in hemostasis parameters that differ from those patterns seen in humans. Employing an alternative mouse strain or inducing other cardiovascular modifiers/risk factors in C57BL/6 mice may provide a more relevant model for studying aging and thrombosis.

6.5 References

1. Branchford BR, Mourani P, Bajaj L, et al. Risk factors for in-hospital venous thromboembolism in children: a case-control study employing diagnostic validation. *Haematologica*. 2012;97(4):509-515.

2. Galson S. The Surgeon Generals Call to Action to Prevent Deep Vein Thrombosis and Pulmonary Embolism. Available at: http://www.surgeongeneral.gov/topics/deepvein/calltoaction/call-to-action-on-dvt-2008.pdf. Accessed April 20, 2012.

3. Spyropoulos AC, Hurley JS, Ciesla GN, de Lissovoy G. Management of acute proximal deep vein thrombosis: pharmacoeconomic evaluation of outpatient treatment with enoxaparin vs inpatient treatment with unfractionated heparin. *Chest*. 2002;122(1):108-114.

4. Wong P, Baglin T. Epidemiology, risk factors and sequelae of venous thromboembolism. *Phlebology*. 2012;27 Suppl 2:2-11.

5. Silverstein RL, Bauer KA, Cushman M, et al. Venous thrombosis in the elderly: more questions than answers. *Blood*. 2007;110(9):3097-3101.

6. Yamamoto K, Shimokawa T, Yi H, et al. Aging accelerates endotoxin-induced thrombosis : increased responses of plasminogen activator inhibitor-1 and lipopolysaccharide signaling with aging. *Am. J. Pathol*. 2002;161(5):1805-1814.

7. Starr ME, Ueda J, Takahashi H, et al. Age-dependent vulnerability to endotoxemia is associated with reduction of anticoagulant factors activated protein C and thrombomodulin. *Blood*. 2010;115(23):4886-4893.

8. Yamamoto K, Shimokawa T, Yi H, et al. Aging and obesity augment the stress-induced expression of tissue factor gene in the mouse. *Blood*. 2002;100(12):4011-4018.

9. McDonald AP, Meier TR, Hawley AE, et al. Aging is associated with impaired thrombus resolution in a mouse model of stasis induced thrombosis. *Thromb. Res*. 2010;125(1):72-78.

10. Stämpfli SF, Akhmedov A, Gebhard C, et al. Aging induces endothelial dysfunction while sparing arterial thrombosis. *Arterioscler. Thromb. Vasc. Biol*. 2010;30(10):1960-1967.

11. Buyue Y, Whinna HC, Sheehan JP. The heparin-binding exosite of factor IXa is a critical regulator of plasma thrombin generation and venous thrombosis. *Blood*. 2008;112(8):3234-3241.

12. Tchaikovski SN, VAN Vlijmen BJM, Rosing J, Tans G. Development of a calibrated automated thrombography based thrombin generation test in mouse plasma. *J. Thromb. Haemost*. 2007;5(10):2079-2086.

13. Versari D, Daghini E, Virdis A, Ghiadoni L, Taddei S. The ageing endothelium, cardiovascular risk and disease in man. *Exp. Physiol*. 2009;94(3):317-321.

14. Mazzoccoli G, Fontana A, Grilli M, et al. Idiopathic deep venous thrombosis and arterial endothelial dysfunction in the elderly. *Age (Dordr)*. 2012;34(3):751-760.

15. Hemmeryckx B, Emmerechts J, Bovill EG, Hoylaerts MF, Lijnen HR. Effect of ageing on the murine venous circulation. *Histochem. Cell Biol*. 2012;137(4):537-546.

16. Segal JB, Moliterno AR. Platelet counts differ by sex, ethnicity, and age in the United States. *Ann Epidemiol*. 2006;16(2):123-130.

17. Sparrow D, Silbert JE, Rowe JW. The influence of age on peripheral lymphocyte count in men: a cross-sectional and longitudinal study. *J Gerontol*. 1980;35(2):163-166.

18. McArthur WP, Bloom K, Taylor M, et al. Peripheral blood leukocyte populations in the elderly with and without periodontal disease. *J. Clin. Periodontol*. 1996;23(9):846-852.

19. Mari D, Mannucci PM, Coppola R, et al. Hypercoagulability in centenarians: the paradox of successful aging. *Blood*. 1995;85(11):3144-3149.

20. Haidl H, Cimenti C, Leschnik B, Zach D, Muntean W. Age-dependency of thrombin generation measured by means of calibrated automated thrombography (CAT). *Thromb. Haemost*. 2006;95(5):772-775.

21. Nakayama T, Sato W, Yoshimura A, et al. Endothelial von Willebrand factor release due to eNOS deficiency predisposes to thrombotic microangiopathy in mouse aging kidney. *Am. J. Pathol*. 2010;176(5):2198-2208.

22. Wolberg AS, Aleman MM, Leiderman K, Machlus KR. Procoagulant activity in hemostasis and thrombosis: Virchow's triad revisited. *Anesth. Analg*. 2012;114(2):275-285.

23. Hume M. Venous thrombosis: mechanisms and treatment. *Adv. Exp. Med. Biol*. 1978;102:215-224.

24. Peterson CW. Venous thrombosis: an overview. *Pharmacotherapy*. 1986;6(4 Pt 2):12S-17S.

25. Zhou J, May L, Liao P, Gross PL, Weitz JI. Inferior vena cava ligation rapidly induces tissue factor expression and venous thrombosis in rats. *Arterioscler. Thromb. Vasc. Biol*. 2009;29(6):863-869.

26. Wrobleski SK, Farris DM, Diaz JA, Myers DD, Wakefield TW. Mouse complete stasis model of inferior vena cava thrombosis. *J Vis Exp*. 2011;(52). Available at: http://www.ncbi.nlm.nih.gov/pubmed/21712794 [Accessed April 20, 2012].

27. Diaz JA, Obi AT, Myers DD, et al. Critical review of mouse models of venous thrombosis. *Arterioscler. Thromb. Vasc. Biol*. 2012;32(3):556-562.

28. Hekimi S, Lapointe J, Wen Y. Taking a "good" look at free radicals in the aging process. *Trends Cell Biol*. 2011;21(10):569-576.

29. Floyd RA, Towner RA, He T, Hensley K, Maples KR. Translational research involving oxidative stress and diseases of aging. *Free Radic. Biol. Med*. 2011;51(5):931-941.

30. Finkel T, Holbrook NJ. Oxidants, oxidative stress and the biology of ageing. *Nature*. 2000;408(6809):239-247.

31. Kregel KC, Zhang HJ. An integrated view of oxidative stress in aging: basic mechanisms, functional effects, and pathological considerations. *Am. J. Physiol. Regul. Integr. Comp. Physiol*. 2007;292(1):R18-36.

Chapter 7

Summary and Future Directions

7.1 Summary and future directions

The complex relationship between aging and the increased risk of VTE is not well understood. Upregulation of the cell cycle inhibitor $p16^{INK4a}$ is an established biomarker of aging and inducer of cellular senescence[1,2]. Cellular senescence may promote vascular dysfunction seen in elderly individuals, predisposing them to venous thrombosis. To date, the contribution of $p16^{INK4a}$ and cellular senescence to the pathophysiology of venous thrombosis has not been examined. This research was focused on determining if $p16^{INK4a}$ is a genetic risk factor for the age-related risk of VTE. We used both *in vitro* and *in vivo* techniques to determine in which cellular compartment $p16^{INK4a}$ expression was contributing to thrombosis.

In Chapter 3, we analyzed the effect of $p16^{INK4a}$ expression on venous thrombosis *in vivo*. Using a transgenic mouse model of ubiquitous overexpression, we compared venous thrombus formation and resolution in several vascular injury models between $p16^{INK4a}$ overexpressing and wild-type littermate control mice. We demonstrated that $p16^{INK4a}$ transgenic mice display faster rates of vascular occlusion and delayed thrombus resolution upon injury to the saphenous vein. Additionally, $p16^{INK4a}$ overexpression was associated with elevated thrombin generation and increased circulating thrombin-antithrombin (TAT) levels in plasma after exposure to low-dose endotoxin. Furthermore, bone marrow

transplantation from a wild-type donor into $p16^{INK4a}$ transgenic mice resulted in correction of the observed prothrombotic phenotype, suggesting that $p16^{INK4a}$ expression in hematopoietic cells contribute to venous thrombosis[3].

Chapter 4 is a continuation of the studies performed in Chapter 3. Here, we further defined the role of $p16^{INK4a}$ expression in hematopoietic cells to venous thrombus formation. Mouse models of stasis-induced thrombosis following inferior vena cava (IVC) ligation demonstrate that leukocytes were important contributors to the natural history of venous thrombogenesis and thrombus resolution[4-6]. We compared thrombi from $p16^{INK4a}$ transgenic and wild-type control mice following IVC ligation for 3 days both grossly to determine morphologic changes and histologically to examine alterations in protein and cellular composition. Mice overexpressing $p16^{INK4a}$ had larger thrombi compared to wild-type mice after IVC ligation, confirming our previous findings in Chapter 3 that $p16^{INK4a}$ expression is prothrombotic in a mouse model. Immunohistochemical analysis demonstrated that $p16^{INK4a}$ transgenic mice had significantly elevated expression of the monocyte and macrophage marker, F4/80. In order to determine the contribution of these cell types, monocytes and macrophages were depleted by approximately 50% in both transgenic and wild-type mice following intravenous injection of clodronate-packaged liposomes. While both $p16^{INK4a}$ overexpressing and control mice demonstrated increased thrombus size following monocyte and macrophage reduction, suggesting a role for these leukocytes in clearance of early forming thrombi, the difference in thrombus size between the two genotypes was abolished. These studies suggest that $p16^{INK4a}$ expression in monocytes and macrophages from the hematopoietic compartment contribute to the observed prothrombotic phenotype in $p16^{INK4a}$ transgenic mice.

In Chapter 5, we analyzed the effect of $p16^{INK4a}$ expression and cellular senescence on cell surface clotting parameters in endothelial cells *in vitro*. Human umbilical vein endothelial cells (HUVEC) were serially passaged to promote upregulation of senescence hallmarks in cell culture. Serial passaging of HUVEC was associated with increases in the rate of plasma clot formation, greater thrombin generation and the formation of denser, and thus more stable fibrin clots on the cell surface. This procoagulant phenotype was not due to increases in tissue factor (TF) activity. Furthermore, serially passaging of HUVEC resulted in a significant reduction in activated protein C (APC) generation on the cell surface. We found this was due to downregulation of thrombomodulin (TM) expression in late passages. These data suggest that senescence in vascular endothelial cells is associated with procoagulant phenotypic changes in cell culture.

Lastly, Chapter 6 examined the contribution of natural aging to thrombus formation, thrombus resolution, and blood hypercoagulability in mice. We observed that mice displayed an age-dependent decrease in vascular occlusion time following $FeCl_3$-mediated injury to the saphenous vein. Additionally, aging in mice is associated with increases in platelet, lymphocyte, and monocyte counts in whole blood. Interestingly, aged mice display reduced thrombin generation by calibrated automated thrombography (CAT) and no change in TAT levels. Furthermore, stasis-induced thrombosis model showed no difference in thrombus size between 1 and 14 days post IVC ligation. These studies show that susceptibility to venous thrombosis in aged mice is dependent on the type and extent of vascular injury. Also, aging in mice results in changes in blood cell composition and plasma coagulability that differ from those hemostatic changes observed in human aging[7-11], making C57BL/6 mice a challenging model to study hemostasis during aging.

In conclusion, this dissertation showed *in vitro* and *in vivo* that $p16^{INK4a}$ expression and cellular senescence associated with aging contributes to venous thrombosis. Future studies should be directed at how $p16^{INK4a}$ expression in monocytes and macrophages contribute to thrombogenesis. Using a monocyte/macrophage-specific $p16^{INK4a}$ knock-out or $p16^{INK4a}$ overexpressing mouse model would confirm data from the liposome depletion study and also be a more direct way of analyzing the role of $p16^{INK4a}$ expression in monocytes and macrophages in driving a prothrombotic phenotype. In addition, isolation of these cell types from whole blood and bone marrow of $p16^{INK4a}$ transgenic mice would allow us to measure expression levels of proteins involved in regulating thrombus growth and resolution to determine if they differ from wild-type controls. Also, it remains to be determined whether the observed changes in serially passaged HUVEC are $p16^{INK4a}$ -dependent or are an artifact of cell culture. Although many attempts have been made thus far to elucidate these mechanisms, we have not yet successfully overexpressed $p16^{INK4a}$ in HUVEC. Alternatively, vascular endothelial cells can be isolated from $p16^{INK4a}$ transgenic and wild-type mice and cultured to determine if they differ with regard to plasma clotting parameters and APC generation.

7.2 References

1. Krishnamurthy J, Torrice C, Ramsey MR, et al. Ink4a/Arf expression is a biomarker of aging. *J. Clin. Invest*. 2004;114(9):1299-1307.

2. Sharpless NE. Ink4a/Arf links senescence and aging. *Exp. Gerontol*. 2004;39(11-12):1751-1759.

3. Cardenas JC, Owens AP, Krishnamurthy J, et al. Overexpression of the cell cycle inhibitor p16INK4a promotes a prothrombotic phenotype following vascular injury in mice. *Arterioscler. Thromb. Vasc. Biol*. 2011;31(4):827-833.

4. Saha P, Humphries J, Modarai B, et al. Leukocytes and the natural history of deep vein thrombosis: current concepts and future directions. *Arterioscler. Thromb. Vasc. Biol*. 2011;31(3):506-512.

5. von Brühl M, Stark K, Steinhart A, et al. Monocytes, neutrophils, and platelets cooperate to initiate and propagate venous thrombosis in mice in vivo. *J. Exp. Med*. 2012;209(4):819-835.

6. Nosaka M, Ishida Y, Kimura A, Kondo T. Time-dependent appearance of intrathrombus neutrophils and macrophages in a stasis-induced deep vein thrombosis model and its application to thrombus age determination. *Int. J. Legal Med*. 2009;123(3):235-240.

7. Segal JB, Moliterno AR. Platelet counts differ by sex, ethnicity, and age in the United States. *Ann Epidemiol*. 2006;16(2):123-130.

8. Sparrow D, Silbert JE, Rowe JW. The influence of age on peripheral lymphocyte count in men: a cross-sectional and longitudinal study. *J Gerontol*. 1980;35(2):163-166.

9. McArthur WP, Bloom K, Taylor M, et al. Peripheral blood leukocyte populations in the elderly with and without periodontal disease. *J. Clin. Periodontol*. 1996;23(9):846-852.

10. Mari D, Mannucci PM, Coppola R, et al. Hypercoagulability in centenarians: the paradox of successful aging. *Blood*. 1995;85(11):3144-3149.

11. Haidl H, Cimenti C, Leschnik B, Zach D, Muntean W. Age-dependency of thrombin generation measured by means of calibrated automated thrombography (CAT). *Thromb. Haemost*. 2006;95(5):772-775.